

Dear Dr Schymanski and reviewers,

Thank you for taking the time to re-review our manuscript. Once again the comments were insightful and we have taken the time to fully respond. In particular, we have taken reviewer 2's suggestion of recasting the attribution in terms of relative humidity and have performed the analysis. We have added it to the manuscript, rather than replacing the specific humidity analysis, as we believe that including both helps to tell the whole story. We think this has greatly added to our analysis, and we would very much like to know the name of reviewer 2 (if they are agreeable) so that we can properly acknowledge them.

Please find below our responses to the editor and reviewers, followed by a marked up version of the manuscript showing the changes made. Note that, since we updated the references, Word has marked all of the citations as changes, even though most are the same as before.

Regards,

Emma Robinson on behalf of the authors

Response to comments by editor

L18: Yes, we have changed this.

L22: Yes, changed.

L298-299: We have added references for the Pen-Pan model and the Penman equation.

L301: We have changed this.

L348: It is specifically for the 0.12m reference crop, we have clarified this.

L372-374: Yes, this was the wrong way round – the increased humidity decreases the evaporative demand. We have amended this.

L394: Changed 'the number of lying snow days' to 'the number of days with snow cover'.

Response to Reviewer 1 (Report 2)

We thank the reviewer for their comment and respond as follows.

“Concerning the issue of reduced transpiration due to interception I have still one comment:

In line 487 – 490 authors argue, that due to evaporation of snow/rain at the upper side of the leaf, the transpiration is reduced by closed stomata due to high relative humidity. I would not agree with that statement. Given a high relative humidity in the surrounding air, the plant will open the stomata as it is able to exchange carbon for “free” – so the reason for no transpiration is the missing gradient in vapour partial pressure – I am sure that can be easily shown in FLUXNET data when looking at carbon fluxes after rain events!”

Yes, we agree that this sentence was wrong – we have changed it to mention the physical mechanism by which increased humidity decreases the evaporative demand.

Response to Reviewer 2 (Report 1)

We thank the reviewer for their detailed and insightful comments, in particular the suggestion to use relative humidity in the attribution. We have implemented the following changes in response.

Major comment:

This is an excellent suggestion, which we believe supplements the analysis with specific humidity to tell the story of the response of PET to changing climate. We find, as the reviewer expected, that the response to air temperature is reduced significantly. There is a negative trend in the relative humidity across our dataset, although this is only statistically significant in spring. This trend in humidity drives an increase in the PET of similar magnitude as the SW down (this is the same as the difference between the increase in PET due to air temperature and the PET decrease due to specific humidity in the first formulation). We have therefore added this to the manuscript in Section 4.4.

Minor:

General: Thompson et al (1981) is a Met Office technical report, which is, unfortunately, difficult to get hold of outside of the Met Office. However, this is the only place that the technical details of MORECS are available (since it is a commercial product). The Field (1983) paper does provide a good summary of the technical details however, so we have also added a reference to it.

General (but optional): We have kept the units of dec-1, largely for intercomparison with other studies.

21-22: We have edited the abstract to be more consistent.

54: We have added that the Princeton forcings are available at 0.25 deg.

85-91 vs 91-96: Yes, we've added some text to make the fact that PET is a representation of AED clearer.

99: We've added "1km resolution" to this sentence to make it clearer.

125: Deleted the "annual means" reference.

168: For the lapse rates, we did indeed use the approximate method, by which we calculate

$$e_{\text{seaM}} = (1 - (\text{elevM} * 0.025)) * e_{\text{M}}$$

where e_{M} is the MORECS vapour pressure (VP), elevM is the elevation of the MORECS square and e_{seaM} is the MORECS VP lapsed to sea level.

To lapse the interpolated VP back from sea-level to the grid square elevation we used the fraction of the sea-level value

$$e_{\text{1km}} = (1 + (\text{elev1km} * 0.025)) * e_{\text{sea1km}}$$

where e_{sea1km} is the interpolated sea level VP, elev1km is the elevation and e_{1km} is the VP used to calculate our specific humidity.

We have added these equations to the text to clarify.

183-184: We have investigated the effect of the 100000Pa assumption on the PET on the same first year of data. We calculated what the VP would have been if we had used the dataset air pressure (p^*) instead of the constant 100000Pa air pressure (p_c).

You are right that there is a larger relative effect on the PET and PETI where the humidity deficit is small. However, this is generally in the winter and the high ground, where the PET(I) itself is small. So even if the relative difference is high ($>\sim 10\%$), the absolute difference is small, so this is still reasonable.

We haven't quantified the effect this approximation would have on the trends or the attribution, although it is clear from the equations in Appendix C that only the temperature and windspeed contributions would be affected.

236-238: This first part of the paper is describing the calculation of a dataset which has already been published. While we agree that for future releases interpolating these data would be an improvement, the existing data set has not been interpolated. We have looked at the output of runs of the JULES model driven by these data and we do not see significant artefacts associated with the CRU grid cell boundaries.

261: You are right that the problem is that many different values are mixed together in the highlands. The wind speed is quite variable over small ranges – there are values of ~ 3 m s⁻¹ and values of ~ 6 m s⁻¹ very close to each other – so it is very hard to see the different colours. We have tried different limits on the colour bar and there's not much improvement, so we don't really have a solution.

289-292: We have added a discussion of this wind speed bias in the description of aerodynamic resistance in the PET calculation. The wind speed bias would lead to a high bias in the PET, but we are calculating a 'reference crop' PET and ignoring the land cover, so this is reasonable.

313-314, 321, 332: We have added statements to identify that the spatially varying p^* is used everywhere apart from the VP calculation.

373-374: Yes, this should have read that the high humidity causes a low humidity deficit, and therefore low evaporative demand. We have fixed this.

402-405: Although the equation allows for intercepted water to take more than one day to evaporate, we assume that after the first day the interception is negligible, so that any day without rainfall does not include the interception correction. We have added this to the text.

End of 455: We have moved the mention of annual trends in Table 2 to the appropriate point in the paragraph.

460: We've amended the discussion of seasonal temperature trends to say that the trend is only significant in spring and autumn.

476: We've mentioned the aerodynamic and radiative components in Table 2 in the text. The extra line in Table 2 was actually part of the previous line, but the formatting was such that it was not obvious where one row ended and the next began. We've added some separating lines for clarity.

479-483: We've explicitly mentioned Fig B2 where applicable.

496-497: We've added the autumn English Lowlands exception

545: We have changed "whole dataset" to "seasonal cycle"

562-563: We haven't changed the variables from downward LW/SW radiation to net LW/SW radiation, but we have added this caveat to the text.

563-564: Yes, the stilling is still significant, so we have changed the text to reflect this.

568: We've changed "decreasing" to "more strongly decreasing"

582: We've changed "negligible" to say that the wind speed has not had a dominant effect.

674: This discussion has now changed somewhat, so we no longer have this sentence.

729-730: We have mentioned the overestimate of SWdown in the text (note that we had the legend text wrong – the black lines are the new dataset, the blue lines are the observations – so that the dataset SWdown is an overestimate compared to the observations.)

748-749 vs rest of paper: We've changed to Tsp (and also psp) throughout.

Beginning of 749: Yes, just a typo, which has been fixed.

Table 1, Specific Humidity line: Yes, also a typo which has been fixed.

Fig A2 caption, lines 1287-1288: Yes, the caption has been fixed.

Fig B1 (and probably B2 as well): We have added annual mean to the caption.

Also Fig B1: Yes, we've amended the caption.

Typos:

Beginning of 593: "or" should be "of": fixed

1292: "Ration" should be "ratio": fixed

1 **Trends in atmospheric evaporative demand in Great Britain**
2 **using high-resolution meteorological data**

3

4 **Emma L. Robinson¹, Eleanor M. Blyth¹, Douglas B. Clark¹, Jon Finch¹ and Alison**
5 **C. Rudd¹**

6 [1]{Centre for Ecology and Hydrology, Maclean Building, Benson Lane, Crowmarsh Gifford,
7 Wallingford OX10 8BB }

8 Correspondence to: Emma L. Robinson (emrobi@ceh.ac.uk)

9

10 Abstract

11 Observations of climate are often available on very different spatial scales from observations
12 of the natural environments and resources that are affected by climate change. In order to help
13 bridge the gap between these scales using modelling, a new dataset of daily meteorological
14 variables was created at 1 km resolution over Great Britain for the years 1961-2012, by
15 interpolating coarser resolution climate data and including the ~~effect~~effects of local topography.
16 These variables were used to calculate atmospheric evaporative demand (AED) at the same
17 spatial and temporal resolution. Two functions that represent AED were chosen: one is a
18 standard form of Potential Evapotranspiration (PET) and the other is a ~~derivative of it~~derived
19 PET measure used by hydrologists that includes the effect of water intercepted by the canopy
20 (PETI). Temporal trends in these functions were calculated, with PET found to be increasing
21 in all regions, and at an overall rate of $0.021 \pm 0.021 \text{ mm d}^{-1} \text{ decade}^{-1}$ in Great Britain, ~~while,~~
22 PETI was found to be increasing at a rate ~~of $0.023019 \pm 0.023020 \text{ mm d}^{-1} \text{ decade}^{-1}$ in England~~
23 ~~$(0.028 \pm 0.025 \text{ mm d}^{-1} \text{ decade}^{-1}$ in the English Lowlands),~~ Great Britain, but ~~this was not~~
24 ~~increasing at a statistically significant rate in Scotland or Wales.~~ However, there was a trend in
25 PETI in England of $0.023 \pm 0.023 \text{ mm d}^{-1} \text{ decade}^{-1}$. The trends were found to vary by season,
26 with spring PET increasing by $0.043 \pm 0.019 \text{ mm d}^{-1} \text{ decade}^{-1}$ ($0.038 \pm 0.018 \text{ mm d}^{-1} \text{ decade}^{-1}$
27 when the interception correction is included) in Great Britain, while there is no statistically
28 significant trend in other seasons. The trends were attributed analytically to trends in the climate
29 variables; the overall positive trend was predominantly driven by rising air temperature,
30 although rising specific humidity had a negative effect on the trend. Recasting the analysis in
31 terms of relative humidity revealed that the overall effect is that falling relative humidity causes
32 the PET to rise. Increasing downward short- and longwave radiation made an overall positive
33 contribution to the PET trend, while ~~the 10 m~~decreasing wind speed ~~had made~~
34 ~~effect.~~contribution to the trend in PET. The trend in spring PET was particularly strong due to
35 a strong decrease in relative humidity and increase in ~~spring~~ downward shortwave radiation in
36 the spring.

37

38 1 Introduction

39 There are many studies showing the ways in which our living environment is changing over
40 time: changing global temperatures (~~IPCC, 2013~~)([IPCC, 2013](#)), radiation (~~Wild, 2009~~)([Wild,](#)
41 [2009](#)) and wind speeds (~~McVicar et al., 2012~~)([McVicar et al., 2012](#)) can have significant
42 impacts on ecosystems and human life (~~IPCC, 2014a~~)([IPCC, 2014a](#)). While there are overall
43 global trends, the impacts can vary between regions (~~IPCC, 2014b~~)([IPCC, 2014b](#)). In the UK,
44 wildlife surveys of both flora (~~Wood et al., 2015; Evans et al., 2008~~)([Wood et al., 2015; Evans](#)
45 [et al., 2008](#)) and fauna (~~Poorek et al., 2015~~)([Pocock et al., 2015](#)) show a shift in patterns and
46 timing (~~Thackeray et al., 2010~~)([Thackeray et al., 2010](#)). In addition, the UK natural resources
47 of freshwater (~~Watts et al., 2015~~)([Watts et al., 2015](#)), soils (~~Reynolds et al., 2013; Reynolds et~~
48 [al., 2013; Bellamy et al., 2005](#)) and vegetation (~~Berry et al., 2002; Hickling et al., 2006; Norton~~
49 [et al., 2012; Hickling et al., 2006; Norton et al., 2012](#)) are changing. The UK is experiencing
50 new environmental stresses on the land and water systems through changes in temperature and
51 river flows (Crooks and Kay, 2015; ~~Watts et al., 2015~~[Watts et al., 2015](#); ~~Hannaford,~~
52 [2015Hannaford, 2015](#)), which ~~is~~[are](#) part of a widespread global pattern of temperature increase
53 and circulation changes (~~Watts et al., 2015~~)([Watts et al., 2015](#)).

54 To explain these changes in terms of climate drivers, there are several gridded meteorological
55 datasets available at global and regional scales. Global datasets can be based on observations –
56 for example the 0.5° resolution Climate Research Unit time series 3.21 (CRU TS 3.21) data
57 (~~Jones and Harris, 2013; Harris et al., 2014~~)([Jones and Harris, 2013; Harris et al., 2014](#)) – while
58 some are based on global meteorological reanalyses bias-corrected to observations – for
59 example the WATCH Forcing Data (WFD, 0.5°; ~~Weedon et al. (2011)~~[Weedon et al. \(2011\)](#)),
60 the WATCH Forcing Data methodology applied to ERA-Interim reanalysis product (WFDEI,
61 0.5°; ~~Weedon et al. (2014)~~[Weedon et al. \(2014\)](#)) and the Princeton Global Meteorological
62 Forcing Dataset (~~1°; Sheffield et al. (2006)~~[0.25°–1°; Sheffield et al. \(2006\)](#)). At the regional
63 scale in Great Britain (GB), there are datasets that are derived directly from observations – for
64 example the Met Office Rainfall and Evaporation Calculation System (MORECS) dataset at 40
65 km resolution (~~Thompson et al., 1981; Hough and Jones, 1997~~)([Thompson et al., 1981; Hough](#)
66 [and Jones, 1997; Field, 1983](#)) and the UKCP09 observed climate data at 5 km resolution
67 (~~Jenkins et al., 2008~~)([Jenkins et al., 2008](#)).

68 However, while regional observations of carbon, methane and water emissions from the land
69 (Baldocchi et al., 1996), the vegetation cover (~~Morton et al., 2011~~)([Morton et al., 2011](#)) and soil

70 properties (~~FAO/IIASA/ISRIC/ISS-CAS/JRC, 2012~~)(~~FAO/IIASA/ISRIC/ISS-CAS/JRC,~~
71 ~~2012~~) are typically made at the finer landscape scale of 100 m to 1000 m, most of these long-
72 term gridded meteorological datasets are only available at a relatively coarse resolution of a
73 few tens of km. These spatial scales may not be representative of the climate experienced by
74 the flora and fauna being studied, and it has also been shown that input resolution can have a
75 strong effect on the performance of hydrological models (~~Kay et al., 2015~~)(~~Kay et al., 2015~~).
76 In addition, the coarse temporal resolution of some datasets, for example the monthly CRU TS
77 3.21 data (~~Harris et al., 2014; Jones and Harris, 2013~~)(~~Harris et al., 2014; Jones and Harris,~~
78 ~~2013~~), can miss important sub-monthly extremes.

79 Regional studies are important to identify drivers and impacts of changing meteorology that
80 may or may not be reflected in trends in global means. For example, in Canada (~~Vincent et al.,~~
81 ~~2015~~)(~~Vincent et al., 2015~~) and Europe (~~Fleig et al., 2015~~)(~~Fleig et al., 2015~~), high resolution
82 meteorological data have been used to identify the impacts of changing circulation patterns,
83 while in Australia wind speed data have been used to quantify the effects of global stilling in
84 the region (~~McVicar et al., 2008~~)(~~McVicar et al., 2008~~). While there are datasets available at
85 finer spatial and temporal resolutions for the UK (such as UKCP09 (~~Jenkins et al.,~~
86 ~~2008~~)(~~Jenkins et al., 2008~~)), these often do not provide all the variables needed to identify the
87 impacts of changing climate.

88 To address this, we have created a meteorological dataset for Great Britain at 1 km resolution
89 (~~Robinson et al., 2015a~~): the Climate Hydrology and Ecology research Support System
90 meteorology dataset for Great Britain (1961-2012) (CHESS-met; Robinson et al. (2015b)). It is
91 derived from the observation-based MORECS dataset (~~Thompson et al., 1981; Hough and~~
92 ~~Jones, 1997~~)(~~Thompson et al., 1981; Hough and Jones, 1997~~), and then downscaled using
93 information about topography. This is augmented by an independent precipitation dataset –
94 Gridded Estimates of daily and monthly Areal Rainfall for the United Kingdom (CEH-GEAR;
95 ~~Tanguy et al. (2014); Keller et al. (2015)~~Tanguy et al. (2014); Keller et al. (2015)) – along with
96 variables from two global datasets – WFD and CRU TS 3.21 – to produce a comprehensive,
97 observation-based, daily meteorological dataset at 1 km × 1 km spatial resolution.

98 In order to understand the effect of meteorology on the water cycle, a key variable in
99 hydrological modelling is the atmospheric evaporative demand (AED), which is determined by
100 meteorological variables (~~Kay et al., 2013~~)(~~Kay et al., 2013~~). It has been shown that water-
101 resource and hydrological model results are largely driven by how this property is defined and

102 used (~~Haddeland et al., 2011~~)([Haddeland et al., 2011](#)). The AED can be expressed in several
103 ways, for instance the evaporation from a wet surface, from a well-watered but dry uniform
104 vegetated cover, or from a hypothetical well-watered but dry version of the actual vegetation.
105 Metrics such as the Palmer Drought Severity Index (PDSI; ~~Palmer (1965)~~) ~~use potential~~
106 ~~evapotranspiration (PET) as an input~~[Palmer \(1965\)](#) ~~use potential evapotranspiration (PET) as~~
107 ~~an input to represent AED~~, while many hydrological models such as Climate and Land use
108 Scenario Simulation in Catchments (CLASSIC; Crooks and Naden (2007)) or Grid-to-Grid
109 (G2G; Bell et al. (2009)), ~~use as input~~[which also require an input representing AED](#), ~~use~~ a
110 distinct form of the PET which includes the intercepted water from rainfall (this is described
111 later in the text) which we hereby name PETI. While hydrological models can make use of high
112 resolution topographic information and precipitation datasets, they are often driven with PET
113 calculated at a coarser resolution (Bell et al., 2011; Bell et al., 2012; ~~Kay et al., 2015~~)[Kay et al.,](#)
114 ~~2015~~). ~~Therefore, we have also created a dataset.~~ ~~Therefore, we have also created a 1 km × 1~~
115 ~~km resolution dataset, the Climate Hydrology and Ecology research Support System Potential~~
116 ~~Evapotranspiration dataset for Great Britain (1961-2012) (CHESS-PE; Robinson et al.~~
117 ~~(2015a))~~, consisting of estimates of PET and PETI, which can be used to run high-resolution
118 hydrological models (~~Robinson et al., 2015b~~).

119 Other regional studies have created gridded estimates of AED in Austria (~~Haslinger and~~
120 ~~Bartsch, 2016~~)([Haslinger and Bartsch, 2016](#)) and Australia (~~Donohue et al., 2010~~)([Donohue et](#)
121 ~~al., 2010~~). Regional studies of trends in AED have seen varied results, with increasing AED
122 seen in Romania (~~Paltineanu et al., 2012~~)([Paltineanu et al., 2012](#)), Serbia (~~Gocic and Trajkovic,~~
123 ~~2013~~)([Gocic and Trajkovic, 2013](#)), Spain (~~Vicente-Serrano et al., 2014~~)([Vicente-Serrano et al.,](#)
124 ~~2014~~), some regions of China (~~Li and Zhou, 2014~~)([Li and Zhou, 2014](#)) and Iran (Azizzadeh and
125 Javan, 2015; ~~Hosseinzadeh Talaei et al., 2013; Tabari et al., 2012~~)[Hosseinzadeh Talaei et al.,](#)
126 ~~2013; Tabari et al., 2012~~), decreasing AED in north east India (~~Jhajharia et al., 2012~~)([Jhajharia](#)
127 ~~et al., 2012~~) and regions in China (~~Yin et al., 2009; Song, 2010; Shan et al., 2015; Zhao et al.,~~
128 ~~2015; Zhang et al., 2015; Lu et al., 2016~~)([Yin et al., 2009; Song, 2010; Shan et al., 2015; Zhao](#)
129 ~~et al., 2015; Zhang et al., 2015; Lu et al., 2016~~) and regional variability in Australia (~~Donohue~~
130 ~~et al., 2010~~)([Donohue et al., 2010](#)) and China (~~Li et al., 2015~~)([Li et al., 2015](#)). In order to
131 understand this variability, it is important to quantify the relative contributions of the changing
132 meteorological variables to trends in AED and regional studies often find different drivers of
133 changing AED (see ~~MeVicar et al. (2012)~~[McVicar et al. \(2012\)](#) for a review). Relative humidity
134 has been shown to drive AED in the Canary Islands (~~Vicente-Serrano et al., 2016~~)([Vicente-](#)

135 [Serrano et al., 2016](#)), wind speed and air temperature were shown to have nearly equal but
136 opposite effects in Australia (~~[Donohue et al., 2010](#)~~)([Donohue et al., 2010](#)), while in China
137 sunshine hours (~~[Li et al., 2015](#)~~)([Li et al., 2015](#)), wind speed (~~[Yin et al., 2009](#)~~)([Yin et al., 2009](#))
138 or a combination of the two (~~[Lu et al., 2016](#)~~)([Lu et al., 2016](#)) have been shown to drive trends.
139 ~~[Rudd and Kay \(2015\)](#)~~[Rudd and Kay \(2015\)](#) investigated projected changes in PET using a
140 regional climate model, but little has been done to investigate historical trends of AED in the
141 UK.

142 The objectives of this paper are (i) to evaluate the trends in key meteorological variables in
143 Great Britain over the years 1961-2012; (ii) to evaluate the AED in Great Britain over the same
144 time period using PET; (iii) to investigate the effect of including interception in the formulation
145 of PET called PETI; (iv) to evaluate trends in PET over the time period of interest; and (v) to
146 attribute the trends in PET to trends in meteorological variables. To address these objectives,
147 the paper is structured as follows. Section 2 presents the calculation of the meteorological
148 variables. Section 3 presents the calculation of PET and PETI from the meteorological variables
149 and assesses the difference between PET and PETI. In Section 4 the trends ~~in annual means~~ of
150 the meteorological variables and AED are calculated and the trends in PET are attributed to
151 trends in meteorological variables. In Section 5 the results are discussed and conclusions are
152 presented in Section 6.

153 **2 Calculation of meteorological variables**

154 The meteorological variables included in this new dataset (~~[Robinson et al., 2015a](#)~~)([Robinson et](#)
155 [al., 2015b](#)) are daily mean values of air temperature, specific humidity, wind speed, downward
156 longwave (LW) and shortwave (SW) radiation, precipitation and air pressure, plus daily
157 temperature range (Table 1). These variables are important drivers of near-surface conditions,
158 and, for instance, are the full set of variables required to drive the JULES land surface model
159 (LSM) (Best et al., 2011; Clark et al., 2011), as well as other LSMs.

160 The data were derived primarily from MORECS, which is a long-term gridded dataset starting
161 in 1961 and updated to the present (~~[Thompson et al., 1981](#)~~; ~~[Hough and Jones, 1997](#)~~)([Thompson](#)
162 [et al., 1981](#); [Hough and Jones, 1997](#)). It interpolates five variables from synoptic stations (daily
163 mean values of air temperature, vapour pressure and wind speed, daily hours of bright sunshine
164 and daily total precipitation) to a 40 km × 40 km resolution grid aligned with the Ordnance
165 Survey National Grid. There are currently 270 stations reporting in real time, while a further
166 170 report the daily readings on a monthly basis, but numbers have varied throughout the run.

195 The algorithm interpolates a varying number of stations (up to nine) for each square, depending
196 on data availability (Hough and Jones, 1997)(Hough and Jones, 1997). The interpolation is such
197 that the value in each grid square is the effective measurement of a station positioned at the
198 centre of the square and at the grid square mean elevation, averaged from 00:00 GMT to 00:00
199 GMT the next day. MORECS is a consistent, quality-controlled time series, which accounts for
200 changing station coverage. The MORECS variables were used to derive the air temperature,
201 specific humidity, wind speed, downward LW and SW radiation and air pressure in the new
202 dataset. The WFD and CRU TS 3.21 datasets were used for surface air pressure and daily
203 temperature range respectively, as they could not be calculated solely from MORECS.
204 Additionally precipitation was obtained from the CEH-GEAR data, which is a product directly
205 interpolated to 1 km from the station data (Keller et al., 2015)(Keller et al., 2015).

206 The spatial coverage of the dataset was determined by the spatial coverage of MORECS, which
207 covers the majority of Great Britain, but excludes some coastal regions and islands at the 1 km
208 scale. For most of these points, the interpolation was extended from the nearest MORECS
209 squares, but some outlying islands (in particular Shetland and the Scilly Isles) were excluded
210 when the entire island was further than 40 km from the nearest MORECS square.

211 2.1 Air temperature

212 Air temperature, T_a (K), was derived from the MORECS air temperature. The MORECS air
213 temperature was reduced to mean sea level, using a lapse rate of -0.006 K m^{-1} (Hough and
214 Jones, 1997)(Hough and Jones, 1997). A bicubic spline was used to interpolate from 40 km
215 resolution to 1 km resolution, then the temperatures were adjusted to the elevation of each 1 km
216 square using the same lapse rate. The 1 km resolution elevation data used were aggregated from
217 the Integrated Hydrological Digital Terrain Model (IHDTM) – a 50 m resolution digital terrain
218 model (Morris and Flavin, 1990).

219 2.2 Specific humidity

220 Specific humidity, q_a (kg kg^{-1}), was derived from the MORECS vapour pressure, e_M (Pa), which
221 was first reduced to mean sea level, using the equation

$$222 e_{sea} = e_M \left(1 - \frac{L_e}{100} h_M \right) \quad (1)$$

223 where L_e is the lapse rate of -0.025 \% m^{-1} and h is the elevation of the MORECS square
 224 (Thompson et al., 1981)(Thompson et al., 1981). The actual lapse rate of humidity will, in
 225 general, vary according to atmospheric conditions. However, calculating this would require
 226 more detailed information than is available in the input data used. Any method of calculating
 227 the variation of specific humidity with height will involve several assumptions, but the method
 228 used here is well-established and is used by the Met Office in calculating MORECS (Thompson
 229 et al., 1981)(Thompson et al., 1981). The value of the vapour pressure lapse rate is chosen to
 230 keep relative humidity approximately constant with altitude, rather than assuming that the
 231 specific humidity vapour pressure itself is constant.

232 A bicubic spline was used to interpolate vapour pressure to 1 km resolution then the values
 233 were adjusted to the 1 km resolution elevation using the IHDTM elevations. Finally the specific
 234 humidity was calculated, using and using the same lapse rate, such that

$$235 \quad e = e_{sea,1km} \left(1 + \frac{L_e}{100} h_{1km} \right), \quad (2)$$

236 where $e_{sea,1km}$ is the sea-level vapour pressure at 1 km resolution and h_{1km} is the 1 km resolution
 237 elevation.

238 Finally the specific humidity was calculated, using

$$239 \quad q_a = \frac{\epsilon e}{p_* - (1 - \epsilon)e}, \quad (43)$$

240 where e is the vapour pressure (Pa) and $\epsilon = 0.622$ is the mass ratio of water to dry air (Gill,
 241 1982)(Gill, 1982). The air pressure, p_* , in this calculation was assumed to have a constant value
 242 of 100000 Pa because this was prescribed in the computer code. It would be better to use a
 243 varying air pressure, as calculated in Section 2.8, but this makes a negligible difference (of a
 244 few percent) to the calculated specific humidity and a constant p_* was retained.

245 **2.3 Downward shortwave radiation**

246 Downward SW radiation, S_d (W m^{-2}), was derived from the MORECS hours of bright sunshine
 247 (defined as the total number of hours in a day for which solar irradiation exceeds 120 W m^{-2}
 248 (WMO, 2013)(WMO, 2013)). The value calculated is the mean SW radiation over 24 hours.
 249 The sunshine hours were used to calculate the cloud cover factor, $C_f = n/N$, where n is the
 250 number of hours of bright sunshine in a day, and N is the total number of hours between sunrise
 251 and sunset (Marthews et al., 2011)(Marthews et al., 2011). The cloud cover factor was

252 interpolated to 1 km resolution using a bicubic spline. The downward SW solar radiation for a
253 horizontal plane at the Earth's surface was then calculated using the solar angle equations of
254 ~~Iqbal (1983)~~Iqbal (1983) and a form of the ~~Angstrom~~Ångström-Prescott equation which relates
255 hours of bright sunshine to solar irradiance (Ångström, 1918; Prescott, 1940~~Prescott, 1940~~),
256 with empirical coefficients calculated by Cowley (1978). They vary spatially and seasonally
257 and effectively account for reduction of irradiance with increasing solar zenith angle, as well
258 as implicitly accounting for spatially- and seasonally-varying aerosol effects. However, they do
259 not vary interannually and thus do not explicitly include long-term trends in aerosol
260 concentration.

261 The downward SW radiation was then corrected for the average inclination and aspect of the
262 surface, assuming that only the direct beam radiation is a function of the inclination and that
263 the diffuse radiation is homogeneous. It was also assumed that the cloud cover is the dominant
264 factor in determining the diffuse fraction (~~Muneer and Munawwar, 2006~~)(Muneer and
265 Munawwar, 2006). The aspect and inclination were calculated using the IHDTM elevation at
266 50 m resolution, following the method of ~~Horn (1981)~~Horn (1981), and were then aggregated
267 to 1 km resolution. The top of atmosphere flux for horizontal and inclined surfaces was
268 calculated following Allen et al. (2006) and the ratio used to scale the direct beam radiation.

269 **2.4 Downward longwave radiation**

270 Downward LW radiation, L_d (W m^{-2}), was derived from the 1 km resolution air temperature
271 (Sect. 2.1), vapour pressure (Sect. 2.2) and cloud cover factor (Sect. 2.3). ~~The downward LW~~
272 ~~radiation for clear sky conditions was calculated as a function of air temperature and~~
273 ~~precipitable water using the method of Dilley and O'Brien (1998), with precipitable water~~
274 ~~calculated from air temperature and humidity following Prata (1996). The additional~~
275 ~~component due to cloud cover was calculated using the equations of Kimball et al. (1982)~~The
276 downward LW radiation for clear sky conditions was calculated as a function of air temperature
277 and precipitable water using the method of Dilley and O'Brien (1998), with precipitable water
278 calculated from air temperature and humidity following Prata (1996). The additional
279 component due to cloud cover was calculated using the equations of Kimball et al. (1982),
280 assuming a constant cloud base height of 1000 m.

281 2.5 Wind speed

282 The wind speed at a height of 10 m, u_{10} (m s^{-1}), was derived from the MORECS 10 m wind
283 speed, which were interpolated to 1 km resolution using a bicubic spline and adjusted for
284 topography using a 1 km resolution dataset of mean wind speeds produced by the UK Energy
285 Technology Support Unit (ETSU) (~~Newton and Burch, 1985; Burch and Ravenscroft, 1992~~).
286 ~~This used Numerical Objective Analysis Boundary Layer (NOABL) methodology and; Newton~~
287 ~~and Burch (1985); Burch and Ravenscroft (1992))~~. This used Numerical Objective Analysis
288 Boundary Layer (NOABL) methodology combined with station wind measurements over the
289 period 1975-84 to produce a map of mean wind speed over the UK. To calculate the topographic
290 correction, the ETSU wind speed was aggregated to 40 km resolution, then the difference
291 between each 1 km value and the corresponding 40 km mean found. This difference was added
292 to the interpolated daily wind speed. In cases where this would result in a negative wind speed,
293 the wind speed was set to zero.

294 2.6 Precipitation

295 Precipitation rate, P ($\text{kg m}^{-2} \text{s}^{-1}$), is taken from the daily CEH-GEAR dataset (~~Tanguy et al.,~~
296 ~~2014; Keller et al., 2015~~)(Tanguy et al., 2014; Keller et al., 2015), scaled to the appropriate
297 units. The CEH-GEAR methodology uses natural neighbour interpolation (~~Gold, 1989~~)(Gold,
298 1989) to interpolate synoptic station data to a 1 km resolution gridded daily dataset of the
299 estimated precipitation in 24 hours between 09:00 GMT and 09:00 GMT the next day.

300 2.7 Daily temperature range

301 Daily temperature range (DTR), D_T (K), was obtained from the CRU TS 3.21 monthly mean
302 daily temperature range estimates on a 0.5° latitude \times 0.5° longitude grid, which is interpolated
303 from monthly climate observations (~~Harris et al., 2014; Jones and Harris, 2013~~)(Harris et al.,
304 2014; Jones and Harris, 2013). There is no standard way to correct DTR for elevation, so these
305 data were reprojected to the 1 km grid with no interpolation and the monthly mean used to
306 populate the daily values in each month. Although DTR is not required in the calculation of
307 AED, it is a required input of the JULES LSM, in order to run at sub-daily timestep with daily
308 input data.

309 2.8 Surface air pressure

310 Surface air pressure, p^* (Pa), was derived from the WFD, an observation-corrected reanalysis
311 product, which provides 3 hourly meteorological data for 1958-2001 on a 0.5° latitude \times 0.5°
312 longitude resolution grid (~~Weedon et al., 2011~~)(Weedon et al., 2011). Mean monthly values of
313 WFD surface air pressure and air temperature were calculated for each 0.5° grid box over the
314 years 1961-2001. These were reprojected to the 1 km grid with no interpolation, then the lapse
315 rate of air temperature (Sect. 2.1) used to calculate the integral of the hypsometric equation, ~~in~~
316 ~~order to obtain the air pressure at the elevation of each 1 km grid~~ (Shuttleworth,
317 ~~2012~~)(Shuttleworth, 2012), ~~in order to obtain the air pressure at the elevation of each 1 km~~
318 ~~grid~~. The mean monthly values were used to populate the daily values in the full dataset, thus
319 the surface air pressure in the new dataset does not vary interannually, but does vary seasonally.
320 This is reasonable as the trend in surface air pressure in the WFD is negligible (~~Weedon et al.,~~
321 ~~2011~~)(Weedon et al., 2011).

322 2.9 Spatial and seasonal patterns of meteorological variables

323 Long-term mean values of the meteorological variables were calculated for each 1 km square
324 over the whole dataset (~~, covering the years 1961-2012~~) (Fig. 1). Four sub-regions of interest
325 were defined (Fig. 2); three of these regions correspond to nations (England, Wales and
326 Scotland), while the fourth is the ‘English lowlands’, a subset of England, covering south-
327 central and south-east England, East Anglia and the East Midlands (~~Folland et al.,~~
328 ~~2015~~)(Folland et al., 2015). Mean-monthly climatologies (~~Fig. 3~~) were calculated over the
329 whole of Great Britain (GB), and over these four regions of interest (~~Fig. 3~~).

330 The maps clearly show the effect of topography on the variables (Fig. 1), with an inverse
331 correlation between elevation and temperature, specific humidity, downward LW radiation and
332 surface air pressure and a positive correlation with wind speed. The precipitation has an east-
333 west gradient due to prevailing weather systems and orography. The fine-scale structure of the
334 downward SW radiation is due to the aspect and elevation of each grid cell, with more spatial
335 variability in areas with more varying terrain. As no topographic correction has been applied to
336 DTR, it varies only on a larger spatial scale. Although specific humidity is inversely
337 proportional to elevation, relative humidity is not, as the saturated specific humidity will also
338 be inversely proportional to elevation due to the decrease in temperature with height. The strong

370 correlation between wind speed and elevation means that it is very variable over short spatial
371 scales, particularly in Scotland.

372 The mean-monthly climatologies (Fig. 3) demonstrate the differences between the regions, with
373 Scotland generally having lower temperatures and more precipitation than the average, and
374 England (particularly the English lowlands) being warmer and drier.

375 **2.10 Validation of meteorology**

376 The precipitation dataset, CEH-GEAR, has previously been validated against observations
377 ~~(Keller et al., 2015)~~(Keller et al., 2015). Other studies discuss the uncertainties in the CRU TS
378 3.21 daily temperature range data ~~(Harris et al., 2014)~~(Harris et al., 2014) and WFDEI air
379 pressure data (Weedon et al., 2014).

380 For the other variables, the MORECS data set is ultimately derived from the synoptic stations
381 around the UK which represent most of the available observed meteorological data- for the
382 country. The only way to validate the gridded meteorology presented here is to compare it to
383 independently observed data, which are available at a few sites where meteorological
384 measurement stations that are not part of the synoptic network are located. Here we carry out a
385 validation exercise with data from four sites from the UK, which have meteorological
386 measurements available for between 5 and 10 years. Details of the sites and data are in
387 Appendix A. Fig. 4 shows the comparison of data set air temperature with the observed air
388 temperature at each of the four sites. This shows a strong correlation (r^2 between 0.94 and 0.97)
389 between the data set and the observations. Fig. 5 shows the mean-monthly climatology
390 calculated from both the data set and from the observations (only for times for which
391 observations were available) and demonstrates that the data set successfully captures the
392 seasonal cycle. This has been repeated for downward SW radiation and for an estimate of the
393 mixing ratio of water vapour, 10 m wind speed and surface air pressure (Appendix A). The air
394 temperature, downward SW radiation and mixing ratio all have high correlations and represent
395 the seasonal cycle well. The downward SW is overestimated at Auchencorth Moss, which may
396 be due to local factors (e.g. shading, or the siting of the station within the grid square). The
397 wind speed is overestimated by the derived data set at two sites, which is likely to be due to
398 land cover effects. The modelling which produced the ETSU dataset uses topography but not
399 land cover (Burch and Ravenscroft, 1992; ~~Newton and Burch, 1985~~Newton and Burch, 1985),
400 so at sites with tall vegetation the wind speed is likely to be less than the modelled value. The

Field Co

401 air pressure has a low correlation because the data set contains a mean-monthly climatological
 402 value. However, the mean bias is low and the RMSE is small, confirming that it is reasonable
 403 to use a climatological value in place of daily data.

404 3 Calculation of potential evapotranspiration (PET)

405 There are several ways to assess the evaporative demand of the atmosphere. Pan evaporation
 406 can be modelled using the Pen-Pan model, ~~or open-water evaporation can be modelled with the~~
 407 ~~Penman equation. (Rotstayn et al., 2006), or open-water evaporation can be modelled with the~~
 408 ~~Penman equation (Penman, 1948).~~ However, neither of these account for the fact that in general
 409 the evaporation is occurring from a vegetated surface. A widely used model is the Penman-
 410 Monteith PET, E_P (mm d^{-1} , equivalent to $\text{kg m}^{-2} \text{d}^{-1}$), which is a physically-based formulation
 411 of ~~the AED of the atmosphere (Monteith, 1965)(Monteith, 1965);~~ including the effect of
 412 stomatal resistance. It provides an estimate of AED dependent on the atmospheric conditions
 413 but allowing for the fact that the water is evaporating through the surface of leaves and thus
 414 the resistance is higher. It ~~is~~ can be calculated from the daily meteorological variables using the
 415 equation

$$416 \quad E_P = \frac{t_d}{\lambda} \frac{\Delta A + \frac{c_p \rho_a}{r_a} (q_s - q_a)}{\Delta + \gamma \left(1 + \frac{r_s}{r_a}\right)}, \quad (24)$$

417 where $t_d = 86400 \text{ s d}^{-1}$ is the length of a day, $\lambda = 2.5 \times 10^6 \text{ J kg}^{-1}$ is the latent heat of evaporation,
 418 q_s is saturated specific humidity (kg kg^{-1}), Δ is the gradient of saturated specific humidity with
 419 respect to temperature ($\text{kg kg}^{-1} \text{K}^{-1}$), A is the available energy (W m^{-2}), $c_p = 1010 \text{ J kg}^{-1} \text{K}^{-1}$ is the
 420 specific heat capacity of air, ρ_a is the density of air (kg m^{-3}), q_a is specific humidity (kg kg^{-1}),
 421 $\gamma = 0.004 \text{ K}^{-1}$ is the psychrometric constant, r_s is stomatal resistance (s m^{-1}) and r_a is aerodynamic
 422 resistance (s m^{-1}) ~~(Stewart, 1989)(Stewart, 1989).~~

423 The saturated specific humidity, q_s (kg kg^{-1}), is calculated from saturated vapour pressure, e_s
 424 (Pa), using Eq. (1).3. The saturated vapour pressure is calculated using an empirical fit to air
 425 temperature

$$426 \quad e_s = p_s p_{sp} \exp\left(\sum_{i=1}^4 a_i \left(1 - \frac{T_s}{T_{ref}}\right)^i\right) \left(\sum_{i=1}^4 a_i \left(1 - \frac{T_{sp}}{T_a}\right)^i\right), \quad (35)$$

428 where $p_s p_{sp} = 101325$ Pa is the steam point pressure, $T_s T_{sp} = 373.15$ K is the steam point
 429 temperature and $a=(13.3185, -1.9760, -0.6445, -0.1299)$ are empirical coefficients (Richards,
 430 1971)(Richards, 1971).

431 The derivative of the saturated specific humidity with respect to temperature, Δ ($\text{kg kg}^{-1} \text{K}^{-1}$),
 432 is therefore

$$433 \Delta = \frac{T_s T_{sp}}{T_a^2 T_a^2} \frac{p_s q_s}{p_s - (1-\epsilon)e_s} \sum_{i=1}^4 i a_i \left(1 - \frac{T_s}{T_a}\right)^{i-1} \left(1 - \frac{T_{sp}}{T_a}\right)^{i-1} \quad (6)$$

435 where the air pressure used is the spatially varying air pressure calculated in Sect.2.8.

436 The available energy, A (W m^{-2}), is the energy balance of the surface,

$$437 A = R_n - G, \quad (57)$$

438 where R_n is the net radiation (W m^{-2}) and G is the soil heat flux (W m^{-2}). The net soil heat flux
 439 is negligible at the daily timescale (Allen et al., 1998), so the available energy is equal to the
 440 net radiation, such that

$$441 A = (1 - \alpha)S_d + \epsilon(L_d - \sigma T_*^4), \quad (68)$$

442 where σ is the Stefan-Boltzmann constant, α is the albedo and ϵ the emissivity of the surface
 443 and T_* is the surface temperature (Shuttleworth, 2012)(Shuttleworth, 2012). For this study the
 444 surface temperature is approximated by using the air temperature, T_a .

445 The air density, ρ_a (kg m^{-3}), is a function of air pressure and temperature,

$$446 \rho_a = \frac{p_s}{r T_a}, \quad (79)$$

447 where $r = 287.05 \text{ J kg}^{-1} \text{K}^{-1}$ is the gas constant of air and the air pressure used is the spatially
 448 varying air pressure calculated in Sect. 2.8.

449 The stomatal and aerodynamic resistances are strongly dependent on land cover due to
 450 differences in roughness length and physiological constraints on transpiration of different
 451 vegetation types. In addition, the albedo and emissivity are also dependent on the land cover.
 452 In order to investigate the effect of meteorology on AED, as distinct from land use effects, the
 453 PET was calculated for a single land cover type over the whole of the domain. If necessary, this
 454 can be adjusted to give an estimate of PET specific to the local land cover, for example using
 455 regression relationships (Crooks and Naden, 2007). As a standard, the Food and Agriculture

483 Organization of the United Nations (FAO) calculate reference crop evaporation for a
 484 hypothetical reference crop, which corresponds to a well-watered grass (Allen et al., 1998).
 485 Following this, the PET in the current study was calculated for a reference crop of 0.12 m
 486 height, with constant stomatal resistance, $r_s = 70.0 \text{ s m}^{-1}$, an albedo of 0.23 and emissivity of
 487 0.92 over the whole of Great Britain. This study therefore neglects the effect of land-use on
 488 evaporation, which could be investigated in future by calculating PET for different land surface
 489 types, with different coverage for each year of the dataset.

490 Following In general, aerodynamic resistance is a function of wind speed and canopy height.
 491 Following Allen et al. (1998), the aerodynamic resistance, r_a (s m^{-1}), of a reference crop of 0.12
 492 m height is a function of the 10 m wind speed

$$493 \quad r_a = \frac{278}{u_{10}}. \quad (810)$$

494 Note that, since the wind speed is likely to be biased high at sites with tall vegetation (Sect.
 495 2.10), this implies that the aerodynamic resistance is likely to be biased low, leading to an
 496 overestimate of PET. However, the estimate of PET here is for a reference crop over the whole
 497 of the dataset, and does not consider the effect of tall vegetation, so the wind speed is
 498 appropriate.

499 Thus the PET is a function of six of the meteorological variables: air temperature, specific
 500 humidity, downward LW and SW radiation, wind speed and surface air pressure.

501 To explore the role of the different meteorological variables in the AED, it is helpful to split
 502 the radiative component (the first part of the numerator in Equation 2Eq. 4) from the wind
 503 component (the second part). Formally, this is defined as follows (Doorenbos, 1977):

504 The radiative component, E_{PR} ,

$$505 \quad E_{PR} = \frac{t_d}{\lambda} \frac{\Delta A}{\Delta + \gamma \left(1 + \frac{r_s}{r_a}\right)}, \quad (911)$$

506 and the aerodynamic component, E_{PA} ,

$$507 \quad E_{PA} = \frac{t_d}{\lambda} \frac{\frac{c_p \rho_a}{r_a} (q_s - q_a)}{\Delta + \gamma \left(1 + \frac{r_s}{r_a}\right)},$$

$$508 \quad (1012)$$

509 such that $E_P = E_{PR} + E_{PA}$.

510 3.1 Potential evapotranspiration with interception (PETI)

511 When rain falls, water is intercepted by the canopy. The evaporation of this water is not
512 constrained by stomatal resistance but is subject to the same aerodynamic resistance as
513 transpiration (~~Shuttleworth, 2012~~)(Shuttleworth, 2012). At the same time, transpiration is
514 inhibited in a wet canopy. Suppression of transpiration is well observed both by comparing
515 eddy-covariance fluxes and observations of sap flow (~~Kume et al., 2006; Moors, 2012~~)(Kume
516 et al., 2006; Moors, 2012), and by observing stomatal and photosynthesis response to wetting
517 (~~Ishibashi and Terashima, 1995~~)(Ishibashi and Terashima, 1995). For plants which have at least
518 some of their stomata on the upper surface of the leaves, this can be due to water directly
519 blocking the stomata. However, in GB most plants have stomata only on the underside of the
520 leaves, so the transpiration is inhibited by other mechanisms.

521 Physically, the suppression may ~~simply~~ be due to the fact that energy is used in evaporating the
522 intercepted water, so less is available for transpiration (~~Bosveld and Bouten, 2003~~) or that the
523 increased humidity of the air, ~~due to evaporation of intercepted water, causes~~ decreases the
524 ~~stomata to close~~ (~~Lange et al., 1971~~)-evaporative demand (Bosveld and Bouten, 2003). It may
525 also be due to the presence of water on the leaf surface causing stomatal closure through
526 physiological reactions, which can be observed even when the stomata are on the underside of
527 a leaf and the water is lying on the upper side (~~Ishibashi and Terashima, 1995~~)(Ishibashi and
528 Terashima, 1995).

529 In the short term after a rain event, potential water losses due to evaporation may be
530 underestimated if only potential transpiration is calculated, and therefore overall rates
531 underestimated. As transpiration is inhibited over the wet fraction of the canopy (~~Ward and
532 Robinson, 2000~~)(Ward and Robinson, 2000)-, the PET over a grid box will be a linear
533 combination of the potential interception and potential transpiration, each weighted by the
534 fraction of the canopy that is wet or dry. This can be accounted for by introducing an
535 interception term to the calculation of PET, giving PETI. This is modelled as an interception
536 store, which is (partially) filled by rainfall, proportionally inhibiting the transpiration. As the
537 interception store dries, the relative contribution of interception is decreased and the
538 transpiration increases. ~~This~~In this dataset, this correction is applied on days with precipitation,
539 while on days without precipitation, the potential is equal to the PET defined in Eq. 24.
540 Although an unconventional definition of PET, a similar interception correction is applied to

541 the PET provided at 40 km resolution by MORECS (~~Thompson et al., 1981~~)(Thompson et al.,
542 1981) which is used widely by hydrologists.

543 This method implicitly assumes that the water is liquid, however snow lying on the canopy will
544 also inhibit transpiration, and will be depleted by melting as well as by sublimation. The rates
545 may be slower, and the snow may stay on the canopy for longer than one day. However, the
546 difference of accounting for canopy snow as distinct from canopy water will have a small effect
547 on large-scale averages, as the number of lyingdays with snow dayscover in GB is relatively
548 low, and they occur during winter when the PET is ~~very~~ small.

549 The PETI is a weighted sum of the PET, E_P , (as calculated in Eq 2.) and potential interception,
550 E_I , which is calculated by substituting zero stomatal resistance, $r_s=0$ s m⁻¹, into Eq. 24. To
551 calculate the relative proportions of interception and transpiration, it is assumed that the wet
552 fraction of the canopy is proportional to the amount of water in the interception store. The
553 interception store, S_I (kg m⁻²), decreases through the day according to an exponential dry down
554 (~~Rutter et al., 1971~~)(Rutter et al., 1971), such that

$$555 S_I(t) = S_0 e^{-\frac{E_I}{S_{tot}}t},$$

556 (113)

557 where E_I is the potential interception, S_{tot} is the total capacity of the interception store (kg m⁻²),
558 S_0 is the precipitation that is intercepted by the canopy (kg m⁻²) and t is the time (in days) since
559 a rain event. The total capacity of the interception store is calculated following Best et al.
560 (2011), such that

$$561 S_{tot} = 0.5 + 0.05\Lambda,$$

562 (1214)

563 where Λ is the leaf area index (LAI); ~~for~~. For the FAO standard grass land cover the LAI is
564 2.88 (Allen et al., 1998). The fraction of precipitation intercepted by the canopy is also found
565 ~~also~~ following Best et al. (2011), assuming that precipitation lasts for an average of 3 hours.

566 The wet fraction of the canopy, C_{wet} , is proportional to the store size, such that

$$567 C_{wet}(t) = \frac{S(t)}{S_{tot}}.$$

568 (1315)

569 The total PETI is the sum of the interception from the wet canopy and the transpiration from
570 the dry canopy,

$$571 E_{PI}(t) = E_I C_{wet}(t) + E_P(1 - C_{wet}(t)).$$

572 ~~(1416)~~

573 This is integrated over one day to find the total PETI, E_{PI} (mm d⁻¹), to be

$$574 E_{PI} = S_0 \left(1 - e^{-\frac{E_I}{S_{tot}}}\right) + E_P \left(1 - \frac{S_0}{E_I} \left(1 - e^{-\frac{E_I}{S_{tot}}}\right)\right).$$

575 ~~(1517)~~

576 This calculation is only carried out for days on which rainfall occurs. On subsequent days it is
577 assumed that the canopy has sufficiently dried out that the interception component is zero.

578 The PETI is a function of the same six meteorological variables as the PET, plus the
579 precipitation.

580 3.2 Spatial and seasonal patterns of PET and PETI

581 Both PET and PETI have a distinct gradient from low in the north-west to high in the south-
582 east, and they are both inversely proportional to the elevation (Fig. 6), reflecting the spatial
583 patterns of the meteorological variables. The PETI is 8 % higher than the PET overall but this
584 difference is larger in the north and west, where precipitation rates, and therefore interception,
585 are higher (Fig. 6). In Scotland, the higher interception and lower AED mean that this increase
586 is a larger proportion of the total, with the mean PETI being 11 % larger than the PET (in some
587 areas the difference is more than 25%). In the English lowlands the difference is smaller, at 6
588 %, but this is a more water limited region where hydrological modelling can be sensitive to
589 even relatively small adjustments to PET (Kay et al., 2013)(Kay et al., 2013).

590 The seasonal climatology of both PET and PETI follow the meteorology (Fig. 7), with high
591 values in the summer and low in the winter. Although the relative difference peaks in winter,
592 the absolute difference between PET and PETI is bimodal, with a peak in March and a smaller
593 peak in October (September in Scotland) (Fig. 7), because in winter the overall AED is low,
594 while in summer the amount of precipitation is low, so the interception correction is small. The
595 seasonal cycle of PET is driven predominantly by the radiative component, which has a much
596 stronger seasonality than the aerodynamic component (Fig. 8).

597 On a monthly or annual timescale, the ratio of PET to precipitation is an indicator of the wet-
598 or dryness of a region (~~Oldekop, 1911~~[\(Oldekop, 1911\)](#); Andréassian et al., 2016). Low values
599 of PET relative to precipitation indicate wet regions, where evaporation is demand-limited,
600 while high values indicate dry, water-limited regions. In the wetter regions (Scotland, Wales)
601 mean-monthly PET and PETI (Fig. 7) are on average lower than the mean-monthly precipitation
602 (Fig. 3) throughout the year, while in drier regions (England, English lowlands) the mean PET
603 and PETI are higher than the precipitation for much of the summer, highlighting the regions'
604 susceptibility to hydrological drought (~~Folland et al., 2015~~[\(Folland et al., 2015\)](#)).

605 **4 Decadal trends**

606 **4.1 Meteorological Variables**

607 Annual means of the meteorological variables (Fig. 9) and the PET and PETI (Fig. 10) were
608 calculated for each region. The trends in these annual means were calculated using linear
609 regression; the significance (P value) and 95% confidence intervals (CI) of the slope are
610 calculated specifically allowing for the non-zero lag-1 autocorrelation, to account for possible
611 correlations between adjacent data points (~~Zwiers and von Storch, 1995; von Storch and Zwiers,~~
612 ~~1999~~[\(Zwiers and von Storch, 1995; von Storch and Zwiers, 1999\)](#)). ~~The annual trends can be~~
613 ~~seen in Table 2.~~ In addition, seasonal means were calculated, with the four seasons defined to
614 be Winter (December-February), Spring (March-May), Summer (June-August) and Autumn
615 (September-November), and trends in these means were also found. ~~The trends can be seen in~~
616 ~~Table 2.~~

617 The trends in the annual and seasonal means for all regions are plotted in Fig. 11; trends that
618 are statistically significant at the 5% level are plotted with solid error bars, those that are not
619 significant are plotted with dashed lines. The analysis was repeated for each pixel in the 1 km
620 resolution dataset; maps of these rates of change can be seen in ~~Appendix B~~[Fig. B1](#).

621 There was a statistically significant trend in air temperature in ~~all regions (except the English~~
622 ~~Lowlands throughout the year. In the other regions the trends were statistically significant in~~
623 ~~winter), which agrees spring and autumn, and for the annual means. The trends agree~~ with recent
624 trends in the Hadley Centre Central England Temperature (HadCET) dataset (~~Parker and~~
625 ~~Horton, 2005~~[\(Parker and Horton, 2005\)](#)) and in temperature records for Scotland (~~Jenkins et~~
626 ~~al., 2008~~[\(Jenkins et al., 2008\)](#)) as well as in the CRUTEM4 dataset (~~Jones et al., 2012~~[\(Jones et](#)
627 ~~al., 2012)~~). An increase in winter precipitation in Scotland is seen in the current dataset, which

628 leads to a statistically significant increase in the annual mean precipitation of GB. However, all
629 other regions and seasons have no statistically significant trends in precipitation. Long term
630 observations show that there has been little trend in annual precipitation, but a change in
631 seasonality with wetting winters and drying summers since records began, although with little
632 change over the past 50 years (~~Jenkins et al., 2008~~)(Jenkins et al., 2008). The statistically
633 significant decline in wind speed in all regions is consistent with the results of ~~McVicar et al.~~
634 ~~(2012)~~McVicar et al. (2012) and ~~Vautard et al. (2010)~~Vautard et al. (2010), who report
635 decreasing wind speeds in the northern hemisphere over the late 20th century.

636 4.2 Potential Evapotranspiration

637 The trends of the meteorological variables are interesting in their own right. But for hydrology,
638 it is the impact that the trends have on evaporation that matters and that depends on their
639 combination, which can be expressed through PET.

640 The regional trends of annual mean PET and PETI and the radiative and aerodynamic
641 components of PET can be seen in Table 2, and the trends in the annual and seasonal means ~~of~~
642 ~~PET, PETI, and the radiative and aerodynamic components of PET~~ are plotted in Fig. 12 for all
643 regions. Maps of the trends can be seen in ~~Appendix B~~Fig. B2. The trend in the radiative
644 component of PET is positive over the whole of GB. However, the trend in the aerodynamic
645 component varies; for much of Wales, Scotland and northern England, it is not significant, or
646 is slightly negative, while in south-east England and north-west Scotland it is positive. This
647 leads to a positive trend in PET over much of GB, but no significant trend in southern Scotland
648 and northern England. There is a statistically significant increase in annual PET in all regions
649 except Wales; the GB trend ($0.021 \pm 0.021 \text{ mm d}^{-1} \text{ decade}^{-1}$) is equivalent to an increase of
650 $0.11 \pm 0.11 \text{ mm d}^{-1}$ ($8.3 \pm 8.1 \%$ of the long term mean) over the whole dataset. Increases in PETI
651 are only statistically significant in England ($0.023 \pm 0.023 \text{ mm d}^{-1} \text{ decade}^{-1}$) and English
652 lowlands ($0.028 \pm 0.025 \text{ mm d}^{-1} \text{ decade}^{-1}$), where the increases over the whole dataset are
653 $0.12 \pm 0.12 \text{ mm d}^{-1}$ ($8.0 \pm 8.0 \%$ of the long term mean) and $0.15 \pm 0.13 \text{ mm d}^{-1}$ ($9.7 \pm 8.8 \%$ of the
654 long term mean) respectively. There is a difference in trend between different seasons. In
655 winter, summer and autumn there are no statistically significant trends in PET or PETI, other
656 than the English lowlands in autumn, but the spring is markedly different, with very significant
657 trends ($P < 0.0005$) in all regions. The GB spring trends in PET ($0.043 \pm 0.019 \text{ mm d}^{-1} \text{ decade}^{-1}$)
658 and PETI ($0.038 \pm 0.018 \text{ mm d}^{-1} \text{ decade}^{-1}$) are equivalent to an increase of $0.22 \pm 0.10 \text{ mm d}^{-1}$
659 ($13.8 \pm 6.2 \%$ of the long-term spring mean) and $0.20 \pm 0.09 \text{ mm d}^{-1}$ ($11.2 \pm 5.3 \%$ of the long-term

660 spring mean) over the length of the dataset respectively. The radiative component of PET has
661 similarly significant trends in spring, while the aerodynamic component has no significant
662 trends in any season (~~Fig. 12~~), indicating that the trend in PET is due to the increasing radiative
663 component, except the English Lowlands in autumn (Fig. 12).

664 There are few studies of long-term trends in AED in the UK. MORECS provides an estimate
665 of Penman-Monteith PET with interception correction calculated directly from the 40 km
666 resolution meteorological data (~~Hough and Jones, 1997; Thompson et al., 1981~~)(Hough and
667 Jones, 1997; Thompson et al., 1981), and increases can be seen over the dataset (~~Rodda and~~
668 Marsh, 2011)(Rodda and Marsh, 2011). But as the PET and PETI in the current dataset are
669 ultimately calculated using the same meteorological data (albeit by different methods), it is not
670 unexpected that similar trends should be seen. Site-based studies suggest an increase over recent
671 decades (Burt and Shahgedanova, 1998; Crane and Hudson, 1997), but it is difficult to separate
672 climate-driven trends from local land-use trends. A global review paper (~~McVicar et al.,~~
673 2012)(McVicar et al., 2012) identified a trend of decreasing AED in the northern hemisphere,
674 driven by decreasing wind speeds, however they also reported significant local variations on
675 trends in pan evaporation, including the increasing trend observed by ~~Stanhill and Möller~~
676 (2008)Stanhill and Möller (2008) at a site in England after 1968. ~~Matsoukas et al.~~
677 (2011)Matsoukas et al. (2011) identified a statistically significant increase in PET in several
678 regions of the globe, including southern England, between 1983 and 2008, attributing it
679 predominantly to an increase in the radiative component of PET, due to global brightening.
680 However, these results were obtained using reanalysis data, which is limited in its ability to
681 capture trends in wind speed. This limitation has been documented in both northern (~~Pryor et~~
682 al., 2009)(Pryor et al., 2009) and southern (~~McVicar et al., 2008~~)(McVicar et al., 2008)
683 hemispheres.

684 Regional changes in actual evaporative losses can be estimated indirectly using regional
685 precipitation and runoff or river flow. Using a combination of observations and modelling,
686 ~~Marsh and Dixon (2012)~~Marsh and Dixon (2012) identified an increase in evaporative losses
687 in Great Britain from 1961-2011. ~~Hannaford and Buys (2012)~~Hannaford and Buys (2012) note
688 seasonal and regional differences in trends in observed river flow, suggesting that decreasing
689 spring flows in the English lowlands are indicative of increasing AED. However, changing
690 evaporative losses can also be due to changing supply through precipitation, so it is important

691 to formally attribute the trends in PET to changing climate, in order to understand changing
692 evapotranspiration.

693 **4.3 Attribution of trends in potential evapotranspiration**

694 In order to attribute changes in PET to changes in climate, the rate of change of PET, dE_p/dt
695 ($\text{mm d}^{-1} \text{ decade}^{-1}$), can be calculated as a function of the rate of change of each variable
696 ~~(Roderick et al., 2007)~~(Roderick et al., 2007),

$$697 \frac{dE_p}{dt} = \frac{dE_p}{dT_a} \frac{dT_a}{dt} + \frac{dE_p}{dq_a} \frac{dq_a}{dt} + \frac{dE_p}{du_{10}} \frac{du_{10}}{dt} + \frac{dE_p}{dL_d} \frac{dL_d}{dt} + \frac{dE_p}{dS_d} \frac{dS_d}{dt} .$$

698 ~~(1618)~~

699 Note that we exclude the surface air pressure, because this dataset uses a mean-monthly
700 climatology as the interannual variability of air pressure is negligible. The derivative of the PET
701 with respect to each of the meteorological variables can be found analytically (Appendix C).
702 The derivatives are calculated from the daily meteorological data at 1 km resolution.
703 Substituting the slopes of the linear regressions of the gridded annual means (Appendix B) for
704 the rate of change of each variable with time, and the overall time-average of the derivatives of
705 PET with respect to the meteorological variables, the contribution of each variable to the rate
706 of change of PET can be calculated at 1 km resolution. These are then averaged over the regions
707 of interest. The same can also be applied to the radiative and aerodynamic components
708 independently.

709 Note that this can also be applied to the regional means of the derivatives of PET and the trends
710 in the meteorological variables. The results are compared in Table 3 and the two approaches
711 are consistent. For the regional analysis, we also quote the 95% CI. However, for the gridded
712 values, there is such high spatial coherence that combining the 95% CI over the region results
713 in unreasonably constrained results. We therefore use the more conservative CI obtained from
714 the regional analysis. Also note that this method assumes that the rate of change of the variables
715 with respect to time is constant over the ~~whole-dataset~~seasonal cycle (and thus the product of
716 the means is equal to the mean of the products), and indeed this is how it is often applied
717 ~~(Donohue et al., 2010; Lu et al., 2016)~~(Donohue et al., 2010; Lu et al., 2016). The effect of this
718 assumption was investigated by repeating the analysis with seasonal trends and means, but this
719 makes negligible difference to the results.

720 Fig.Figure 13 shows the contribution of each meteorological variable to the rate of change of
721 the annual mean PET and to the radiative and aerodynamic components and compares the total
722 attributed trend to that obtained by linear regression. The percentage contribution is in Table 4,
723 calculated as a fraction of the fitted trend. The final ~~column~~ shows the total attributed
724 trend (i.e. the sum of the previous columns) as a percentage of the fitted trend, to demonstrate
725 the success of the attribution at recovering the fitted trends. For the PET trend and for the trend
726 in the radiative component, these values generally sum to the linear regression to within a few
727 percent. However, for the aerodynamic component, the fitted ~~trend is very small (an order of~~
728 ~~magnitude smaller than the PET and radiative component trends), and trends are~~ much smaller
729 than the statistical uncertainty. This means that there can be a large and/or negative percentage
730 difference between the attributed and fitted trends, even when the absolute difference is
731 negligible.

732 The largest overall contribution to the rate of change of PET comes from increasing air
733 temperature, which has the effect of increasing the aerodynamic component (as it makes the air
734 more able to hold water), but it decreases the radiative component (due to increasing outgoing
735 LW radiation). ~~However, the decrease due to increasing specific humidity largely cancels this~~
736 ~~increase in the aerodynamic component. Note that in this calculation we are assuming that air~~
737 ~~temperature and downward LW radiation vary independently, while in reality (and implicit in~~
738 ~~the calculation of downward LW in Sect. 2.4), downward LW radiation is also proportional to~~
739 ~~the air temperature so that increases in downward LW broadly cancel the increasing outgoing~~
740 ~~LW radiation. If we instead used net LW radiation as the independent variable, it is likely that~~
741 ~~dependence of the rate of change of the radiative component on air temperature would be~~
742 ~~reduced and compensated by the rate of change of net LW radiation.~~

743 Overall the next largest increases are caused by increasing downward SW radiation, particularly
744 in the English regions in the spring, as it increases the radiative component of PET. However,
745 in Scotland and Wales, the increasing downward LW radiation is also important.
746 Finally, Increasing specific humidity strongly decreases the PET by decreasing the aerodynamic
747 component, while the decreasing wind speed has the effect of increasing the radiative
748 component, but more strongly decreasing the aerodynamic component, so overall it tends to
749 cause a decrease in PET.

750 Since the increasing air temperature and downward LW and SW radiation have the effect of
751 increasing PET, but the increasing specific humidity and decreasing wind speed tend to

752 decrease it, then the overall trend is positive, but smaller than the trend due to air temperature
753 alone.

754 **4.4 Relative humidity**

755 The increase in PET due to increasing air temperature is largely cancelled by the decrease due
756 to increasing specific humidity. However, although we have assumed that specific humidity
757 and air temperature are independent variables, they are in fact coevolving as part of a warming
758 atmosphere. An alternative way of assessing the drivers of AED is to consider relative humidity,
759 R_h , the independent humidity variable. In this case, the PET can be recast in terms of relative
760 humidity, such that

$$761 E_P = \frac{t_d}{\lambda} \frac{\Delta A + \frac{c_p \rho_a}{r_a} q_s (1 - R_h)}{\Delta + \gamma \left(1 + \frac{r_s}{r_a}\right)}. \quad (19)$$

762 Relative humidity can be calculated from the specific humidity using

$$763 R_h = \frac{q_a}{q_s}. \quad (20)$$

764 Although in this case relative humidity is a function of air temperature, through the saturated
765 specific humidity, in reality they are often found to behave as independent variables. It has been
766 shown that there is little cancellation of the air temperature and relative humidity terms when
767 studying both historical data (Vicente-Serrano et al., 2016) and future climate projections
768 (Scheff and Frierson, 2014).

769 The relative humidity annual means, mean-monthly climatology and seasonal trends can be
770 seen in Fig. 14. We find that there is a statistically significant negative trend in relative
771 humidity, in the spring and autumn (except Wales in the autumn) but no overall negative trend
772 in winter or summer, or for the annual means. Maps of the overall mean relative humidity and
773 its trend are in Fig B3.(Jenkins et al., 2008; Dai, 2006)

774 Figure 15 shows the contribution of the different variables to the rate of change of PET with
775 this alternative formulation. The total attributed change is nearly the same as that in Fig. 13,
776 although there are small differences due to statistical uncertainty in the fits. The contribution of
777 air temperature to the rate of change is significantly reduced, so much as to be negligible. It
778 causes the radiative component to decrease as before (due to increased outgoing LW radiation)
779 and the aerodynamic component to decrease (because the rising air temperature increases the
780 saturated specific humidity). Although it is not statistically significant, there is a negative trend

781 in relative humidity, and this leads to an increase in the aerodynamic component, larger than
782 the increase due to increasing downward SW radiation.

783 **5 Discussion**

784 These high resolution datasets provide insight into the effect of the changing climate of Great
785 Britain on AED over the past five decades. There have been significant climatic trends in the
786 UK since 1961; in particular rising air temperature and specific humidity, decreasing wind
787 speed and decreasing cloudiness. Although some are positive and some negative, these
788 meteorological trends combine to give statistically significant trends in PET.

789 Wind speeds have decreased more significantly in the west than the east, and show a consistent
790 decrease across seasons. ~~Contrary to Donohue et al. (2010)~~Contrary to Donohue et al. (2010)
791 and ~~McVicar et al. (2012)~~McVicar et al. (2012), this study finds that the change in wind speed
792 of the late 20th and early 21st centuries has not had a negligibledominant influence on PET over
793 the period of study, although it has mitigated the increasing trend in PET. However, the previous
794 studies were concerned with open-water Penman evaporation, which has a simpler
795 (proportional) dependence on wind speed than the Penman-Monteith PET considered here
796 ~~(Schymanski and Or, 2015)~~(Schymanski and Or, 2015).

797 The air temperature trend in this study of 0.21 ± 0.15 K decade⁻¹ in GB is consistent with
798 observed global and regional trends ~~(Hartmann et al., 2013; Jenkins et al., 2008)~~(Hartmann et
799 al., 2013; Jenkins et al., 2008). The temperature trend is responsible for a large contribution to
800 the trend in PET, although the large negative contribution from the specific humidity (as well
801 as a small negative contribution from wind speed) means that the overall trend is smaller than
802 the temperature trend alone.

803 ~~Although the contribution is smaller than that of air temperature, the trends in LW radiation in~~
804 ~~these datasets contribute to between 15% and 28% of the trends in PET and between 27% and~~
805 ~~46% of the trends in the radiative component. Observations of LW radiation are often uncertain,~~
806 ~~but the trend in this dataset, although small, is consistent with observed trends (Wang and Liang,~~
807 ~~2009), as well as with trends in the WFDEI bias corrected reanalysis product (Weedon et al.,~~
808 ~~2014).~~

809 When the attribution is recast in terms of relative humidity, the effect of air temperature is
810 negligible, supporting the hypothesis that the temperature and specific humidity components
811 cancel because their changes are part of the same thermodynamic warming processes. However,

812 although the relative humidity does not have a statistically significant trend (except in spring
813 and for some regions in autumn), it is large enough that the negative trend in relative humidity
814 is the largest contribution to the increasing PET, followed by the downward SW radiation.

815 The trend in relative humidity is consistent with that seen in historical regional (Jenkins et al.,
816 2008) and global (Dai, 2006; Willett et al., 2014) analyses. Although not statistically significant
817 overall, it contributes to between 57 % and 68 % of the trends in PET (between 39 % and 46 %
818 or the trends in spring PET). Globally trends in relative humidity vary spatially, with mid-
819 latitudes showing a decrease and the tropics and high-latitudes showing an increase, despite an
820 overall increase in specific humidity over land particularly in the Northern Hemisphere (Dai,
821 2006; Willett et al., 2014). In these global analyses, Great Britain is in a region of transition
822 between decreasing relative humidity in Western Europe and increasing relative humidity in
823 Scandinavia, so that small decreasing trends are found, but they are not significant; this is
824 consistent with our findings. We have found the relative humidity to be decreasing significantly
825 in spring, when the downward SW is increasing. This is again consistent with reduced
826 precipitation and cloud cover due to changing weather patterns (Sutton and Dong, 2012).

827 Increasing solar radiation has been shown to increase spring and annual AED, contributing to
828 between 18% and 50% of the fitted trend in annual PET, and to between 43% and 53% of
829 the fitted trend in spring PET. Two main mechanisms can be responsible for changing solar
830 radiation – changing cloud cover and changing aerosol concentrations. Changing aerosol
831 emissions have been shown to have had a significant effect on solar radiation in the 20th century.
832 In Europe, global dimming due to increased aerosol concentrations peaked around 1980,
833 followed by global brightening as aerosol concentrations decreased (Wild, 2009)(Wild, 2009).
834 Observations of changing continental runoff and river flow in Europe over the 20th century have
835 been attributed to changing aerosol concentrations, via their effect on solar radiation, and thus
836 AED (Gedney et al., 2014)(Gedney et al., 2014).

837 In this study we use the duration of bright sunshine to calculate the solar radiation, using
838 empirical coefficients which do not vary with year, so aerosol effects are not explicitly included.
839 The coefficients used in this study to convert sunshine hours to radiation fluxes were
840 empirically derived in 1978; the derivation used data from the decade 1966-75, as this period
841 was identified to be before reductions in aerosol emissions had begun to significantly alter
842 observed solar radiation (Cowley, 1978). Despite this, the trend in SW radiation in the current
843 dataset from 1979 onwards ($1.4 \pm 1.4 \text{ W m}^{-2} \text{ decade}^{-1}$) is consistent, within uncertainties, with

875 that seen over GB in the WFDEI data ($0.9 \pm 1.1 \text{ W m}^{-2} \text{ decade}^{-1}$), which is bias-corrected to
876 observations and includes explicit aerosol effects (~~Weedon et al., 2014~~)([Weedon et al., 2014](#)).

877 It has been suggested that aerosol effects also implicitly affect sunshine duration since in
878 polluted areas, there will be fewer hours above the official 'sunshine hours' threshold of 120
879 Wm^{-2} (~~Helmes and Jaenicke, 1986~~)([Helmes and Jaenicke, 1986](#)). Several regional studies have
880 shown trends in sunshine hours that are consistent with the periods of dimming and brightening
881 across the globe (~~eg Liley, 2009; Sanchez-Lorenzo et al., 2009; Sanchez-Lorenzo et al., 2008;~~
882 ~~Stanhill and Cohen, 2005~~)([eg Liley, 2009; Sanchez-Lorenzo et al., 2009; Sanchez-Lorenzo et](#)
883 [al., 2008; Stanhill and Cohen, 2005](#)), and several have attempted to quantify the relative
884 contribution of trends in cloud cover and aerosol loading (e.g. ~~Sanchez-Lorenzo and Wild~~
885 ~~(2012)~~[Sanchez-Lorenzo and Wild \(2012\)](#) in Switzerland, see ~~Sanchez-Romero et al.~~
886 ~~(2014)~~[Sanchez-Romero et al. \(2014\)](#) for a review). Therefore, it may be that some of the
887 brightening trend seen in the current dataset is due to the implicit signal of aerosol trends in the
888 MORECS sunshine duration, although this is likely to be small compared to the effects of
889 changing cloud cover.

890 The trends in the MORECS sunshine duration used in this study are consistent with changing
891 weather patterns which may be attributed to the Atlantic Multidecadal Oscillation (AMO). The
892 AMO has been shown to cause a decrease in spring precipitation (and therefore cloud cover) in
893 northern Europe over recent decades (~~Sutton and Dong, 2012~~)([Sutton and Dong, 2012](#)), and the
894 trend in MORECS sunshine hours is dominated by an increase in the spring mean. This has also
895 been seen in Europe-wide sunshine hours data (~~Sanchez-Lorenzo et al., 2008~~)([Sanchez-](#)
896 [Lorenzo et al., 2008](#)). On the other hand, the effect of changing aerosols on sunshine hours is
897 expected to be largest in the winter ([Sanchez-Lorenzo et al., 2008](#)). However, it would not be
898 possible to directly identify either of these effects on the sunshine duration without access to
899 longer data records.

900 The inclusion of explicit aerosol effects in the coefficients of the ~~Angstrom~~[Ångström](#)-Prescott
901 equation would be expected to reduce the positive trend in AED in the first two decades of the
902 dataset, and increase it after 1980. ~~Gedney et al. (2014)~~[Gedney et al. \(2014\)](#) attribute a decrease
903 in European solar radiation of 10 W m^{-2} between the periods 1901-10 and 1974-80, and an
904 increase of 4 W m^{-2} from 1974-84 to 1990-99 to changing aerosol contributions. Applying these
905 trends to the current dataset, with a turning point at 1980, would double the overall increase in

Field Co

906 solar radiation in Great Britain, which would lead to a 40 % increase in the overall trend in
907 PET. So, if this effect were to be included, it would confirm the results found in this paper.

908 (Willett et al., 2014; Dai, 2006; Sutton and Dong, 2012)Although the contribution is generally
909 smaller (except in Scotland), the trends in LW radiation in these datasets contribute to between
910 15% and 28% of the trends in PET and between 27% and 46% of the trends in the radiative
911 component. In Scotland the downward LW radiation is the dominant driver of changing PET.
912 Observations of LW radiation are often uncertain, but the trend in this dataset, although small,
913 is consistent with observed trends (Wang and Liang, 2009), as well as with trends in the WFDEI
914 bias-corrected reanalysis product (Weedon et al., 2014).

915 Trends in temperature and cloud cover in the UK are expected to continue into the coming
916 decades, with precipitation expected to increase in the winter but decrease in the summer
917 ~~(Murphy et al., 2009)~~(Murphy et al., 2009). Therefore it is likely that AED will increase,
918 increasing water stress in the summer when precipitation is lower and potentially affecting
919 water resources, agriculture and biodiversity. This has been demonstrated for southern England
920 and Wales by ~~Rudd and Kay (2015)~~Rudd and Kay (2015), who calculated present and future
921 PET using high-resolution RCM output and ~~include~~included the effects of CO₂ on stomatal
922 opening.

923 The current study is concerned only with the effects of changing climate on AED and has
924 assumed a constant bulk canopy resistance throughout. However, plants are expected to react
925 to increased CO₂ in the atmosphere by closing stomata and limiting the exchange of gases,
926 including water ~~(Kruijt et al., 2008)~~(Kruijt et al., 2008), and observed changes in runoff have
927 been attributed to this effect ~~(Gedney et al., 2006; Gedney et al., 2014)~~(Gedney et al., 2006;
928 Gedney et al., 2014). It is possible that the resulting change of canopy resistance could partially
929 offset the increased atmospheric demand ~~(Rudd and Kay, 2015)~~(Rudd and Kay, 2015) and may
930 impact runoff ~~(Gedney et al., 2006; Prudhomme et al., 2014)~~(Gedney et al., 2006; Prudhomme
931 et al., 2014), but further studies would be required to quantify this.

932 **6 Conclusion**

933 This paper has presented a unique, high-resolution, observation-based dataset of meteorological
934 variables and AED in Great Britain since 1961. Key trends in the meteorological variables are
935 (i) increasing air temperature and specific humidity, consistent with global temperature trends;
936 (ii) increasing solar radiation, particularly in the spring, consistent with changes in aerosol
937 emissions and weather patterns in recent decades; (iii) decreasing wind speed, consistent with

938 observations of global stilling; and (iv) increasing precipitation, driven by increasing winter
939 precipitation in Scotland. The meteorological variables were used to evaluate AED in Great
940 Britain via calculation of PET and PETI. It has been demonstrated that including the
941 interception component in the calculation of PETI gives a mean estimate that is overall 8%
942 larger than PET alone, with strong seasonality and spatial variation of the difference. PET was
943 found to be increasing by $0.021 \pm 0.021 \text{ mm d}^{-1} \text{ decade}^{-1}$ in GB over the study period. With the
944 interception component included, the trend in PETI is weaker, $(0.019 \pm 0.020 \text{ mm d}^{-1})$, and over
945 GB is not significant at the 5% level. The trend in PET was analytically attributed to the trends
946 in the meteorological variables, and it was found that the dominant effect was that increasing
947 air temperature was driving increasing PET. ~~This, with smaller increases from increased~~
948 ~~downward SW and LW radiation. However, the effect of temperature~~ is largely compensated
949 by the associated increase in specific humidity, ~~as the water cycle is intensified under climate~~
950 ~~change and by while~~ decreasing wind speed. ~~However, tended to decrease~~ the PET. ~~When the~~
951 ~~attribution was recast in terms of relative humidity, temperature was found to have a negligible~~
952 ~~effect on the trend in PET, while the decreasing relative humidity caused PET to increase, at a~~
953 ~~similar rate to the downward SW radiation (and downward LW radiation in Scotland). The~~
954 ~~increase in PET due to these variables is mitigated by the observed northern hemisphere wind~~
955 ~~stilling, which causes a decrease in PET, however, the overall trend in PET is also driven by~~
956 ~~increasing solar radiation, particularly in the spring~~ positive over the period of study.

957 In addition to providing meteorological data and estimates of AED for analysis, the
958 meteorological variables provided are sufficient to run LSMs and hydrological models. The
959 high spatial (1 km) and temporal (daily) resolution will allow this dataset to be used to study
960 the effects of climate on physical and biological systems at a range of scales, from local to
961 national.

962 **Data Access**

963 The data can be downloaded from the Environmental Information Platform at the Centre for
964 Ecology & Hydrology. The meteorological variables (CHES-met) can be found at
965 <https://catalogue.ceh.ac.uk/documents/80887755-1426-4dab-a4a6-250919d5020c>,
966 while the PET and PETI (CHES-PE) can be accessed at
967 <https://catalogue.ceh.ac.uk/documents/d329f4d6-95ba-4134-b77a-a377e0755653>.

968 **Author contribution**

969 EB, JF and DBC designed the study. JF, ACR, DBC and ELR developed code to create
970 meteorological data. ELR created the PET and PETI. ELR and EB analysed trends. ELR, EB,
971 ACR and DBC wrote the manuscript.

972 **Acknowledgements**

973 The meteorological variables presented are based largely on GB meteorological data under
974 licence from the Met Office, and those organisations contributing to this national dataset
975 (including the Met Office, Environment Agency, Scottish Environment Protection Agency
976 (SEPA) and Natural Resources Wales) are gratefully acknowledged. The CRU TS 3.21 daily
977 temperature range data were created by the University of East Anglia Climatic Research Unit,
978 and the WFD air pressure data were created as part of the EU FP6 project WATCH (Contract
979 036946). Collection of flux data was funded by EU FP4 EuroFlux (Griffin Forest); EU FP5
980 CarboEuroFlux (Griffin Forest); EU FP5 GreenGrass (Easter Bush); EU FP6 CarboEuropeIP
981 (Alice Holt , Griffin Forest, Auchencorth Moss, Easter Bush); EU FP6 IMECC (Griffin
982 Forest); the Forestry Commission (Alice Holt); the Natural Environment Research Council,
983 UK (Auchencorth Moss, Easter Bush).

984 ~~Thanks to Nicola Gedney and Graham Weedon for useful discussions.~~

985 Fig. 1 and panels a) and b) of Fig. 6 were produced with the python implementation of the
986 cubehelix colour scheme (Green, 2011).

987 Thanks to Nicola Gedney and Graham Weedon for useful discussions.

988 Thanks to three anonymous reviewers, who provided insightful and helpful comments.

989 This work was partially funded by the Natural Environment Research Council in the
990 Changing Water Cycle programme: NERC Reference: NE/I006087/1.

991

992 Appendix A: Data validation

993 Meteorological data were downloaded from the European Fluxes Database Cluster
994 (<http://gaia.agraria.unitus.it>) for four sites positioned around Great Britain. Two were woodland
995 sites (Alice Holt (~~Wilkinson et al., 2012; Heinemeyer et al., 2012~~)([Wilkinson et al., 2012;](#)
996 [Heinemeyer et al., 2012](#)) and Griffin Forest (Clement, 2003)), while two had grass and crop
997 cover (Auchencorth Moss (Billett et al., 2004) and Easter Bush (~~Gilmanov et al., 2007;~~
998 ~~Soussana et al., 2007~~)([Gilmanov et al., 2007; Soussana et al., 2007](#))). Table A1 gives details of
999 the data used. The data are provided as half-hourly measurements, which were used to create
1000 daily means, where full daily data coverage was available. The daily means of the observed
1001 data were compared to the daily data from the grid square containing the site and the Pearson
1002 correlation (r^2), mean bias and root mean square error (RMSE) were calculated. For each site,
1003 monthly means were calculated where the full month had available data, then a climatology
1004 calculated from available months. The same values were calculated from the relevant grid
1005 squares, using only time periods for which observed data were available.

1006 Fig. A1 shows the comparison of the data set downward SW radiation against daily mean air
1007 temperature observed at the four sites. Fig. A2 shows the mean-monthly climatology of the
1008 daily values. The observed values of the mixing ratio of water vapour in air were compared
1009 with values calculated from the meteorological dataset, using the equation

$$1010 \quad r_w = q_a \left(\frac{m_a}{m_w} \right) \quad \text{---} \quad \text{(A1)}$$

1011 where m_a is the molecular mass of dry air and m_w is the molecular mass of water. The
1012 comparisons are shown in Figs. A3 and A4.

1013 Table A2 shows the r^2 , mean bias and RMSE for each of the variables included in the validation
1014 exercise. The correlations indicate a good relationship between the dataset variables and the
1015 independent observations at the sites, while the mean-monthly climatologies demonstrate that
1016 the data represent the seasonal cycle well. [The data set downward SW in Auchencorth Moss is](#)
1017 [biased high compared to the observations, while the wind speed is biased high at two sites.](#)

1018 Appendix B: Trend maps

1019 Fig. B1 shows the rate of change of each of the meteorological variables at the 1 km resolution,
1020 while Fig. B2 shows the rate of change of the PET, PETI, and the two components of PET at

1040 the same resolution. This shows that the regional trends are consistent with spatial variation and
 1041 are not dominated by individual extreme points.

1042 **Appendix C: Derivatives of PET**

1043 The wind speed affects the PET through the aerodynamic resistance. The derivative with respect
 1044 to wind speed is

$$1045 \quad \frac{\partial E_P}{\partial u_{10}} = \frac{(\Delta + \gamma)E_{PA} - \gamma \frac{r_s}{r_a} E_{PR}}{u_{10} \left(\Delta + \gamma \left(1 + \frac{r_s}{r_a} \right) \right)}. \quad (C1)$$

1046 The downward LW and SW radiation affect PET through the net radiation, and the derivatives
 1047 are

$$1048 \quad \frac{\partial E_P}{\partial L_d} = E_{PR} \frac{\epsilon}{R_n} \quad (C2)$$

$$1049 \quad \frac{\partial E_P}{\partial S_d} = E_{PR} \frac{(1 - \alpha)}{R_n}. \quad (C3)$$

1050 The derivative of PET with respect to specific humidity is

$$1051 \quad \frac{\partial E_P}{\partial q_a} = \frac{E_{PA}}{q_a - q_s}. \quad (C4)$$

1052 The air temperature affects PET through the saturated specific humidity and its derivative, the
 1053 net radiation and the air density, so that the derivative of PET with respect to air temperature is

$$1054 \quad \frac{\partial E_P}{\partial T_a} = E_{PR} \left(\frac{\gamma \left(1 + \frac{r_s}{r_a} \right)}{T_a^2 \left(\Delta + \gamma \left(1 + \frac{r_s}{r_a} \right) \right)} \left[T_{sp} \left(\frac{\sum_{i=1}^4 i a_i T_r^{i-1}}{\sum_{i=1}^4 i a_i T_r^{i-1}} + \frac{\sum_{i=1}^4 i a_i T_r^{i-1}}{\sum_{i=1}^4 i(i-1) a_i T_r^{i-2}} + \frac{2(1-\epsilon) \sum_{i=1}^4 i a_i T_r^{i-1} q_s}{\epsilon} \right) - \right. \right. \\
 1055 \quad \left. \left. \frac{2T_a}{\epsilon} \right] - \frac{4\epsilon\sigma T_a^3}{R_n} \right) + E_{PA} \left(\frac{\Delta}{q_s - q_a} - \frac{1}{T_a} - \frac{\Delta}{T_a^2 \left(\Delta + \gamma \left(1 + \frac{r_s}{r_a} \right) \right)} \left[T_{sp} \left(\frac{\sum_{i=1}^4 i a_i T_r^{i-1}}{\sum_{i=1}^4 i a_i T_r^{i-1}} + \frac{\sum_{i=1}^4 i a_i T_r^{i-1}}{\sum_{i=1}^4 i(i-1) a_i T_r^{i-2}} + \right. \right. \right. \\
 1056 \quad \left. \left. \frac{2(1-\epsilon) \sum_{i=1}^4 i a_i T_r^{i-1} q_s}{\epsilon} \right) - \frac{2T_a}{\epsilon} \right] \right) \left[\left(1 - \right. \right. \\
 1057 \quad \left. \left. \frac{\Delta}{\Delta + \gamma \left(1 + \frac{r_s}{r_a} \right)} \right) \left(\frac{T_{sp} \sum_{i=1}^4 i(i-1) a_i T_r^{i-2}}{T_a^2 \sum_{i=1}^4 i a_i T_r^{i-1}} + \Delta \frac{p_* + (1-\epsilon)e_s}{p_* q_s} - \frac{2}{T_a} \right) - \frac{4\epsilon\sigma T_a^3}{R_n} \right] + E_{PA} \left[\frac{\Delta}{q_s - q_a} - \frac{1}{T_a} - \right. \\
 1058 \quad \left. \frac{\Delta}{\Delta + \gamma \left(1 + \frac{r_s}{r_a} \right)} \left(\frac{T_{sp} \sum_{i=1}^4 i(i-1) a_i T_r^{i-2}}{T_a^2 \sum_{i=1}^4 i a_i T_r^{i-1}} + \Delta \frac{p_* + (1-\epsilon)e_s}{p_* q_s} - \frac{2}{T_a} \right) \right]. \quad (C5)$$

Formatted

1059 When calculating the attribution with relative humidity as the dependent variable, the derivative
 1060 of PET with respect to relative humidity is

$$1061 \frac{\partial E_P}{\partial R_h} = \frac{E_{PA}}{R_h - 1}, \quad (C6)$$

1062 and the derivative of PET with respect to air temperature is

$$1063 \frac{\partial E_P}{\partial T_a} = E_{PR} \left[\left(1 - \frac{\Delta}{\Delta + \gamma \left(1 + \frac{r_s}{r_a} \right)} \right) \left(\frac{T_{sp}}{T_a^2} \frac{\sum_{i=1}^4 i(i-1) a_i T_r^{i-2}}{\sum_{i=1}^4 i a_i T_r^{i-1}} + \Delta \frac{p_* + (1-\varepsilon) e_s}{p_* q_s} - \frac{2}{T_a} \right) - \frac{4\epsilon\sigma T_a^3}{R_n} \right] +$$

$$1064 E_{PA} \left[\frac{\Delta}{q_s} - \frac{1}{T_a} - \frac{\Delta}{\Delta + \gamma \left(1 + \frac{r_s}{r_a} \right)} \left(\frac{T_{sp}}{T_a^2} \frac{\sum_{i=1}^4 i(i-1) a_i T_r^{i-2}}{\sum_{i=1}^4 i a_i T_r^{i-1}} + \Delta \frac{p_* + (1-\varepsilon) e_s}{p_* q_s} - \frac{2}{T_a} \right) \right]. \quad (C7)$$

1065 The difference between Eq. C7 and Eq. C5 is the factor of Δ/q_s instead of $\Delta/(q_s - q_a)$ in the
 1066 second bracket.

1067 7 References

- 1068 Allen, R. G., Pereira, L. S., Raes, D., and Smith, M.: Crop evapotranspiration - Guidelines for
 1069 computing crop water requirements, Food and Agriculture Organization of the United
 1070 Nations, Rome, Italy, FAO Irrigation and Drainage Paper, 1998.
- 1071 Allen, R. G., Trezza, R., and Tasumi, M.: Analytical integrated functions for daily solar
 1072 radiation on slopes, *Agr Forest Meteorol*, 139, 55-73, doi:10.1016/j.agrformet.2006.05.012,
 1073 2006.
- 1074 Andréassian, V., Mander, Ü., and Pae, T.: The Budyko hypothesis before Budyko: The
 1075 hydrological legacy of Evald Oldekop, *Journal of Hydrology*, 535, 386-391,
 1076 <http://dx.doi.org/10.1016/j.jhydrol.2016.02.002>, <http://dx.doi.org/10.1016/j.jhydrol.2016.02.002>,
 1077 2, 2016.
- 1078 Ångström, A.: A study of the radiation of the atmosphere, *Smithsonian Miscellaneous*
 1079 *Collections*, 65, 159-161, 1918.
- 1080 Azizzadeh, M., and Javan, K.: Analyzing Trends in Reference Evapotranspiration in
 1081 Northwest Part of Iran, *Journal of Ecological Engineering*, 16, 1-12,
 1082 10.12911/22998993/1853, 2015.
- 1083 Baldocchi, D., Valentini, R., Running, S., Oechel, W., and Dahlman, R.: Strategies for
 1084 measuring and modelling carbon dioxide and water vapour fluxes over terrestrial ecosystems,
 1085 *Global Change Biology*, 2, 159-168, doi:10.1111/j.1365-2486.1996.tb00069.x, 1996.
- 1086 Bell, V. A., Kay, A. L., Jones, R. G., Moore, R. J., and Reynard, N. S.: Use of soil data in a
 1087 grid-based hydrological model to estimate spatial variation in changing flood risk across the
 1088 UK, *Journal of Hydrology*, 377, 335-350, doi:10.1016/j.jhydrol.2009.08.031, 2009.
- 1089 Bell, V. A., Gedney, N., Kay, A. L., Smith, R. N. B., Jones, R. G., and Moore, R. J.:
 1090 Estimating Potential Evaporation from Vegetated Surfaces for Water Management Impact
 1091 Assessments Using Climate Model Output, *Journal of Hydrometeorology*, 12, 1127-1136,
 1092 doi:10.1175/2011jhm1379.1, 2011.

1093 Bell, V. A., Kay, A. L., Cole, S. J., Jones, R. G., Moore, R. J., and Reynard, N. S.: How might
1094 climate change affect river flows across the Thames Basin? An area-wide analysis using the
1095 UKCP09 Regional Climate Model ensemble, *Journal of Hydrology*, 442-443, 89-104,
1096 doi:10.1016/j.jhydrol.2012.04.001, 2012.

1097 Bellamy, P. H., Loveland, P. J., Bradley, R. I., Lark, R. M., and Kirk, G. J.: Carbon losses
1098 from all soils across England and Wales 1978-2003, *Nature*, 437, 245-248,
1099 doi:10.1038/nature04038, 2005.

1100 Berry, P. M., Dawson, T. P., Harrison, P. A., and Pearson, R. G.: Modelling potential impacts
1101 of climate change on the bioclimatic envelope of species in Britain and Ireland, *Global Ecol*
1102 *Biogeogr*, 11, 453-462, doi:10.1046/j.1466-822x.2002.00304.x, 2002.

1103 Best, M. J., Pryor, M., Clark, D. B., Rooney, G. G., Essery, R. L. H., Ménard, C. B., Edwards,
1104 J. M., Hendry, M. A., Porson, A., Gedney, N., Mercado, L. M., Sitch, S., Blyth, E., Boucher,
1105 O., Cox, P. M., Grimmond, C. S. B., and Harding, R. J.: The Joint UK Land Environment
1106 Simulator (JULES), model description – Part 1: Energy and water fluxes, *Geoscientific Model*
1107 *Development*, 4, 677-699, doi:10.5194/gmd-4-677-2011, 2011.

1108 Billett, M. F., Palmer, S. M., Hope, D., Deacon, C., Storeton-West, R., Hargreaves, K. J.,
1109 Flechard, C., and Fowler, D.: Linking land-atmosphere-stream carbon fluxes in a lowland
1110 peatland system, *Global Biogeochemical Cycles*, 18, n/a-n/a, 10.1029/2003gb002058, 2004.

1111 Bosveld, F. C., and Bouten, W.: Evaluating a Model of Evaporation and Transpiration with
1112 Observations in a Partially Wet Douglas-Fir Forest, *Boundary-Layer Meteorology*, 108, 365-
1113 396, 10.1023/a:1024148707239, 2003.

1114 Burch, S. F., and Ravenscroft, F.: Computer modelling of the UK wind energy resource: Final
1115 overview report., AEA Industrial Technology, 1992.

1116 Burt, T. P., and Shahgedanova, M.: An historical record of evaporation losses since 1815
1117 calculated using long-term observations from the Radcliffe Meteorological Station, Oxford,
1118 England, *Journal of Hydrology*, 205, 101-111, doi:10.1016/S0022-1694(97)00143-1, 1998.

1119 Clark, D. B., Mercado, L. M., Sitch, S., Jones, C. D., Gedney, N., Best, M. J., Pryor, M.,
1120 Rooney, G. G., Essery, R. L. H., Blyth, E., Boucher, O., Harding, R. J., Huntingford, C., and
1121 Cox, P. M.: The Joint UK Land Environment Simulator (JULES), model description – Part 2:
1122 Carbon fluxes and vegetation dynamics, *Geoscientific Model Development*, 4, 701-722,
1123 doi:10.5194/gmd-4-701-2011, 2011.

1124 Clement, R. M., J.B.; Jarvis, P.G.: Net carbon productivity of Sitka Spruce forest in Scotland,
1125 *Scottish Forestry*, 5-10, 2003.

1126 Cowley, J. P.: The distribution over Great Britain of global solar irradiation on a horizontal
1127 surface, *Meteorological Magazine*, 107, 357-372, 1978.

1128 Crane, S. B., and Hudson, J. A.: The impact of site factors and climate variability on the
1129 calculation of potential evaporation at Moel Cynnedd, Plynlimon, *Hydrol. Earth Syst. Sci.*, 1,
1130 429-445, doi:10.5194/hess-1-429-1997, 1997.

1131 Crooks, S. M., and Naden, P. S.: CLASSIC: a semi-distributed rainfall-runoff modelling
1132 system, *Hydrol. Earth Syst. Sci.*, 11, 516-531, doi:10.5194/hess-11-516-2007, 2007.

1133 Crooks, S. M., and Kay, A. L.: Simulation of river flow in the Thames over 120 years:
1134 Evidence of change in rainfall-runoff response?, *Journal of Hydrology: Regional Studies*, 4,
1135 Part B, 172-195, doi:10.1016/j.ejrh.2015.05.014, 2015.

- 1136 [Dai, A.: Recent Climatology, Variability, and Trends in Global Surface Humidity, *Journal of*](#)
1137 [Climate, 19, 3589-3606, doi:10.1175/JCLI3816.1, 2006.](#)
- 1138 Dilley, A. C., and O'Brien, D. M.: Estimating downward clear sky long-wave irradiance at the
1139 surface from screen temperature and precipitable water, *Quarterly Journal of the Royal*
1140 *Meteorological Society*, 124, 1391-1401, doi:10.1256/Smsqj.54902, 1998.
- 1141 Donohue, R. J., McVicar, T. R., and Roderick, M. L.: Assessing the ability of potential
1142 evaporation formulations to capture the dynamics in evaporative demand within a changing
1143 climate, *Journal of Hydrology*, 386, 186-197, doi:10.1016/j.jhydrol.2010.03.020, 2010.
- 1144 Doorenbos, J. a. P., W. O.: Crop water requirements. FAO Irrigation and Drainage Paper 24.,
1145 FAO, Rome, Italy, 1977.
- 1146 Evans, N., Baierl, A., Semenov, M. A., Gladders, P., and Fitt, B. D.: Range and severity of a
1147 plant disease increased by global warming, *Journal of the Royal Society, Interface / the Royal*
1148 *Society*, 5, 525-531, doi:10.1098/rsif.2007.1136, 2008.
- 1149 FAO/IIASA/ISRIC/ISS-CAS/JRC: Harmonized World Soil Database, 2012.
- 1150 [Field, M.: The meteorological office rainfall and evaporation calculation system —](#)
1151 [MORECS, *Agricultural Water Management*, 6, 297-306, \[http://dx.doi.org/10.1016/0378-\]\(http://dx.doi.org/10.1016/0378-3774\(83\)90017-3\)](#)
1152 [3774\(83\)90017-3, 1983.](#)
- 1153 Fleig, A. K., Tallaksen, L. M., James, P., Hisdal, H., and Stahl, K.: Attribution of European
1154 precipitation and temperature trends to changes in synoptic circulation, *Hydrology and Earth*
1155 *System Sciences*, 19, 3093-3107, 10.5194/hess-19-3093-2015, 2015.
- 1156 Folland, C. K., Hannaford, J., Bloomfield, J. P., Kendon, M., Svensson, C., Marchant, B. P.,
1157 Prior, J., and Wallace, E.: Multi-annual droughts in the English Lowlands: a review of their
1158 characteristics and climate drivers in the winter half-year, *Hydrology and Earth System*
1159 *Sciences*, 19, 2353-2375, doi:10.5194/hess-19-2353-2015, 2015.
- 1160 Gedney, N., Cox, P. M., Betts, R. A., Boucher, O., Huntingford, C., and Stott, P. A.:
1161 Detection of a direct carbon dioxide effect in continental river runoff records, *Nature*, 439,
1162 835-838, doi:10.1038/nature04504, 2006.
- 1163 Gedney, N., Huntingford, C., Weedon, G. P., Bellouin, N., Boucher, O., and Cox, P. M.:
1164 Detection of solar dimming and brightening effects on Northern Hemisphere river flow,
1165 *Nature Geoscience*, 7, 796-800, doi:10.1038/ngeo2263, 2014.
- 1166 Gill, A. E.: *Atmosphere-ocean Dynamics*, Academic Press, San Diego, California, USA,
1167 1982.
- 1168 Gilmanov, T. G., Soussana, J. F., Aires, L., Allard, V., Ammann, C., Balzarolo, M., Barcza,
1169 Z., Bernhofer, C., Campbell, C. L., Cernusca, A., Cescatti, A., Clifton-Brown, J., Dirks, B. O.
1170 M., Dore, S., Eugster, W., Fuhrer, J., Gimeno, C., Gruenwald, T., Haszpra, L., Hensen, A.,
1171 Ibrom, A., Jacobs, A. F. G., Jones, M. B., Lanigan, G., Laurila, T., Lohila, A., G.Manca,
1172 Marcolla, B., Nagy, Z., Pilegaard, K., Pinter, K., Pio, C., Raschi, A., Rogiers, N., Sanz, M. J.,
1173 Stefani, P., Sutton, M., Tuba, Z., Valentini, R., Williams, M. L., and Wohlfahrt, G.:
1174 Partitioning European grassland net ecosystem CO₂ exchange into gross primary productivity
1175 and ecosystem respiration using light response function analysis, *Agriculture, Ecosystems &*
1176 *Environment*, 121, 93-120, 10.1016/j.agee.2006.12.008, 2007.
- 1177 Gocic, M., and Trajkovic, S.: Analysis of trends in reference evapotranspiration data in a
1178 humid climate, *Hydrological Sciences Journal*, 59, 165-180, 10.1080/02626667.2013.798659,
1179 2013.

- 1180 Gold, C. M.: Surface interpolation, spatial adjacency and GIS, in: Three Dimensional
1181 Applications in Geographical Information Systems, edited by: Raper, J., Taylor and Francis,
1182 London, 1989.
- 1183 [Green, D. A.: A colour scheme for the display of astronomical intensity images, Bulletin of](#)
1184 [the Astronomical Society of India, 39, 2011.](#)
- 1185 Haddeland, I., Clark, D. B., Franssen, W., Ludwig, F., Voß, F., Arnell, N. W., Bertrand, N.,
1186 Best, M., Folwell, S., Gerten, D., Gomes, S., Gosling, S. N., Hagemann, S., Hanasaki, N.,
1187 Harding, R., Heinke, J., Kabat, P., Koirala, S., Oki, T., Polcher, J., Stacke, T., Viterbo, P.,
1188 Weedon, G. P., and Yeh, P.: Multimodel Estimate of the Global Terrestrial Water Balance:
1189 Setup and First Results, *Journal of Hydrometeorology*, 12, 869-884, 10.1175/2011jhm1324.1,
1190 2011.
- 1191 Hannaford, J., and Buys, G.: Trends in seasonal river flow regimes in the UK, *Journal of*
1192 *Hydrology*, 475, 158-174, doi:10.1016/j.jhydrol.2012.09.044, 2012.
- 1193 Hannaford, J.: Climate-driven changes in UK river flows: A review of the evidence, *Progress*
1194 *in Physical Geography*, 39, 29-48, doi:10.1177/0309133314536755, 2015.
- 1195 Harris, I., Jones, P. D., Osborn, T. J., and Lister, D. H.: Updated high-resolution grids of
1196 monthly climatic observations - the CRU TS3.10 Dataset, *International Journal of*
1197 *Climatology*, 34, 623-642, doi:10.1002/Joc.3711, 2014.
- 1198 Hartmann, D. L., Klein Tank, A. M. G., Rusticucci, M., Alexander, L. V., Brönnimann, S.,
1199 Charabi, Y., Dentener, F. J., Dlugokencky, E. J., Easterling, D. R., Kaplan, A., Soden, B. J.,
1200 Thorne, P. W., Wild, M., and Zhai, P. M.: Observations: Atmosphere and Surface, in: *Climate*
1201 *Change 2013: The Physical Science Basis. Contribution of Working Group I to the Fifth*
1202 *Assessment Report of the Intergovernmental Panel on Climate Change*, edited by: Stocker, T.
1203 F., Qin, D., Plattner, G.-K., Tignor, M., Allen, S. K., Boschung, J., Nauels, A., Xia, Y., Bex,
1204 V., and Midgley, P. M., Cambridge University Press, Cambridge, United Kingdom and New
1205 York, NY, USA, 159–254, 2013.
- 1206 Haslinger, K., and Bartsch, A.: Creating long-term gridded fields of reference
1207 evapotranspiration in Alpine terrain based on a recalibrated Hargreaves method, *Hydrology*
1208 *and Earth System Sciences*, 20, 1211-1223, 10.5194/hess-20-1211-2016, 2016.
- 1209 Heinemeyer, A., Wilkinson, M., Vargas, R., Subke, J. A., Casella, E., Morison, J. I. L., and
1210 Ineson, P.: Exploring the "overflow tap" theory: linking forest soil CO₂ fluxes
1211 and individual mycorrhizosphere components to photosynthesis, *Biogeosciences*, 9, 79-95,
1212 10.5194/bg-9-79-2012, 2012.
- 1213 Helmes, L., and Jaenicke, R.: Atmospheric turbidity determined from sunshine records,
1214 *Journal of Aerosol Science*, 17, 261-263, doi:10.1016/0021-8502(86)90080-7, 1986.
- 1215 Hickling, R., Roy, D. B., Hill, J. K., Fox, R., and Thomas, C. D.: The distributions of a wide
1216 range of taxonomic groups are expanding polewards, *Global Change Biology*, 12, 450-455,
1217 doi:10.1111/j.1365-2486.2006.01116.x, 2006.
- 1218 Horn, B. K. P.: Hill Shading and the Reflectance Map, *P Ieee*, 69, 14-47,
1219 doi:10.1109/Proc.1981.11918, 1981.
- 1220 Hosseinzadeh Talaei, P., Shifteh Some'e, B., and Sobhan Ardakani, S.: Time trend and
1221 change point of reference evapotranspiration over Iran, *Theoretical and Applied Climatology*,
1222 116, 639-647, 10.1007/s00704-013-0978-x, 2013.

- 1223 Hough, M. N., and Jones, R. J. A.: The United Kingdom Meteorological Office rainfall and
 1224 evaporation calculation system: MORECS version 2.0-an overview, *Hydrology and Earth*
 1225 *System Sciences*, 1, 227-239, doi:10.5194/hess-1-227-1997, 1997.
- 1226 IPCC: Climate Change 2013: The Physical Science Basis. Contribution of Working Group I
 1227 to the Fifth Assessment Report of the Intergovernmental Panel on Climate Change,
 1228 Cambridge University Press, Cambridge, United Kingdom and New York, NY, USA, 1535
 1229 pp., 2013.
- 1230 IPCC: Climate Change 2014: Impacts, Adaptation, and Vulnerability. Part A: Global and
 1231 Sectoral Aspects. Contribution of Working Group II to the Fifth Assessment Report of the
 1232 Intergovernmental Panel on Climate Change [Field, C.B., V.R. Barros, D.J. Dokken, K.J.
 1233 Mach, M.D. Mastrandrea, T.E. Bilir, M. Chatterjee, K.L. Ebi, Y.O. Estrada, R.C. Genova, B.
 1234 Girma, E.S. Kissel, A.N. Levy, S. MacCracken, P.R. Mastrandrea, and L.L. White (eds.)],
 1235 Cambridge University Press, Cambridge, United Kingdom and New York, NY, USA, 1132
 1236 pp., 2014a.
- 1237 IPCC: Climate Change 2014: Impacts, Adaptation, and Vulnerability. Part B: Regional
 1238 Aspects. Contribution of Working Group II to the Fifth Assessment Report of the
 1239 Intergovernmental Panel on Climate Change [Barros, V.R., C.B. Field, D.J. Dokken, M.D.
 1240 Mastrandrea, K.J. Mach, T.E. Bilir, M. Chatterjee, K.L. Ebi, Y.O. Estrada, R.C. Genova, B.
 1241 Girma, E.S. Kissel, A.N. Levy, S. MacCracken, P.R. Mastrandrea, and L.L. White (eds.)],
 1242 Cambridge University Press, Cambridge, United Kingdom and New York, NY, USA, 688
 1243 pp., 2014b.
- 1244 Iqbal, M.: An introduction to solar radiation, Academic Press, London, 1983.
- 1245 Ishibashi, M., and Terashima, I.: Effects of continuous leaf wetness on photosynthesis:
 1246 adverse aspects of rainfall, *Plant, Cell & Environment*, 18, 431-438, 10.1111/j.1365-
 1247 3040.1995.tb00377.x, 1995.
- 1248 Jenkins, G. J., Perry, M. C., and Prior, M. J.: The climate of the United Kingdom and recent
 1249 trends, Met Office Hadley Centre, Exeter, UK, 2008.
- 1250 Jhajharia, D., Dinpashoh, Y., Kahya, E., Singh, V. P., and Fakheri-Fard, A.: Trends in
 1251 reference evapotranspiration in the humid region of northeast India, *Hydrological Processes*,
 1252 26, 421-435, 10.1002/hyp.8140, 2012.
- 1253 Jones, P. D., Lister, D. H., Osborn, T. J., Harpham, C., Salmon, M., and Morice, C. P.:
 1254 Hemispheric and large-scale land-surface air temperature variations: An extensive revision
 1255 and an update to 2010, *Journal of Geophysical Research: Atmospheres*, 117, n/a-n/a,
 1256 doi:10.1029/2011JD017139, 2012.
- 1257 Jones, P. D., and Harris, I.: CRU TS3.21: Climatic Research Unit (CRU) Time-Series (TS)
 1258 Version 3.21 of High Resolution Gridded Data of Month-by-month Variation in Climate (Jan.
 1259 1901- Dec. 2012). University of East Anglia Climatic Research Unit,
 1260 doi:10.5285/D0E1585D-3417-485F-87AE-4FCECF10A992, 2013.
- 1261 Kay, A. L., Bell, V. A., Blyth, E. M., Crooks, S. M., Davies, H. N., and Reynard, N. S.: A
 1262 hydrological perspective on evaporation: historical trends and future projections in Britain,
 1263 *Journal of Water and Climate Change*, 4, 193, doi:10.2166/wcc.2013.014, 2013.
- 1264 Kay, A. L., Rudd, A. C., Davies, H. N., Kendon, E. J., and Jones, R. G.: Use of very high
 1265 resolution climate model data for hydrological modelling: baseline performance and future
 1266 flood changes, *Climatic Change*, doi:10.1007/s10584-015-1455-6, 2015.

- 1267 Keller, V. D. J., Tanguy, M., Prosdocimi, I., Terry, J. A., Hitt, O., Cole, S. J., Fry, M., Morris,
1268 D. G., and Dixon, H.: CEH-GEAR: 1 km resolution daily and monthly areal rainfall estimates
1269 for the UK for hydrological and other applications, *Earth Syst. Sci. Data*, 7, 143-155,
1270 doi:10.5194/essd-7-143-2015, 2015.
- 1271 Kimball, B. A., Idso, S. B., and Aase, J. K.: A Model of Thermal-Radiation from Partly
1272 Cloudy and Overcast Skies, *Water Resources Research*, 18, 931-936,
1273 doi:10.1029/Wr018i004p00931, 1982.
- 1274 Kruijt, B., Witte, J.-P. M., Jacobs, C. M. J., and Kroon, T.: Effects of rising atmospheric CO₂
1275 on evapotranspiration and soil moisture: A practical approach for the Netherlands, *Journal of*
1276 *Hydrology*, 349, 257-267, doi:10.1016/j.jhydrol.2007.10.052, 2008.
- 1277 Kume, T., Kuraji, K., Yoshifuji, N., Morooka, T., Sawano, S., Chong, L., and Suzuki, M.:
1278 Estimation of canopy drying time after rainfall using sap flow measurements in an emergent
1279 tree in a lowland mixed-dipterocarp forest in Sarawak, Malaysia, *Hydrological Processes*, 20,
1280 565-578, 10.1002/hyp.5924, 2006.
- 1281 Lange, O. L., Lösch, R., Schulze, E.-D., and Kappen, L.: Responses of stomata to changes in
1282 humidity, *Planta*, 100, 76-86, 10.1007/bf00386887, 1971.
- 1283 Li, B., Chen, F., and Guo, H.: Regional complexity in trends of potential evapotranspiration
1284 and its driving factors in the Upper Mekong River Basin, *Quaternary International*, 380-381,
1285 83-94, 10.1016/j.quaint.2014.12.052, 2015.
- 1286 Li, Y., and Zhou, M.: Trends in Dryness Index Based on Potential Evapotranspiration and
1287 Precipitation over 1961–2099 in Xinjiang, China, *Advances in Meteorology*, 2014, 1-15,
1288 10.1155/2014/548230, 2014.
- 1289 Liley, J. B.: New Zealand dimming and brightening, *Journal of Geophysical Research*, 114,
1290 doi:10.1029/2008jd011401, 2009.
- 1291 Lu, X., Bai, H., and Mu, X.: Explaining the evaporation paradox in Jiangxi Province of
1292 China: Spatial distribution and temporal trends in potential evapotranspiration of Jiangxi
1293 Province from 1961 to 2013, *International Soil and Water Conservation Research*, 4, 45-51,
1294 10.1016/j.iswcr.2016.02.004, 2016.
- 1295 Marsh, T., and Dixon, H.: The UK water balance – how much has it changed in a warming
1296 world?, 01-05, doi:10.7558/bhs.2012.ns32, 2012.
- 1297 Marthews, T. R., Malhi, Y., and Iwata, H.: Calculating downward longwave radiation under
1298 clear and cloudy conditions over a tropical lowland forest site: an evaluation of model
1299 schemes for hourly data, *Theoretical and Applied Climatology*, 107, 461-477,
1300 10.1007/s00704-011-0486-9, 2011.
- 1301 Matsoukas, C., Benas, N., Hatzianastassiou, N., Pavlakis, K. G., Kanakidou, M., and
1302 Vardavas, I.: Potential evaporation trends over land between 1983–2008: driven by radiative
1303 fluxes or vapour-pressure deficit?, *Atmospheric Chemistry and Physics*, 11, 7601-7616,
1304 doi:10.5194/acp-11-7601-2011, 2011.
- 1305 McVicar, T. R., Van Niel, T. G., Li, L. T., Roderick, M. L., Rayner, D. P., Ricciardulli, L.,
1306 and Donohue, R. J.: Wind speed climatology and trends for Australia, 1975–2006: Capturing
1307 the stilling phenomenon and comparison with near-surface reanalysis output, *Geophysical*
1308 *Research Letters*, 35, n/a-n/a, 10.1029/2008GL035627, 2008.
- 1309 McVicar, T. R., Roderick, M. L., Donohue, R. J., Li, L. T., Van Niel, T. G., Thomas, A.,
1310 Grieser, J., Jhajharia, D., Himri, Y., Mahowald, N. M., Mescherskaya, A. V., Kruger, A. C.,

- 1311 Rehman, S., and Dinpashoh, Y.: Global review and synthesis of trends in observed terrestrial
1312 near-surface wind speeds: Implications for evaporation, *Journal of Hydrology*, 416, 182-205,
1313 doi:10.1016/j.jhydrol.2011.10.024, 2012.
- 1314 Monteith, J. L.: Evaporation and environment, in: 19th Symposia of the Society for
1315 Experimental Biology, University Press, Cambridge, 1965.
- 1316 Moors, E.: Water Use of Forests in the Netherlands, PhD, Vrije Universiteit, Amsterdam, the
1317 Netherlands, 2012.
- 1318 Morris, D. G., and Flavin, R. W.: A digital terrain model for hydrology., *Proceedings of the*
1319 *4th International Symposium on Spatial Data Handling*, 1, 250-262, 1990.
- 1320 Morton, D., Rowland, C., Wood, C., Meek, L., Marston, C., Smith, G., Wadsworth, R., and
1321 Simpson, I. C.: Final Report for LCM2007 - the new UK land cover map, NERC/Centre for
1322 Ecology & Hydrology 11/07 (CEH Project Number: C03259), 2011.
- 1323 Muneer, T., and Munawwar, S.: Potential for improvement in estimation of solar diffuse
1324 irradiance, *Energy Convers Manage*, 47, 68-86, doi:10.1016/j.enconman.2005.03.015, 2006.
- 1325 Murphy, J. M., Sexton, D. M. H., Jenkins, G. J., Boorman, P. M., Booth, B. B. B., Brown, C.
1326 C., Clark, R. T., Collins, M., Harris, G. R., Kendon, E. J., Betts, R. A., Brown, S. J., Howard,
1327 T. P., Humphrey, K. A., McCarthy, M. P., McDonald, R. E., Stephens, A., Wallace, C.,
1328 Warren, R., Wilby, R., and Wood, R. A.: UK Climate Projections Science Report: Climate
1329 change projections, Met Office Hadley Centre, Exeter, 2009.
- 1330 Newton, K., and Burch, S. F.: Estimation of the UK wind energy resource using computer
1331 modelling techniques and map data, *Energy Technology Support Unit*, 50, 1985.
- 1332 Norton, L. R., Maskell, L. C., Smart, S. S., Dunbar, M. J., Emmett, B. A., Carey, P. D.,
1333 Williams, P., Crowe, A., Chandler, K., Scott, W. A., and Wood, C. M.: Measuring stock and
1334 change in the GB countryside for policy--key findings and developments from the
1335 Countryside Survey 2007 field survey, *Journal of environmental management*, 113, 117-127,
1336 doi:10.1016/j.jenvman.2012.07.030, 2012.
- 1337 Oldekop, E.: Evaporation from the surface of river basins, in: *Collection of the Works of*
1338 *Students of the Meteorological Observatory, University of Tartu-Jurjew-Dorpat, Tartu,*
1339 *Estonia*, 209, 1911.
- 1340 Palmer, W. C.: *Meteorological Drought*. Res. Paper No.45, Dept. of Commerce, Washington,
1341 D.C., 1965.
- 1342 Paltineanu, C., Chitu, E., and Mateescu, E.: New trends for reference evapotranspiration and
1343 climatic water deficit, *International Agrophysics*, 26, 10.2478/v10247-012-0023-9, 2012.
- 1344 Parker, D., and Horton, B.: Uncertainties in central England temperature 1878-2003 and some
1345 improvements to the maximum and minimum series, *International Journal of Climatology*, 25,
1346 1173-1188, doi:10.1002/joc.1190, 2005.
- 1347 [Penman, H. L.: Natural Evaporation from Open Water, Bare Soil and Grass, Proceedings of](#)
1348 [the Royal Society of London. Series A. Mathematical and Physical Sciences, 193, 120-145,](#)
1349 [10.1098/rspa.1948.0037, 1948.](#)
- 1350 Pocock, M. J., Roy, H. E., Preston, C. D., and Roy, D. B.: The Biological Records Centre in
1351 the United Kingdom: a pioneer of citizen science., *Biological Journal of the Linnean Society*,
1352 doi:10.1111/bij.12548, 2015.

1353 Prata, A. J.: A new long-wave formula for estimating downward clear-sky radiation at the
1354 surface, *Quarterly Journal of the Royal Meteorological Society*, 122, 1127-1151,
1355 doi:10.1002/qj.49712253306, 1996.

1356 Prescott, J. A.: Evaporation from a water surface in relation to solar radiation, *Transaction of*
1357 *the Royal Society of South Australia*, 64, 114-125, 1940.

1358 Prudhomme, C., Giuntoli, I., Robinson, E. L., Clark, D. B., Arnell, N. W., Dankers, R.,
1359 Fekete, B. M., Franssen, W., Gerten, D., Gosling, S. N., Hagemann, S., Hannah, D. M., Kim,
1360 H., Masaki, Y., Satoh, Y., Stacke, T., Wada, Y., and Wisser, D.: Hydrological droughts in the
1361 21st century, hotspots and uncertainties from a global multimodel ensemble experiment,
1362 *Proceedings of the National Academy of Sciences*, 111, 3262-3267,
1363 doi:10.1073/pnas.1222473110, 2014.

1364 Pryor, S. C., Barthelmie, R. J., Young, D. T., Takle, E. S., Arritt, R. W., Flory, D., Gutowski,
1365 W. J., Nunes, A., and Roads, J.: Wind speed trends over the contiguous United States, *Journal*
1366 *of Geophysical Research: Atmospheres*, 114, n/a-n/a, 10.1029/2008JD011416, 2009.

1367 Reynolds, B., Chamberlain, P. M., Poskitt, J., Woods, C., Scott, W. A., Rowe, E. C.,
1368 Robinson, D. A., Frogbrook, Z. L., Keith, A. M., Henrys, P. A., Black, H. I. J., and Emmett,
1369 B. A.: Countryside Survey: National “Soil Change” 1978–2007 for Topsoils in Great
1370 Britain—Acidity, Carbon, and Total Nitrogen Status, *Vadose Zone Journal*, 12, 0,
1371 doi:10.2136/vzj2012.0114, 2013.

1372 Richards, J. M.: A simple expression for the saturation vapour pressure of water in the range
1373 –50 to 140°C, *Journal of Physics D: Applied Physics*, 4, L15, 1971.

1374 Robinson, E. L., Blyth, E., Clark, D. B., Finch, J., and Rudd, A. [C.: Climate hydrology and](#)
1375 [ecology research support system potential evapotranspiration dataset for Great Britain \(1961-](#)
1376 [2012\) \[CHESS-PE\], NERC-Environmental Information Data Centre, 2015a.](#)

1377 [Robinson, E. L., Blyth, E., Clark, D. B., Finch, J., and Rudd, A. C.:](#) Climate hydrology and
1378 ecology research support system meteorology dataset for Great Britain (1961-2012) [CHESS-
1379 met], NERC-Environmental Information Data Centre, [2015a.](#)

1380 ~~[Robinson, E. L., Blyth, E., Clark, D. B., Finch, J., and Rudd, A. C.:](#) Climate hydrology and~~
1381 ~~[ecology research support system potential evapotranspiration dataset for Great Britain \(1961-](#)~~
1382 ~~[2012\) \[CHESS-PE\], NERC-Environmental Information Data Centre, 2015b.](#)~~

1383 Rodda, J. C., and Marsh, T. J.: The 1975-76 Drought - a contemporary and retrospective
1384 review, Wallingford, UK, 2011.

1385 Roderick, M. L., Rotstayn, L. D., Farquhar, G. D., and Hobbins, M. T.: On the attribution of
1386 changing pan evaporation, *Geophysical Research Letters*, 34, 10.1029/2007gl031166, 2007.

1387 [Rotstayn, L. D., Roderick, M. L., and Farquhar, G. D.:](#) A simple pan-evaporation model for
1388 [analysis of climate simulations: Evaluation over Australia, *Geophysical Research Letters*, 33,](#)
1389 [10.1029/2006gl027114, 2006.](#)

1390 Rudd, A. C., and Kay, A. L.: Use of very high resolution climate model data for hydrological
1391 modelling: estimation of potential evaporation, *Hydrology Research*, doi:
1392 10.2166/nh.2015.028, 2015.

1393 Rutter, A. J., Kershaw, K. A., Robins, P. C., and Morton, A. J.: A predictive model of rainfall
1394 interception in forests, 1. Derivation of the model from observations in a plantation of
1395 Corsican pine, *Agricultural Meteorology*, 9, 367-384, doi:10.1016/0002-1571(71)90034-3,
1396 1971.

- 1397 Sanchez-Lorenzo, A., Calbó, J., and Martin-Vide, J.: Spatial and Temporal Trends in
 1398 Sunshine Duration over Western Europe (1938–2004), *Journal of Climate*, 21, 6089-6098,
 1399 doi:10.1175/2008jcli2442.1, 2008.
- 1400 Sanchez-Lorenzo, A., Calbó, J., Brunetti, M., and Deser, C.: Dimming/brightening over the
 1401 Iberian Peninsula: Trends in sunshine duration and cloud cover and their relations with
 1402 atmospheric circulation, *Journal of Geophysical Research*, 114, doi:10.1029/2008jd011394,
 1403 2009.
- 1404 Sanchez-Lorenzo, A., and Wild, M.: Decadal variations in estimated surface solar radiation
 1405 over Switzerland since the late 19th century, *Atmospheric Chemistry and Physics*, 12, 8635-
 1406 8644, doi:10.5194/acp-12-8635-2012, 2012.
- 1407 Sanchez-Romero, A., Sanchez-Lorenzo, A., Calbó, J., González, J. A., and Azorin-Molina,
 1408 C.: The signal of aerosol-induced changes in sunshine duration records: A review of the
 1409 evidence, *Journal of Geophysical Research: Atmospheres*, 119, 4657-4673,
 1410 doi:10.1002/2013JD021393, 2014.
- 1411 [Scheff, J., and Frierson, D. M. W.: Scaling Potential Evapotranspiration with Greenhouse](#)
 1412 [Warming, *Journal of Climate*, 27, 1539-1558, doi:10.1175/JCLI-D-13-00233.1, 2014.](#)
- 1413 Schymanski, S. J., and Or, D.: Wind effects on leaf transpiration challenge the concept of
 1414 "potential evaporation", *Proceedings of the International Association of Hydrological*
 1415 *Sciences*, 371, 99-107, 10.5194/piahs-371-99-2015, 2015.
- 1416 Shan, N., Shi, Z., Yang, X., Zhang, X., Guo, H., Zhang, B., and Zhang, Z.: Trends in potential
 1417 evapotranspiration from 1960 to 2013 for a desertification-prone region of China,
 1418 *International Journal of Climatology*, n/a-n/a, 10.1002/joc.4566, 2015.
- 1419 Sheffield, J., Goteti, G., and Wood, E. F.: Development of a 50-Year High-Resolution Global
 1420 Dataset of Meteorological Forcings for Land Surface Modeling, *Journal of Climate*, 19, 3088-
 1421 3111, doi:10.1175/JCLI3790.1, 2006.
- 1422 Shuttleworth, W. J.: *Terrestrial Hydrometeorology*, John Wiley & Sons, Ltd, 2012.
- 1423 Song, Z. W. Z., H. L. ; Snyder, R. L. ;Anderson, F. E. ;Chen, F. : Distribution and Trends in
 1424 Reference Evapotranspiration in the North China Plain, *Journal of Irrigation and Drainage*
 1425 *Engineering*, 136, 240-247, doi:10.1061/(ASCE)IR.1943-4774.0000175, 2010.
- 1426 Soussana, J. F., Allard, V., Pilegaard, K., Ambus, P., Amman, C., Campbell, C., Ceschia, E.,
 1427 Clifton-Brown, J., Czobel, S., Domingues, R., Flechard, C., Fuhrer, J., Hensen, A., Horvath,
 1428 L., Jones, M., Kasper, G., Martin, C., Nagy, Z., Neftel, A., Raschi, A., Baronti, S., Rees, R.
 1429 M., Skiba, U., Stefani, P., Manca, G., Sutton, M., Tuba, Z., and Valentini, R.: Full accounting
 1430 of the greenhouse gas (CO₂, N₂O, CH₄) budget of nine European grassland sites,
 1431 *Agriculture, Ecosystems & Environment*, 121, 121-134, 10.1016/j.agee.2006.12.022, 2007.
- 1432 Stanhill, G., and Cohen, S.: Solar Radiation Changes in the United States during the
 1433 Twentieth Century: Evidence from Sunshine Duration Measurements, *Journal of Climate*, 18,
 1434 1503-1512, doi:10.1175/JCLI3354.1, 2005.
- 1435 Stanhill, G., and Möller, M.: Evaporative climate change in the British Isles, *International*
 1436 *Journal of Climatology*, 28, 1127-1137, doi:10.1002/joc.1619, 2008.
- 1437 Stewart, J. B.: On the use of the Penman-Monteith equation for determining areal
 1438 evapotranspiration, in: *Estimation of Areal Evapotranspiration (Proceedings of a workshop*
 1439 *held at Vancouver, B.C., Canada, August 1987)*. edited by: Black, T. A. S., D. L.; Novak, M.
 1440 D.; Price, D. T., IAHS, Wallingford, Oxfordshire, UK, 1989.

- 1441 Sutton, R. T., and Dong, B.: Atlantic Ocean influence on a shift in European climate in the
1442 1990s, *Nature Geosci*, 5, 788-792, doi:10.1038/ngeo1595, 2012.
- 1443 Tabari, H., Nikbakht, J., and Hosseinzadeh Talaei, P.: Identification of Trend in Reference
1444 Evapotranspiration Series with Serial Dependence in Iran, *Water Resources Management*, 26,
1445 2219-2232, 10.1007/s11269-012-0011-7, 2012.
- 1446 Tanguy, M., Dixon, H., Prosdocimi, I., Morris, D. G., and Keller, V. D. J.: Gridded estimates
1447 of daily and monthly areal rainfall for the United Kingdom (1890-2012) [CEH-GEAR],
1448 NERC Environmental Information Data Centre, doi:10.5285/5dc179dc-f692-49ba-9326-
1449 a6893a503f6e, 2014.
- 1450 Thackeray, S. J., Sparks, T. H., Frederiksen, M., Burthe, S., Bacon, P. J., Bell, J. R., Botham,
1451 M. S., Brereton, T. M., Bright, P. W., Carvalho, L., Clutton-Brock, T., Dawson, A., Edwards,
1452 M., Elliott, J. M., Harrington, R., Johns, D., Jones, I. D., Jones, J. T., Leech, D. I., Roy, D. B.,
1453 Scott, W. A., Smith, M., Smithers, R. J., Winfield, I. J., and Wanless, S.: Trophic level
1454 asynchrony in rates of phenological change for marine, freshwater and terrestrial
1455 environments, *Global Change Biology*, 16, 3304-3313, doi:10.1111/j.1365-
1456 2486.2010.02165.x, 2010.
- 1457 Thompson, N., Barrie, I. A., and Ayles, M.: The Meteorological Office rainfall and
1458 evaporation calculation system: MORECS, Meteorological Office, Bracknell, 1981.
- 1459 Vautard, R., Cattiaux, J., Yiou, P., Thepaut, J. N., and Ciais, P.: Northern Hemisphere
1460 atmospheric stilling partly attributed to an increase in surface roughness, *Nature Geoscience*,
1461 3, 756-761, doi:10.1038/Ngeo979, 2010.
- 1462 Vicente-Serrano, S. M., Azorin-Molina, C., Sanchez-Lorenzo, A., Revuelto, J., López-
1463 Moreno, J. I., González-Hidalgo, J. C., Moran-Tejeda, E., and Espejo, F.: Reference
1464 evapotranspiration variability and trends in Spain, 1961–2011, *Global and Planetary Change*,
1465 121, 26-40, 10.1016/j.gloplacha.2014.06.005, 2014.
- 1466 Vicente-Serrano, S. M., Azorin-Molina, C., Sanchez-Lorenzo, A., El Kenawy, A., Martín-
1467 Hernández, N., Peña-Gallardo, M., Beguería, S., and Tomas-Burguera, M.: Recent changes
1468 and drivers of the atmospheric evaporative demand in the Canary Islands, *Hydrology and
1469 Earth System Sciences Discussions*, 1-35, 10.5194/hess-2016-15, 2016.
- 1470 Vincent, L. A., Zhang, X., Brown, R. D., Feng, Y., Mekis, E., Milewska, E. J., Wan, H., and
1471 Wang, X. L.: Observed Trends in Canada's Climate and Influence of Low-Frequency
1472 Variability Modes, *Journal of Climate*, 28, 4545-4560, 10.1175/jcli-d-14-00697.1, 2015.
- 1473 von Storch, H., and Zwiers, F. W.: *Statistical analysis in climate research*, Cambridge
1474 University Press, Cambridge ; New York, x, 484 p. pp., 1999.
- 1475 Wang, K., and Liang, S.: Global atmospheric downward longwave radiation over land surface
1476 under all-sky conditions from 1973 to 2008, *Journal of Geophysical Research*, 114,
1477 doi:10.1029/2009jd011800, 2009.
- 1478 Ward, R. C., and Robinson, M.: *Principles of Hydrology*, McGraw Hill, 2000.
- 1479 Watts, G., Battarbee, R. W., Bloomfield, J. P., Crossman, J., Daccache, A., Durance, I.,
1480 Elliott, J. A., Garner, G., Hannaford, J., Hannah, D. M., Hess, T., Jackson, C. R., Kay, A. L.,
1481 Kernan, M., Knox, J., Mackay, J., Monteith, D. T., Ormerod, S. J., Rance, J., Stuart, M. E.,
1482 Wade, A. J., Wade, S. D., Weatherhead, K., Whitehead, P. G., and Wilby, R. L.: Climate
1483 change and water in the UK - past changes and future prospects, *Progress in Physical
1484 Geography*, 39, 6-28, doi:10.1177/0309133314542957, 2015.

1485 Weedon, G. P., Gomes, S., Viterbo, P., Shuttleworth, W. J., Blyth, E., Osterle, H., Adam, J.
1486 C., Bellouin, N., Boucher, O., and Best, M.: Creation of the WATCH Forcing Data and Its
1487 Use to Assess Global and Regional Reference Crop Evaporation over Land during the
1488 Twentieth Century, *Journal of Hydrometeorology*, 12, 823-848, doi:10.1175/2011jhm1369.1,
1489 2011.

1490 Weedon, G. P., Balsamo, G., Bellouin, N., Gomes, S., Best, M. J., and Viterbo, P.: The
1491 WFDEI meteorological forcing data set: WATCH Forcing Data methodology applied to
1492 ERA-Interim reanalysis data, *Water Resources Research*, 50, 7505-7514,
1493 doi:10.1002/2014WR015638, 2014.

1494 Wild, M.: Global dimming and brightening: A review, *Journal of Geophysical Research*, 114,
1495 doi:10.1029/2008jd011470, 2009.

1496 Wilkinson, M., Eaton, E. L., Broadmeadow, M. S. J., and Morison, J. I. L.: Inter-annual
1497 variation of carbon uptake by a plantation oak woodland in south-eastern England,
1498 *Biogeosciences*, 9, 5373-5389, 10.5194/bg-9-5373-2012, 2012.

1499 [Willett, K. M., Dunn, R. J. H., Thorne, P. W., Bell, S., de Podesta, M., Parker, D. E., Jones, P.
1500 D., and Williams Jr, C. N.: HadISDH land surface multi-variable humidity and temperature
1501 record for climate monitoring, *Climate of the Past*, 10, 1983-2006, 10.5194/cp-10-1983-2014,
1502 2014.](#)

1503 WMO: Manual on the Global Observing System, Secretariat of the World Meteorological
1504 Organization, Geneva, Switzerland, 2013.

1505 Wood, C. M., Smart, S. M., and Bunce, R. G. H.: Woodland survey of Great Britain 1971–
1506 2001, *Earth System Science Data Discussions*, 8, 259-277, doi:10.5194/essdd-8-259-2015,
1507 2015.

1508 Yin, Y., Wu, S., Chen, G., and Dai, E.: Attribution analyses of potential evapotranspiration
1509 changes in China since the 1960s, *Theoretical and Applied Climatology*, 101, 19-28,
1510 10.1007/s00704-009-0197-7, 2009.

1511 Zhang, K.-x., Pan, S.-m., Zhang, W., Xu, Y.-h., Cao, L.-g., Hao, Y.-p., and Wang, Y.:
1512 Influence of climate change on reference evapotranspiration and aridity index and their
1513 temporal-spatial variations in the Yellow River Basin, China, from 1961 to 2012, *Quaternary
1514 International*, 380-381, 75-82, 10.1016/j.quaint.2014.12.037, 2015.

1515 Zhao, J., Xu, Z.-x., Zuo, D.-p., and Wang, X.-m.: Temporal variations of reference
1516 evapotranspiration and its sensitivity to meteorological factors in Heihe River Basin, China,
1517 *Water Science and Engineering*, 8, 1-8, 10.1016/j.wse.2015.01.004, 2015.

1518 Zwiers, F. W., and von Storch, H.: Taking Serial-Correlation into Account in Tests of the
1519 Mean, *Journal of Climate*, 8, 336-351, doi:10.1175/1520-
1520 0442(1995)008<0336:Tsciai>2.0.Co;2, 1995.

1521

1522

1524 Table 1. Description of input meteorological variables

Variable (units)	Source data	Ancillary files	Assumptions	Height
Air temperature (K)	MORECS air temperature	IHDTM elevation	Lapsed to IHDTM elevation	1.2 m
Specific humidity (kg kg ⁻¹)	MORECS vapour pressure, air temperature	IHDTM elevation	Lapsed to IHDTM elevation Constant air pressure = 1 kPa	1.2 m
Downward LW radiation (W m ⁻²)	MORECS air temperature, vapour pressure, sunshine hours	IHDTM elevation	Constant cloud base height	1.2 m
Downward SW radiation (W m ⁻²)	MORECS sunshine hours	IHDTM elevation Spatially-varying aerosol correction	No time-varying aerosol correction	1.2 m
Wind speed (m s ⁻¹)	MORECS wind speed	ETSU average wind speeds	Wind speed correction is constant	10 m
Precipitation (kg m ⁻² s ⁻¹)	CEH-GEAR precipitation	-	No transformations performed	n/a
Daily temperature range (K)	CRU TS 3.21 daily temperature range	-	No spatial interpolation from 0.5° resolution. No temporal interpolation (constant values for each month)	1.2 m

Format

Surface air pressure (Pa)	WFD air pressure	IHD TM elevation	Mean-monthly values from WFD used (each year has same values). Lapsed to IHD TM elevation. No temporal interpolation (constant values for each month).	n/a
---------------------------	------------------	------------------	--	-----

1525
1526

1531 Table 2: Rate of change of annual means of meteorological and potential evapotranspiration
 1532 variables in Great Britain. Bold indicates trends that are significant at the 5% level. The
 1533 ranges are given by the 95% CI.

Variable	Rate of change \pm 95% CI				
	Great Britain	England	Scotland	Wales	English lowlands
Air temperature (K dec ⁻¹)	0.21 \pm 0.15	0.23 \pm 0.14	0.17 \pm 0.12	0.21 \pm 0.15	0.25 \pm 0.17
Specific humidity (g kg ⁻¹ dec ⁻¹)	0.049 \pm 0.037	0.054 \pm 0.04	0.040 \pm 0.036	0.055 \pm 0.037	0.053 \pm 0.044
Downward SW radiation (W m ⁻² dec ⁻¹)	1.0 \pm 0.8	1.3 \pm 1.0	0.5 \pm 0.6	1.1 \pm 0.9	1.5 \pm 1.0
Downward LW radiation (W m ⁻² dec ⁻¹)	0.50 \pm 0.48	0.45 \pm 0.48	0.58 \pm 0.48	0.50 \pm 0.55	0.42 \pm 0.48
Wind speed (m s ⁻¹ dec ⁻¹)	-0.18 \pm 0.09	-0.16 \pm 0.09	-0.20 \pm 0.10	-0.25 \pm 0.16	-0.13 \pm 0.07
Precipitation (mm d ⁻¹ dec ⁻¹)	0.08 \pm 0.06	0.04 \pm 0.06	0.14 \pm 0.09	0.08 \pm 0.09	0.03 \pm 0.05
Daily temperature range (K dec ⁻¹)	-0.06 \pm 0.06	-0.03 \pm 0.06	-0.13 \pm 0.08	0.00 \pm 0.06	-0.04 \pm 0.07
<u>Relative humidity (% dec⁻¹)</u>	<u>-0.39 \pm 0.44</u>	<u>-0.43 \pm 0.46</u>	<u>-0.33 \pm 0.33</u>	<u>-0.36 \pm 0.4</u>	<u>-0.50 \pm 0.53</u>
PET (mm d ⁻¹ dec ⁻¹)	0.021 \pm 0.021	0.025 \pm 0.024	0.015 \pm 0.015	0.017 \pm 0.021	0.03 \pm 0.026
Radiative component of PET (mm d ⁻¹ dec ⁻¹)	0.016 \pm 0.010	0.018 \pm 0.011	0.013 \pm 0.008	0.020 \pm 0.013	0.018 \pm 0.011
Aerodynamic component of PET (mm d ⁻¹ dec ⁻¹)	0.007 \pm 0.011	0.009 \pm 0.013	0.004 \pm 0.009	0.001 \pm 0.013	0.015 \pm 0.015
PETI (mm d ⁻¹ dec ⁻¹)	0.019 \pm 0.020	0.023 \pm 0.023	0.014 \pm 0.014	0.016 \pm 0.020	0.028 \pm 0.025

1534

1541 Table 3. Contributions to the rate of change of PET and its radiative and aerodynamic
 1542 components. For each variable, the first column shows the contribution calculated using
 1543 regional averages, along with the associated 95% CI. The second column shows the
 1544 contribution calculated at 1 km resolution, then averaged over each region. The uncertainty on
 1545 this value is difficult to calculate as the pixels are highly spatially correlated, so the
 1546 uncertainty range from the regional analysis is used in Fig. 13.

a) Contribution to rate of change of PET (mm d ⁻¹ decade ⁻¹)												
	Air temperature		Specific humidity		Wind speed		Downward LW		Downward SW		Total	
	Regional	Pixel	Regional	Pixel	Regional	Pixel	Regional	Pixel	Regional	Pixel	Regional	Pixel
England	0.041 ± 0.025	0.039	-0.025 ± 0.019	-0.024	-0.010 ± 0.005	-0.007	0.005 ± 0.006	0.005	0.013 ± 0.009	0.012	0.025 ± 0.034	0.024
Scotland	0.029 ± 0.021	0.023	-0.020 ± 0.018	-0.017	-0.010 ± 0.005	-0.007	0.006 ± 0.005	0.006	0.005 ± 0.005	0.004	0.010 ± 0.029	0.008
Wales	0.039 ± 0.028	0.036	-0.026 ± 0.018	-0.025	-0.011 ± 0.007	-0.009	0.006 ± 0.006	0.006	0.010 ± 0.009	0.009	0.017 ± 0.036	0.017
English lowlands	0.043 ± 0.029	0.042	-0.024 ± 0.020	-0.023	-0.008 ± 0.004	-0.008	0.005 ± 0.006	0.005	0.015 ± 0.010	0.015	0.031 ± 0.038	0.030
Great Britain	0.037 ± 0.026	0.031	-0.023 ± 0.018	-0.022	-0.010 ± 0.005	-0.007	0.006 ± 0.005	0.005	0.010 ± 0.007	0.007	0.019 ± 0.033	0.014
b) Contribution to rate of change of radiative component of (mm d ⁻¹ decade ⁻¹)												
	Air temperature		Specific humidity		Wind speed		Downward LW		Downward SW		Total	
	Regional	Pixel	Regional	Pixel	Regional	Pixel	Regional	Pixel	Regional	Pixel	Regional	Pixel
England	-0.009 ± 0.006	-0.009	n/a	n/a	0.009 ± 0.005	0.007	0.005 ± 0.006	0.005	0.014 ± 0.010	0.013	0.018 ± 0.013	0.016
Scotland	-0.006 ± 0.005	-0.006	n/a	n/a	0.009 ± 0.004	0.007	0.006 ± 0.005	0.006	0.005 ± 0.005	0.004	0.014 ± 0.010	0.012
Wales	-0.007 ± 0.005	-0.007	n/a	n/a	0.014 ± 0.009	0.013	0.006 ± 0.006	0.006	0.010 ± 0.009	0.010	0.023 ± 0.015	0.022
English lowlands	-0.010 ± 0.007	-0.010	n/a	n/a	0.007 ± 0.004	0.006	0.005 ± 0.006	0.005	0.016 ± 0.011	0.015	0.017 ± 0.014	0.017
Great Britain	-0.008 ± 0.006	-0.007	n/a	n/a	0.009 ± 0.005	0.007	0.006 ± 0.006	0.006	0.010 ± 0.008	0.008	0.017 ± 0.012	0.013
c) Contribution to rate of change of aerodynamic component of PET (mm d ⁻¹ decade ⁻¹)												
	Air temperature		Specific humidity		Wind speed		Downward LW		Downward SW		Total	
	Regional	Pixel	Regional	Pixel	Regional	Pixel	Regional	Pixel	Regional	Pixel	Regional	Pixel

England	0.052 ± 0.032	0.050	-0.026 ± 0.020	-0.026	-0.018 ± 0.010	-0.015	n/a	n/a	n/a	n/a	0.007 ± 0.039	0.009
Scotland	0.037 ± 0.027	0.033	-0.021 ± 0.019	-0.019	-0.019 ± 0.010	-0.015	n/a	n/a	n/a	n/a	-0.003 ± 0.034	-0.001
Wales	0.048 ± 0.035	0.046	-0.028 ± 0.019	-0.027	-0.026 ± 0.016	-0.023	n/a	n/a	n/a	n/a	-0.005 ± 0.042	-0.003
England and Wales	0.056 ± 0.037	0.055	-0.026 ± 0.021	-0.025	-0.015 ± 0.008	-0.014	n/a	n/a	n/a	n/a	0.015 ± 0.044	0.015
Great Britain	0.046 ± 0.033	0.041	-0.025 ± 0.019	-0.023	-0.020 ± 0.010	-0.015	n/a	n/a	n/a	n/a	0.002 ± 0.039	0.003

1547
1548

1554 Table 4. Contribution of the trend in each variable to the trends in annual mean PET and its
 1555 radiative and aerodynamic components as a percentage of the fitted trend in PET and its
 1556 components.

a) Potential evapotranspiration (PET)						
	Air temperature	Specific humidity	Wind speed	Downward LW	Downward SW	Total
England	154 %	-88 %	-22 %	17 %	47 %	108 %
Scotland	150 %	-74 %	-23 %	26 %	18 %	97 %
Wales	200 %	-130 %	-38 %	28 %	50 %	109 %
English lowlands	142 %	-77 %	-20 %	15 %	45 %	105 %
Great Britain	155 %	-87 %	-23 %	19 %	31 %	96 %
b) Radiative component of PET						
	Air temperature	Specific humidity	Wind speed	Downward LW	Downward SW	Total
England	-47 %	n/a	40 %	28 %	71 %	92 %
Scotland	-42 %	n/a	62 %	46 %	36 %	102 %
Wales	-34 %	n/a	69 %	29 %	52 %	116 %
English lowlands	-53 %	n/a	35 %	27 %	86 %	95 %
Great Britain	-44 %	n/a	46 %	31 %	53 %	87 %
c) Aerodynamic component of PET						
	Air temperature	Specific humidity	Wind speed	Downward LW	Downward SW	Total
England	245 %	-115 %	-48 %	n/a	n/a	82 %
Scotland	68 %	-14 %	-33 %	n/a	n/a	21 %
Wales	-135 %	72 %	-42 %	n/a	n/a	-105 %
English lowlands	282 %	-126 %	-47 %	n/a	n/a	109 %
Great Britain	168 %	-76 %	-44 %	n/a	n/a	48 %

1557
 1558

1566
1567
1568
1569
1570
1571
1572

Table A1. Details of sites used for validation of meteorological data. Contributions to the rate of change of PET and its radiative and aerodynamic components. For each variable, the first column shows the contribution calculated using regional averages, along with the associated 95% CI. The second column shows the contribution calculated at 1 km resolution, then averaged over each region. The uncertainty on this value is difficult to calculate as the pixels are highly spatially correlated, so the uncertainty range from the regional analysis is used in Fig. 13.

Site (ID)		Contribution to rate of change of PET (mm d ⁻¹ decade ⁻¹)		Latitude	Longitude	Years	Land cover	Citation			
Air temperature				Relative humidity	Wind speed	Downward LW	Downward SW	Total			
Re	Pixel	Re	Pixel	Re	Pixel	Re	Pixel	Re	Pixel		
gional		gional	el	gional	el	gional	el	gional	el		
Al	54	-0.000		0.0	0.0	20		0.0	0.0	0.0	0.0
ie	1			15	13	0		13	12	21	23
e	5			±		86		±		±	
H	0.0			0.0		01		0.0		0.0	
ol	02			16		0 ±		09		20	
t	±					0.0					
(0.0					05					
U	01					07					
K											
-											
H											
a											
m											
)E											
ngl											
d											
Sc	±	0.000		0.0	0.0	±		0.0	0.0	0.0	0.0
otl	0.0			11	08	0		06	06	05	04
an	01			±		10		±		±	
d	±			0.0		±		0.0		0.0	
	0.0			11		0		05		05	14
	01					05					
W	±	-0.000		0.0	0.0	±		0.0	0.0	0.0	0.0
ale	0.0			13	12	0		06	06	10	09
s	02			±		11		±		±	
	±			0.0		±		0.0		0.0	
	0.0			14		0		06		09	19
	01					07					

Formatted
Deleted
Formatted
Deleted
Deleted
Deleted
Formatted
Inserted
Inserted
Formatted
Inserted
Inserted
Inserted
Formatted
Formatted
Formatted
Formatted
Formatted
Formatted

En	=	-0.000	0.0	0.0	=	=	0.0	0.0	0.0	0.0	0.0	0.0
gli	0.0		17	17	0.0	0.0	0.05	0.05	0.15	0.15	0.26	0.28
sh	0.03		±		0.08	0.08	±		±		±	
lo	±		0.0		±		0.0		0.0		0.0	
wl	0.0		18		0.0		0.06		0.10		0.22	
an	0.02				0.04							
ds												
Gr	=	0.000	0.0	0.0	=	=	0.0	0.0	0.0	0.0	0.0	0.0
eat	0.0		13	11	0.0	0.0	0.06	0.05	0.10	0.07	0.16	0.16
Bri	0.02		±		0.10	0.07	±		±		±	
tai	±		0.0		±		0.0		0.0		0.0	
n	0.0		15		0.0		0.05		0.07		0.18	
	0.01				0.05							

b) Contribution to rate of change of radiative component of (mm d⁻¹ decade⁻¹)

Air temperature			Relative humidity		Wind speed		Downward LW		Downward SW		Total	
—	Re	Pixel	Re	Pixel	Re	Pixel	Re	Pixel	Re	Pixel	Re	Pixel
	gion		gion	el	gion	el	gion	el	gion	el	gion	el
	nal		nal	nal	nal	nal	nal	nal	nal	nal	nal	nal
En	=	-0.009	n/a	n/a	0.0	0.0	0.0	0.0	0.0	0.0	0.0	0.0
gla	0.0				0.09	0.07	0.05	0.05	0.14	0.13	0.18	0.16
nd	0.0				±		±		±		±	
	±				0.0		0.0		0.0		0.0	
	0.0				0.05		0.06		0.10		0.13	
	0.06											
Sc	=	-0.006	n/a	n/a	0.0	0.0	0.0	0.0	0.0	0.0	0.0	0.0
otl	0.0				0.09	0.07	0.06	0.06	0.05	0.04	0.14	0.12
an	0.06				±		±		±		±	
d	±				0.0		0.0		0.0		0.0	
	0.0				0.04		0.05		0.05		0.10	
	0.05											
W	=	-0.007	n/a	n/a	0.0	0.0	0.0	0.0	0.0	0.0	0.0	0.0
ale	0.0				0.14	0.13	0.06	0.06	0.10	0.10	0.23	0.22
s	0.07				±		±		±		±	
	±				0.0		0.0		0.0		0.0	
	0.0				0.09		0.06		0.09		0.15	
	0.05											
En	=	-0.010	n/a	n/a	0.0	0.0	0.0	0.0	0.0	0.0	0.0	0.0
gli	0.0				0.07	0.06	0.05	0.05	0.16	0.15	0.17	0.17
sh	0.10				±		±		±		±	
lo	±				0.0		0.0		0.0		0.0	
wl	0.0				0.04		0.06		0.11		0.14	
an	0.07											
ds												
Gr	=	-0.007	n/a	n/a	0.0	0.0	0.0	0.0	0.0	0.0	0.0	0.0
eat	0.0				0.09	0.07	0.06	0.06	0.10	0.08	0.17	0.13
Bri	0.08				±		±		±		±	
tai	±				0.0		0.0		0.0		0.0	
n	0.0				0.05		0.06		0.08		0.12	
	0.06											

c) Contribution to rate of change of aerodynamic component of PET (mm d⁻¹ decade⁻¹)

Air temperature			Specific humidity		Wind speed		Downward LW		Downward SW		Total	
—	Re	Pixel	Re	Pixel	Re	Pixel	Re	Pixel	Re	Pixel	Re	Pixel
	gion		gion	el	gion	el	gion	el	gion	el	gion	el
	nal		nal	nal	nal	nal	nal	nal	nal	nal	nal	nal
En	0.0	0.006	0.0	0.0	=	=	n/a	n/a	n/a	n/a	0.0	0.0
gla	0.06		15	14	0.0	0.0					0.03	0.04
nd	±		±		0.18	0.15					±	
	0.0		0.0		±						0.0	
	0.04		17		0.0						0.20	
					0.10							

Sc otl an d	<u>0.0</u> <u>04</u> ± <u>0.0</u> <u>03</u>	<u>0.004</u>	<u>0.0</u> <u>11</u> ± <u>0.0</u> <u>11</u>	<u>0.0</u> <u>09</u> 	<u>±</u> <u>0.0</u> <u>19</u> <u>±</u> <u>0.0</u> <u>10</u>	<u>±</u> <u>0.0</u> <u>15</u> 	n/a	n/a	n/a	n/a	<u>±</u> <u>0.0</u> <u>04</u> ± <u>0.0</u> <u>15</u>	<u>±</u> <u>0.0</u> <u>02</u>
W ale s	<u>0.0</u> <u>05</u> ± <u>0.0</u> <u>04</u>	<u>0.005</u>	<u>0.0</u> <u>13</u> ± <u>0.0</u> <u>15</u>	<u>0.0</u> <u>12</u> 	<u>±</u> <u>0.0</u> <u>26</u> <u>±</u> <u>0.0</u> <u>16</u>	<u>±</u> <u>0.0</u> <u>23</u> 	n/a	n/a	n/a	n/a	<u>±</u> <u>0.0</u> <u>07</u> ± <u>0.0</u> <u>22</u>	<u>±</u> <u>0.0</u> <u>06</u>
En gli sh lo wl an ds	<u>0.0</u> <u>07</u> ± <u>0.0</u> <u>04</u>	<u>0.006</u>	<u>0.0</u> <u>18</u> ± <u>0.0</u> <u>19</u>	<u>0.0</u> <u>17</u> 	<u>±</u> <u>0.0</u> <u>15</u> <u>±</u> <u>0.0</u> <u>08</u>	<u>±</u> <u>0.0</u> <u>14</u> 	n/a	n/a	n/a	n/a	<u>±</u> <u>0.0</u> <u>09</u> ± <u>0.0</u> <u>21</u>	<u>±</u> <u>0.0</u> <u>10</u>
Gr eat Bri tai n	<u>0.0</u> <u>05</u> ± <u>0.0</u> <u>04</u>	<u>0.005</u>	<u>0.0</u> <u>14</u> ± <u>0.0</u> <u>15</u>	<u>0.0</u> <u>11</u> 	<u>±</u> <u>0.0</u> <u>20</u> <u>±</u> <u>0.0</u> <u>10</u>	<u>±</u> <u>0.0</u> <u>15</u> 	n/a	n/a	n/a	n/a	<u>±</u> <u>0.0</u> <u>01</u> ± <u>0.0</u> <u>19</u>	<u>±</u> <u>0.0</u> <u>00</u>

1573
1574

1575 Table 6. Contribution of the trend in each variable to the trends in annual mean PET and its
 1576 radiative and aerodynamic components as a percentage of the fitted trend in PET and its
 1577 components when relative humidity is used.

<u>a) Potential evapotranspiration (PET)</u>						
	<u>Air</u> <u>temperature</u>	<u>Relative</u> <u>humidity</u>	<u>Wind</u> <u>speed</u>	<u>Downward</u> <u>LW</u>	<u>Downward</u> <u>SW</u>	<u>Total</u>
<u>England</u>	<u>-0%</u>	<u>57%</u>	<u>-22%</u>	<u>17%</u>	<u>47%</u>	<u>99%</u>
<u>Scotland</u>	<u>0%</u>	<u>65%</u>	<u>-23%</u>	<u>26%</u>	<u>18%</u>	<u>85%</u>
<u>Wales</u>	<u>-0%</u>	<u>68%</u>	<u>-38%</u>	<u>27%</u>	<u>50%</u>	<u>107%</u>
<u>English</u> <u>lowlands</u>	<u>-0%</u>	<u>57%</u>	<u>-20%</u>	<u>15%</u>	<u>45%</u>	<u>97%</u>
<u>Great Britain</u>	<u>0%</u>	<u>60%</u>	<u>-23%</u>	<u>19%</u>	<u>31%</u>	<u>87%</u>
<u>b) Radiative component of PET</u>						
	<u>Air</u> <u>temperature</u>	<u>Relative</u> <u>humidity</u>	<u>Wind</u> <u>speed</u>	<u>Downward</u> <u>LW</u>	<u>Downward</u> <u>SW</u>	<u>Total</u>
<u>England</u>	<u>-47%</u>	<u>n/a</u>	<u>40%</u>	<u>28%</u>	<u>71%</u>	<u>92%</u>
<u>Scotland</u>	<u>-42%</u>	<u>n/a</u>	<u>62%</u>	<u>46%</u>	<u>36%</u>	<u>102%</u>
<u>Wales</u>	<u>-34%</u>	<u>n/a</u>	<u>69%</u>	<u>29%</u>	<u>52%</u>	<u>116%</u>
<u>English</u> <u>lowlands</u>	<u>-53%</u>	<u>n/a</u>	<u>35%</u>	<u>27%</u>	<u>86%</u>	<u>95%</u>
<u>Great Britain</u>	<u>-44%</u>	<u>n/a</u>	<u>46%</u>	<u>31%</u>	<u>53%</u>	<u>87%</u>
<u>c) Aerodynamic component of PET</u>						
	<u>Air</u> <u>temperature</u>	<u>Relative</u> <u>humidity</u>	<u>Wind</u> <u>speed</u>	<u>Downward</u> <u>LW</u>	<u>Downward</u> <u>SW</u>	<u>Total</u>
<u>England</u>	<u>29%</u>	<u>78%</u>	<u>-48%</u>	<u>n/a</u>	<u>n/a</u>	<u>59%</u>
<u>Scotland</u>	<u>8%</u>	<u>14%</u>	<u>-33%</u>	<u>n/a</u>	<u>n/a</u>	<u>-11%</u>
<u>Wales</u>	<u>-15%</u>	<u>-33%</u>	<u>-42%</u>	<u>n/a</u>	<u>n/a</u>	<u>-90%</u>
<u>English</u> <u>lowlands</u>	<u>33%</u>	<u>98%</u>	<u>-47%</u>	<u>n/a</u>	<u>n/a</u>	<u>84%</u>
<u>Great Britain</u>	<u>19%</u>	<u>52%</u>	<u>-44%</u>	<u>n/a</u>	<u>n/a</u>	<u>27%</u>

1578
1579

1582

Table A1. Details of sites used for validation of meteorological data.

<u>Site (ID)</u>	<u>Latitude</u>	<u>Longitude</u>	<u>Years</u>	<u>Land cover</u>	<u>Citation</u>
<u>Alice Holt (UK-Ham)</u>	<u>51.15</u>	<u>-0.86</u>	<u>2004-2012</u>	<u>Deciduous broadleaf woodland</u>	<u>(Wilkinson et al., 2012; Heinemeyer et al., 2012)</u>
Griffin Forest (UK-Gri)	56.61	-3.80	1997-2001, 2004-2008	Evergreen needleleaf woodland	(Clement, 2003)
Auchencorth Moss (UK-AMo)	55.79	-3.24	2002-2006	Grass and crop	(Billett et al., 2004)
Easter Bush (UK-EBu)	55.87	-3.21	2004-2008	Grass	(Gilmanov et al., 2007; Soussana et al., 2007) (Gilmanov et al., 2007; Soussana et al., 2007)

Formatted

1583

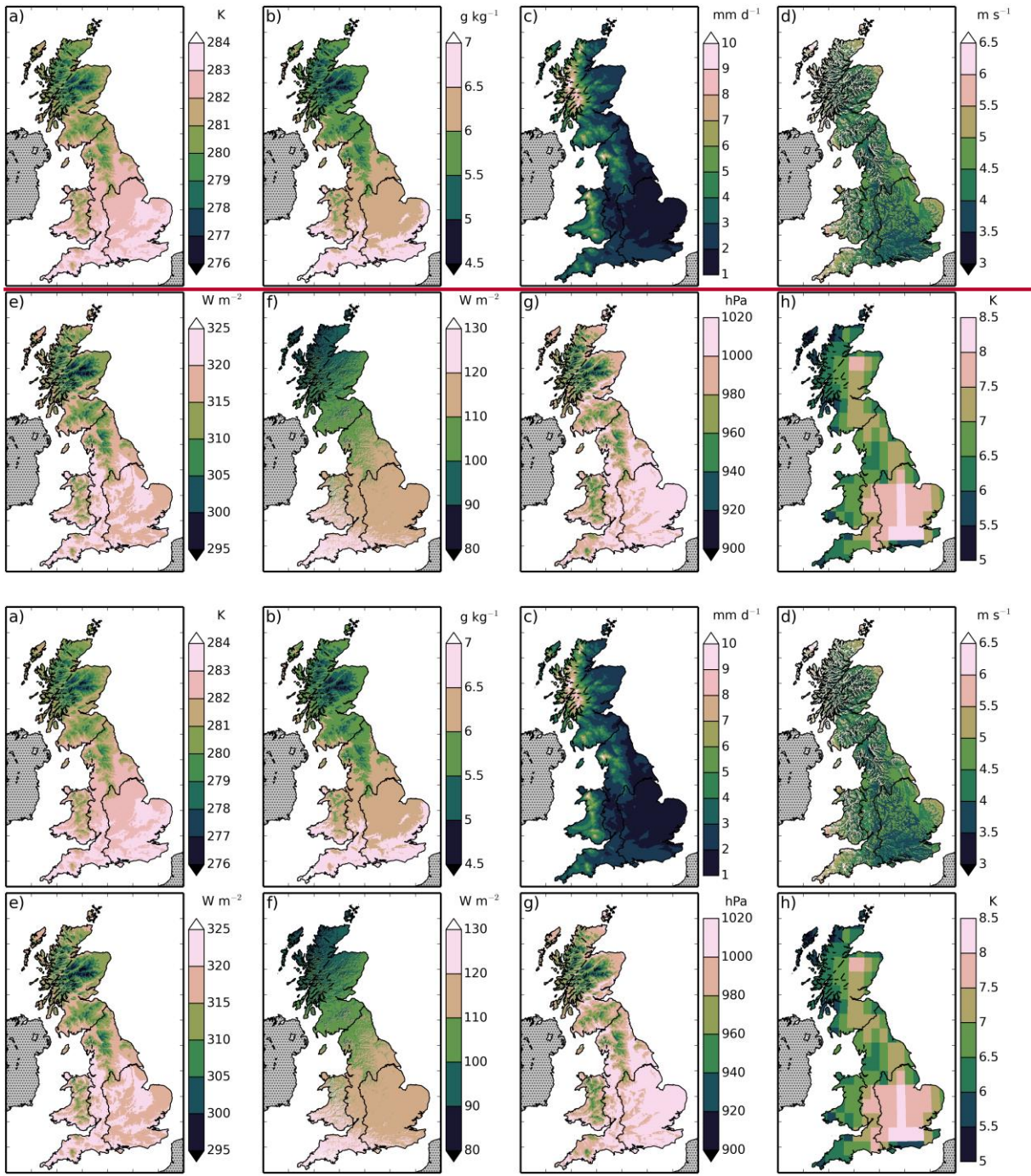
1586

Table A2. Correlation statistics for meteorological variables with data from four sites.

a) Air temperature			
Site	r^2	Mean bias	RMSE
Alice Holt	0.95	0.10 K	1.17 K
Griffin Forest	0.94	0.21 K	1.17 K
Auchencorth Moss	0.98	-0.02 K	0.78 K
Easter Bush	0.97	-0.46 K	0.96 K
b) Downward SW radiation			
Site	r^2	Mean bias	RMSE
Alice Holt	0.94	-3.01 W m ⁻²	22.92 W m ⁻²
Griffin Forest	0.85	-4.90 W m ⁻²	31.29 W m ⁻²
Auchencorth Moss	0.91	14.27 W m ⁻²	27.96 W m ⁻²
Easter Bush	0.88	5.73 W m ⁻²	27.15 W m ⁻²
c) Mixing ratio			
Site	r^2	Mean bias	RMSE
Alice Holt	0.90	-0.02 mmol mol ⁻¹	1.09 mmol mol ⁻¹
Griffin Forest	0.76	0.08 mmol mol ⁻¹	1.56 mmol mol ⁻¹
d) Wind speed			
Site	r^2	mean bias	RMSE
Alice Holt	0.88	1.24 m s ⁻¹	1.45 m s ⁻¹
Griffin Forest	0.59	1.36 m s ⁻¹	1.81 m s ⁻¹
Auchencorth Moss	0.63	-0.38 m s ⁻¹	1.37 m s ⁻¹
Easter Bush	0.82	0.44 m s ⁻¹	1.03 m s ⁻¹
e) Surface air pressure			
Site	r^2	Mean bias	RMSE
Griffin Forest	0.05	-0.42 hPa	1.38 hPa
Auchencorth Moss	0.01	-1.06 hPa	1.57 hPa
Easter Bush	0.03	0.01 hPa	1.33 hPa

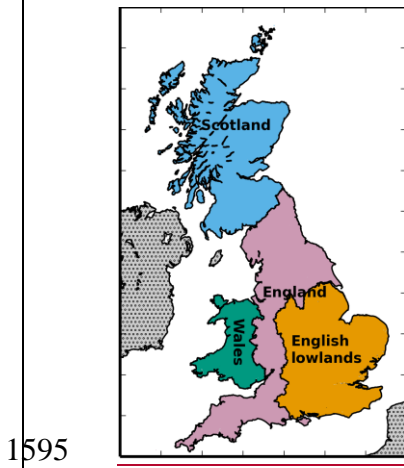
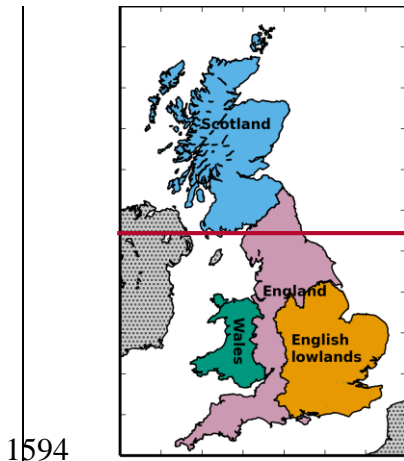
1587

1588

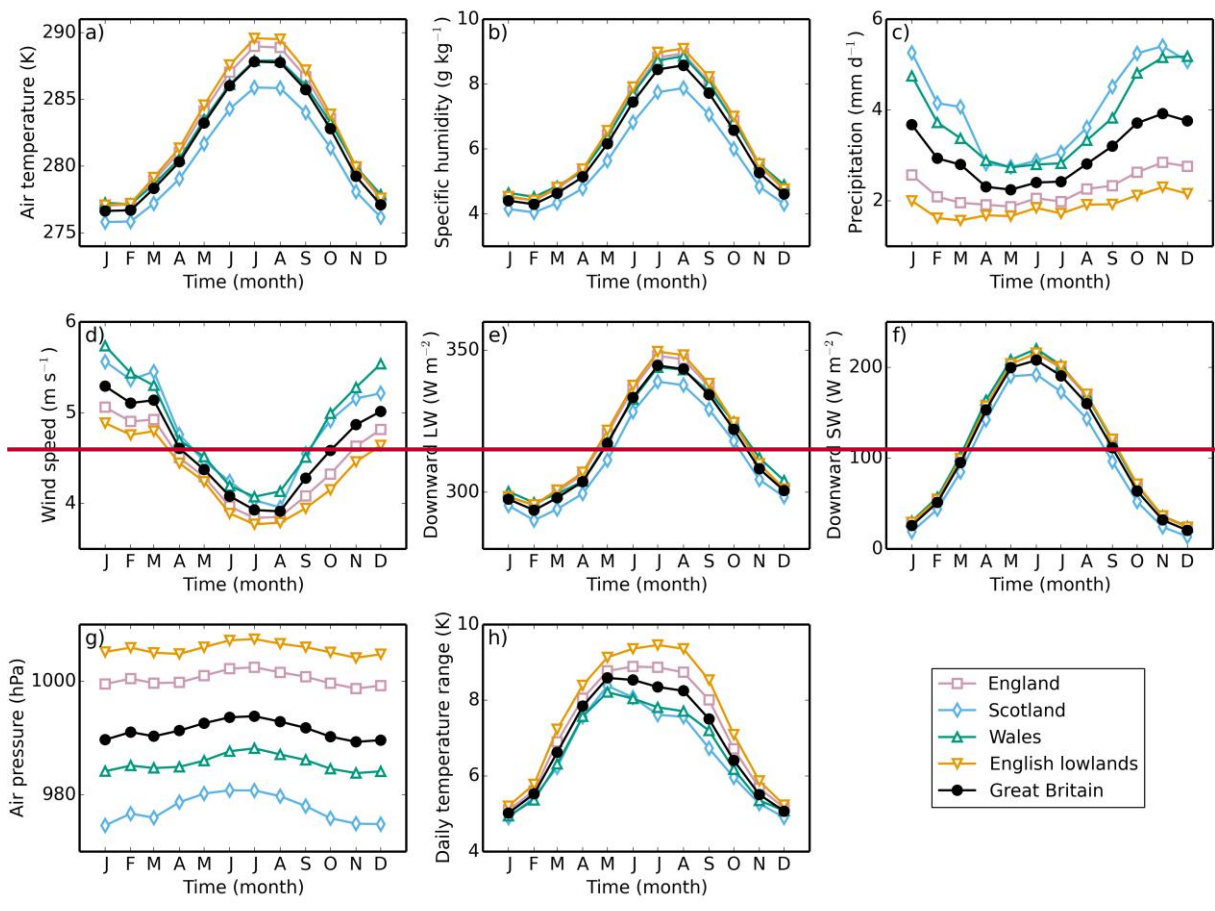


1589

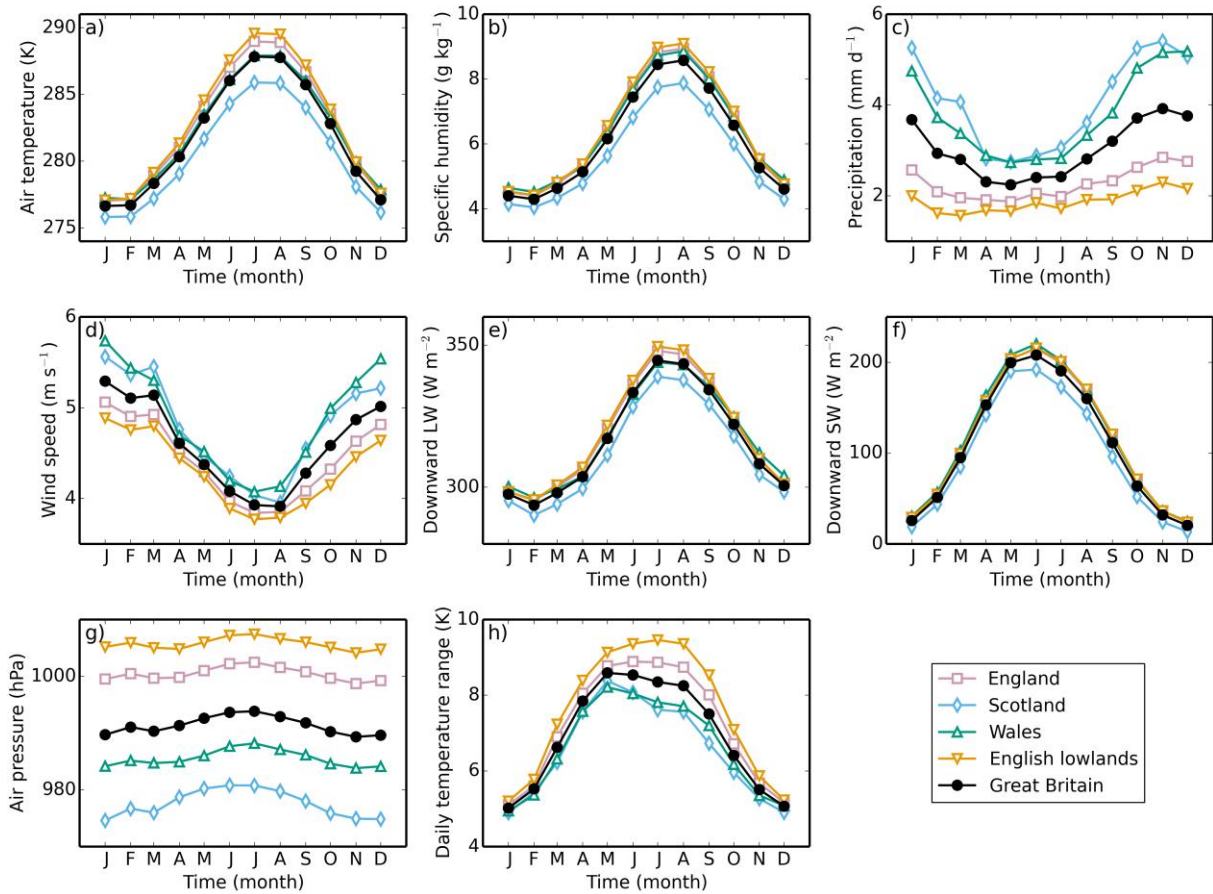
1590 Figure 1. Means of the meteorological variables over the years 1961-2012. The variables are
1591 a) 1.2 m air temperature, b) 1.2 m specific humidity, c) precipitation, d) 10 m wind speed, e)
1592 downward LW radiation, f) downward SW radiation, g) surface air pressure, h) daily air
1593 temperature range.



1596 Figure 2. The regions used to calculate the area means. The English lowlands are a sub-region
1597 of England. England, Scotland and Wales together form the fifth region, Great Britain.

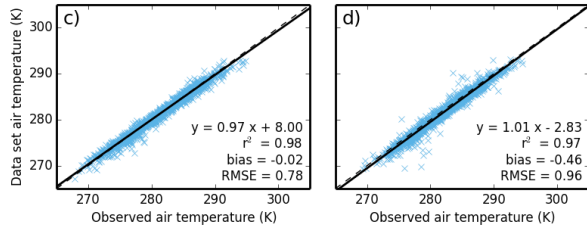
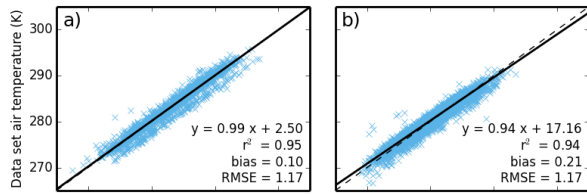
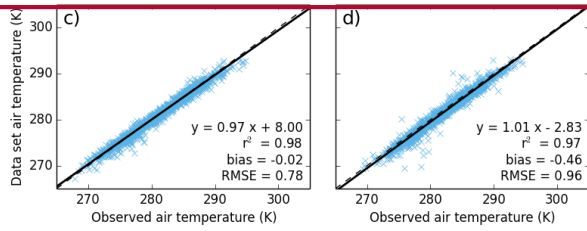
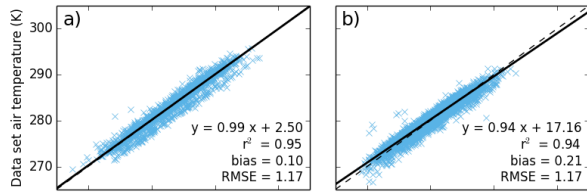


1598



1599

1600 Figure 3. Mean monthly climatology of meteorological variables, a) 1.2 m air temperature, b)
 1601 1.2 m specific humidity, c) precipitation, d) 10 m wind speed, e) downward LW radiation, f)
 1602 downward SW radiation, g) surface air pressure, h) daily air temperature range, for five
 1603 different regions of Great Britain, calculated over the years 1961-2012.
 1604



1605

1606

1607

1608

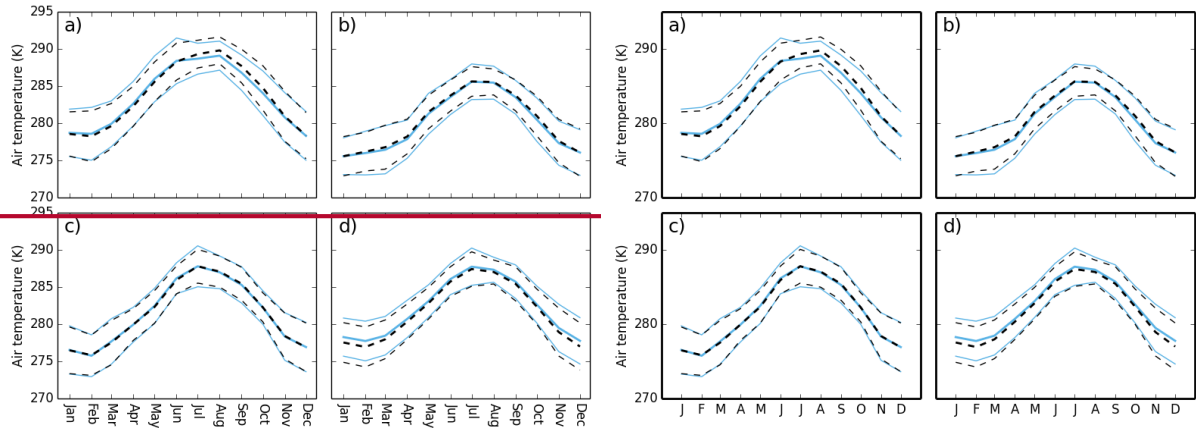
1609

1610

1611

1612

Figure 4. Plot of data set air temperature against daily mean observed air temperature at four sites. The dashed line shows the one to one line, while the solid line shows the linear regression, the equation of which is shown in the lower right of each plot, along with the r^2 value, the mean bias and the RMSE. The sites are a) Alice Holt; b) Griffin Forest; c) Auchencorth Moss; d) Easter Bush.

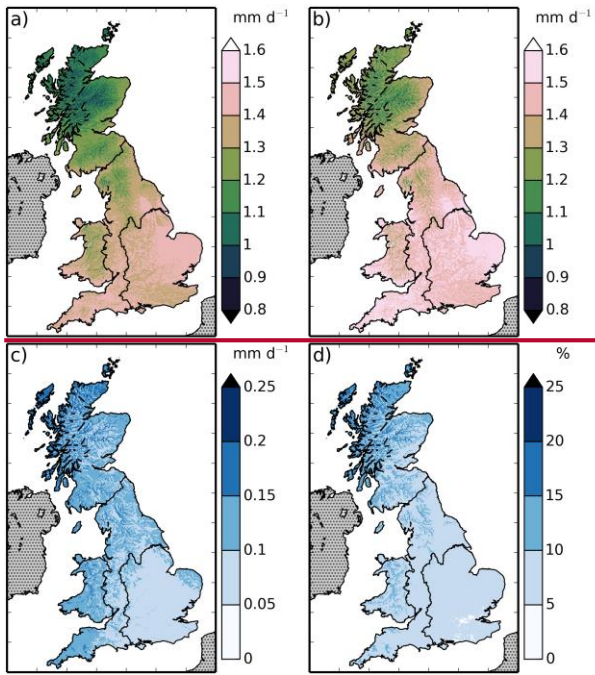


1614

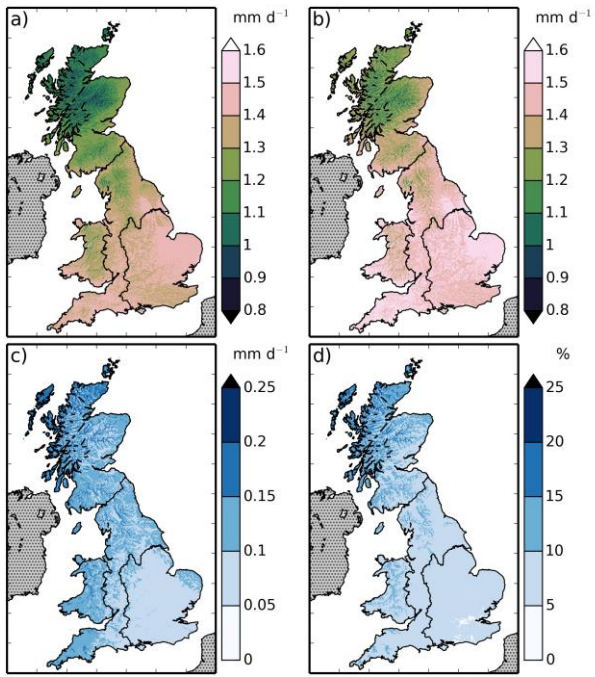
1615 Figure 5. Mean monthly climatology of the dataset (black, dashed lines) and observed (blue,
 1616 solid lines) ~~and observed~~ air temperatures (~~black, dashed lines~~), calculated for the period of
 1617 observations. The thicker lines show the means, while the thinner lines show the standard errors
 1618 on each measurement. Sites as in Fig. 4.

1619

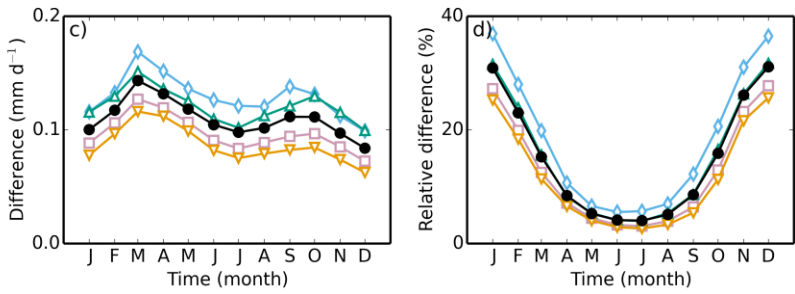
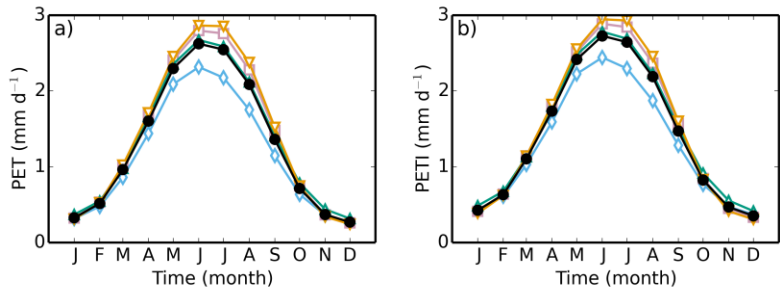
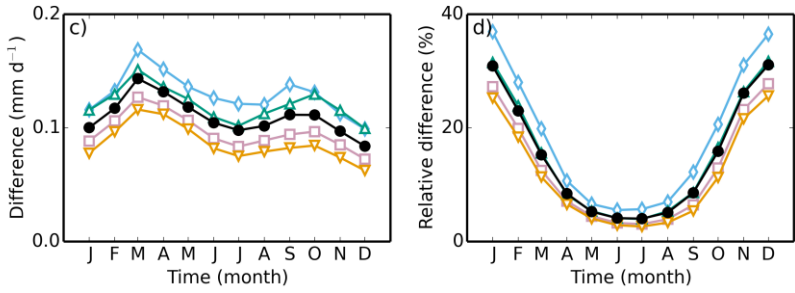
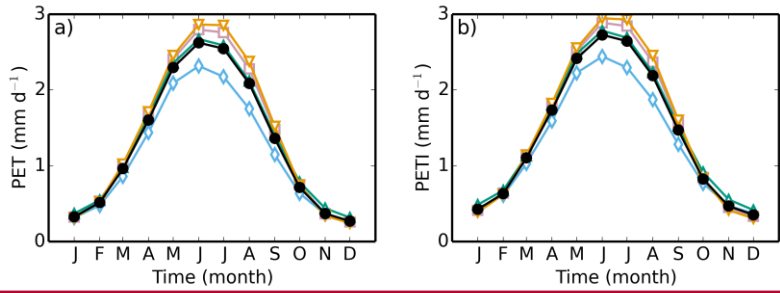
1620



1621



1622 Figure 6. Mean a) PET, b) PETI, c) absolute difference between PETI and PET and d) relative
1623 difference calculated over the years 1961-2012.

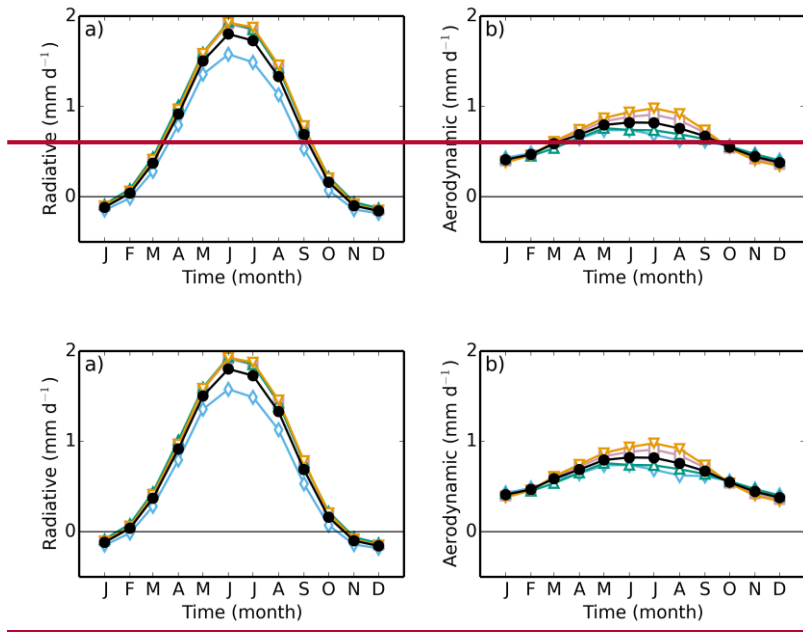


1624

1625

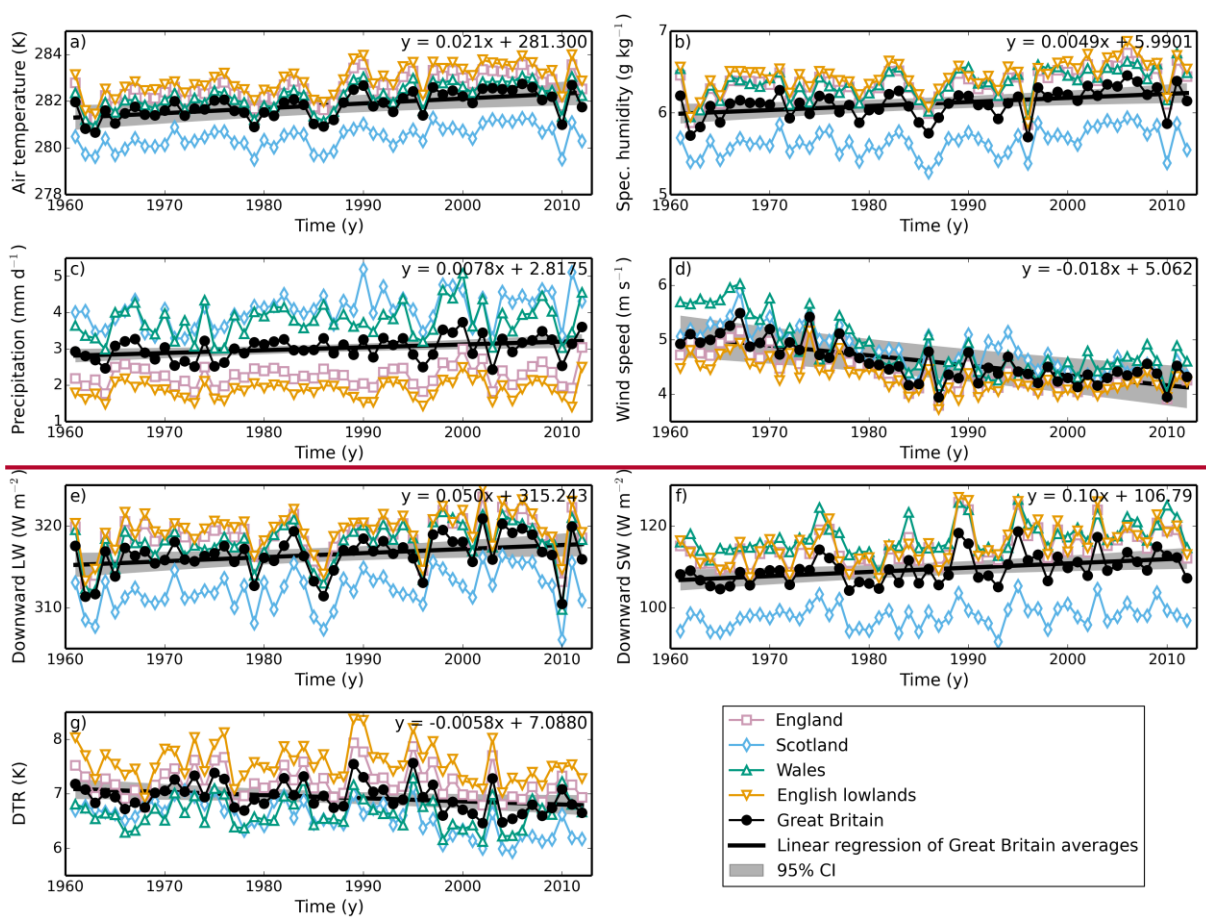
1626 Figure 7. Mean monthly climatology of a) PET, b) PETI, c) absolute difference between PETI
 1627 and PET, d) relative difference, for five different regions of Great Britain, calculated over the
 1628 years 1961-2012. Symbols as in Fig. 3.

1629

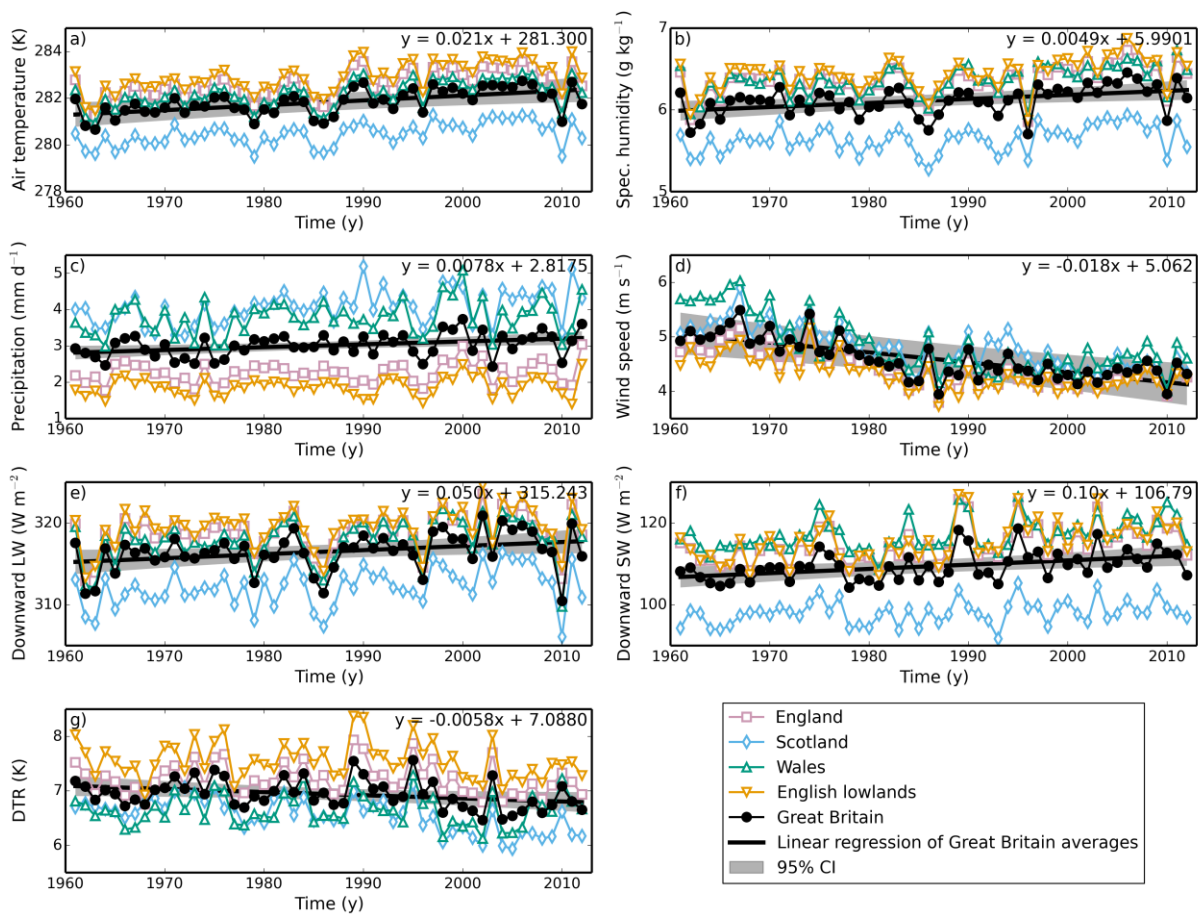


1630

1631 Figure 8. Mean-monthly climatology of the a) radiative and b) aerodynamic components of the
1632 PET for five different regions of Great Britain, calculated over the years 1961-2012. Symbols
1633 as in Fig. 3.

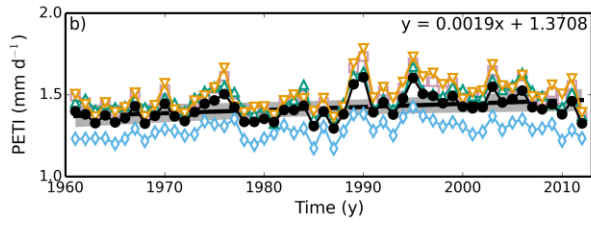
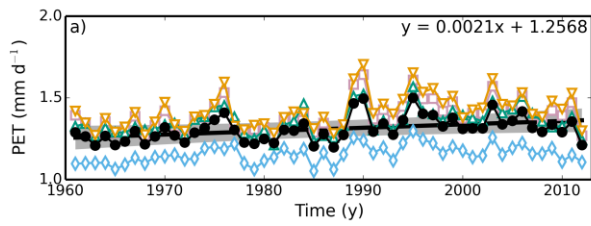
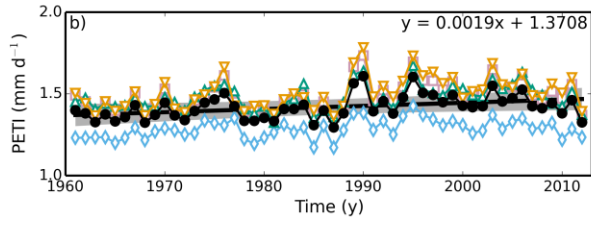
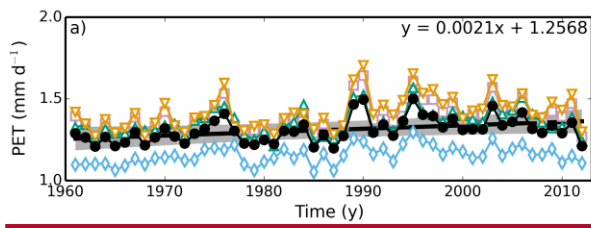


1634



1635

1636 Figure 9. Annual means of the meteorological variables, a) 1.2 m air temperature, b) 1.2 m
 1637 specific humidity, c) precipitation, d) 10 m wind speed, e) downward LW radiation, f) 1.2 m
 1638 downward SW radiation, g) daily air temperature range, over five regions of Great Britain. The
 1639 solid black lines show the linear regression fit to the Great Britain annual means, while the grey
 1640 strip shows the 95% CI of the same fit, assuming a non-zero lag-1 correlation coefficient. The
 1641 equation of this fit is shown in the top right-hand corner of each plot.

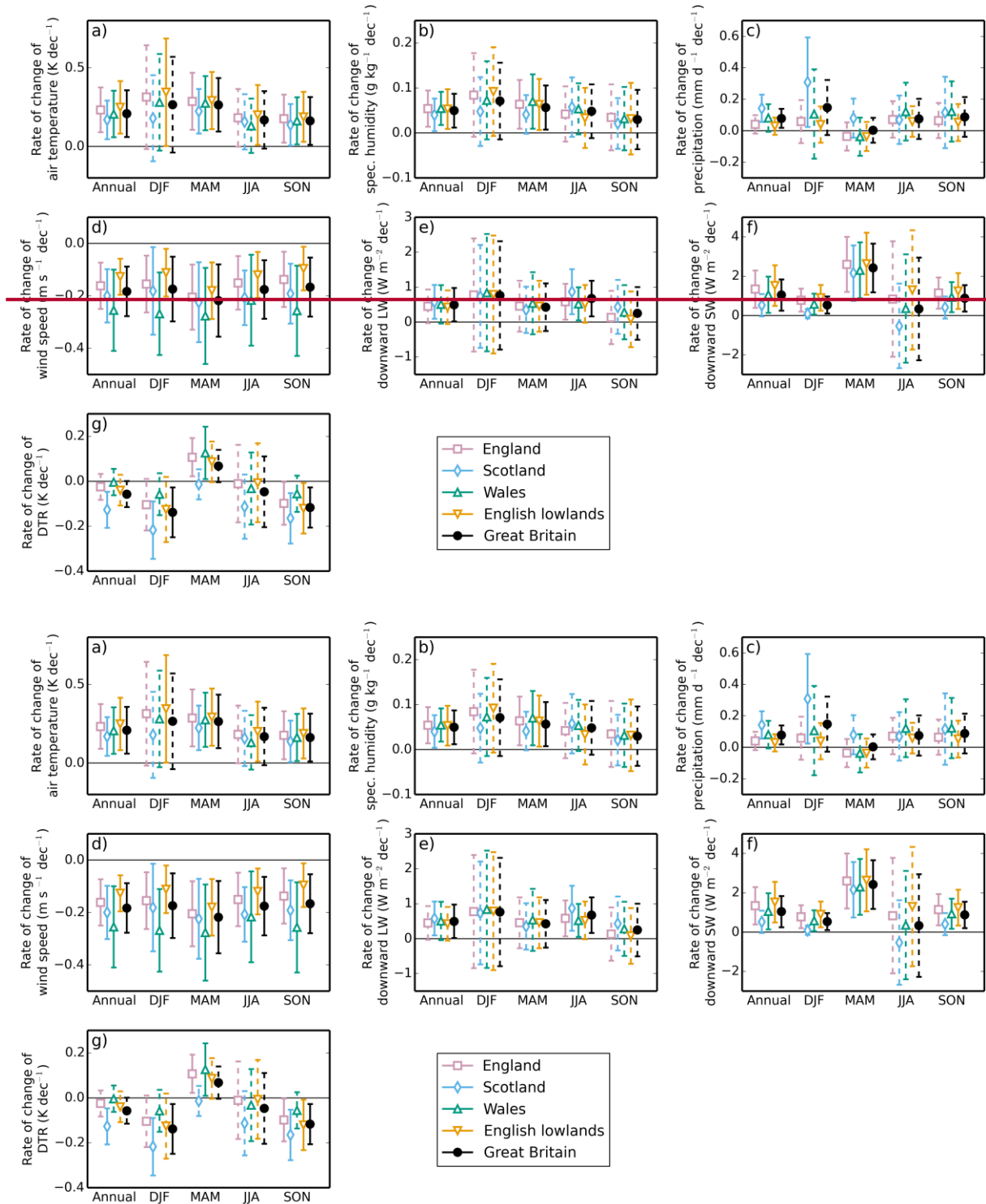


1642

1643

1644 Figure 10. Annual means of a) PET and b) PETI for five regions of Great Britain. Symbols as
 1645 in Fig. 9.

1646

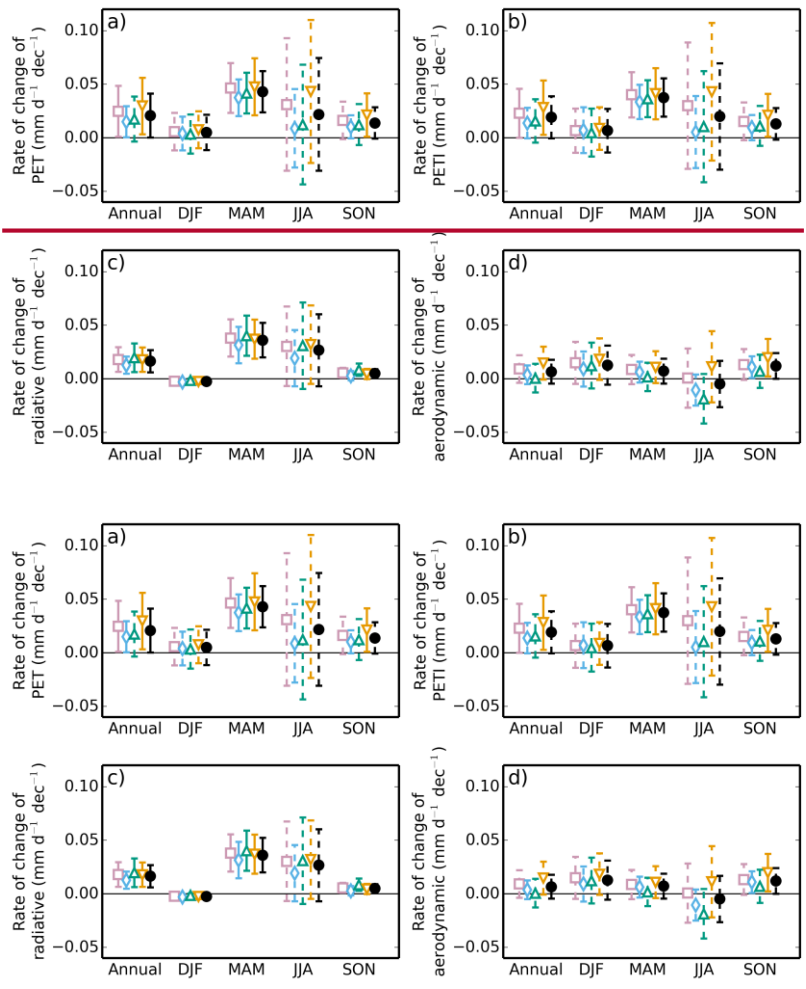


1647

1648

1649 Figure 11. Rate of change of annual and seasonal means of meteorological variables, a) 1.2 m
 1650 air temperature, b) 1.2 m specific humidity, c) precipitation, d) 10 m wind speed, e) downward
 1651 LW radiation, f) downward SW radiation, g) daily air temperature range, for five regions of
 1652 Great Britain for the years 1961-2012. Error bars are the 95% CI calculated assuming a non-

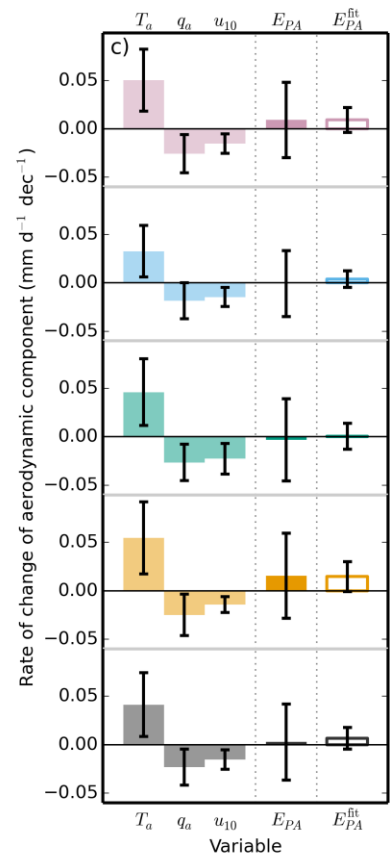
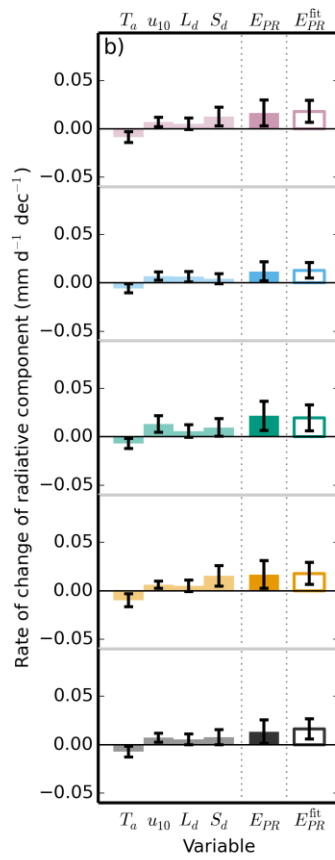
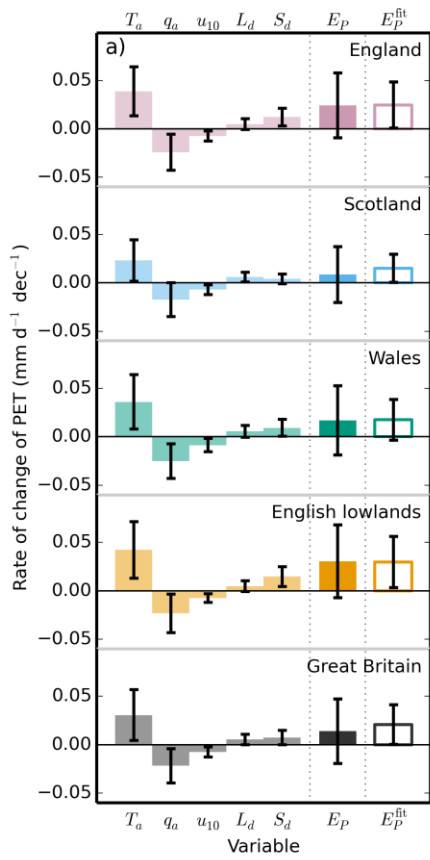
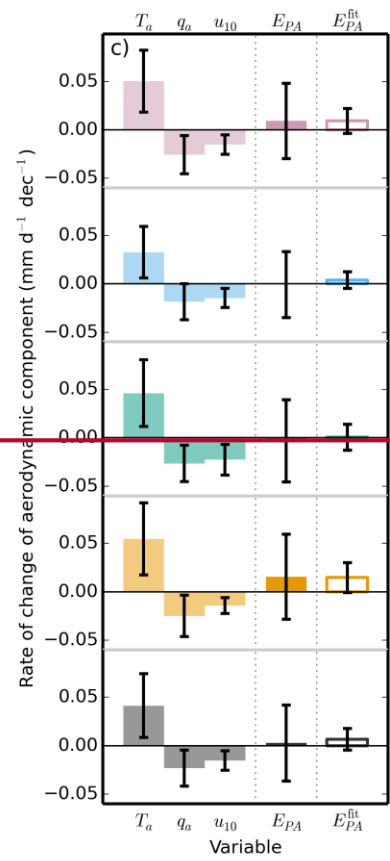
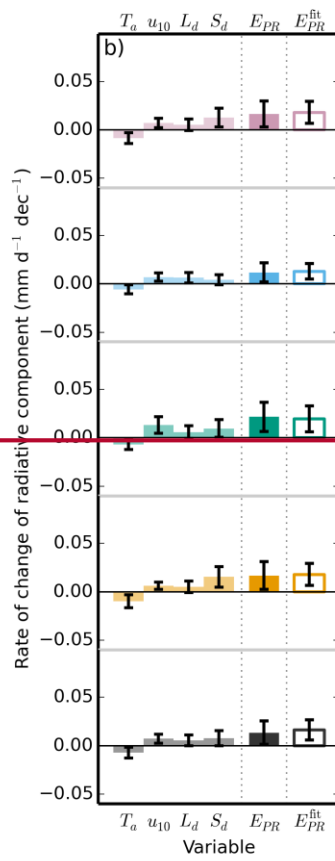
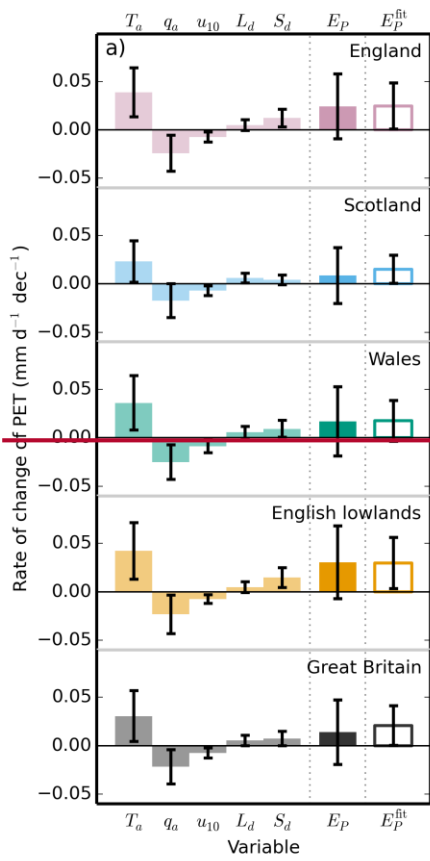
1653 zero lag-1 correlation coefficient. Solid error bars indicate slopes that are statistically significant
1654 at the 5% level, dashed error bars indicate slopes that are not significant at the 5% level.
1655



1656

1657

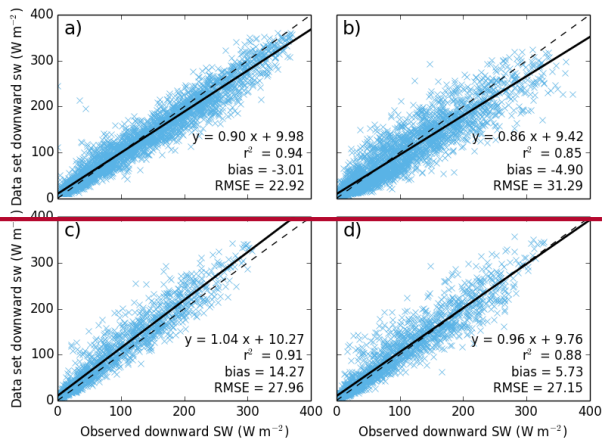
1658 Figure 12. Rate of change of annual and seasonal means of a) PET, b) PETI, c) the radiative
 1659 component of PET and d) the aerodynamic component of PET for five regions of Great Britain
 1660 for the years 1961-2012. Symbols as in Fig. 11.



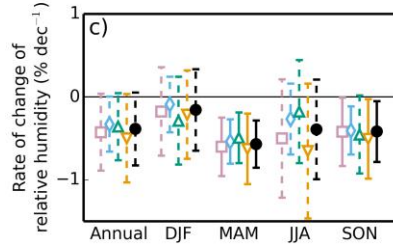
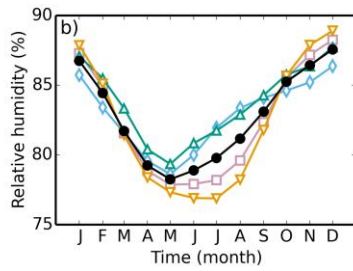
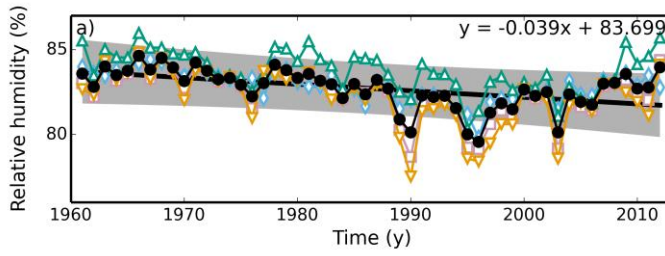
1661

1662

1663 Figure 13. The contribution of the rate of change of each meteorological variable to the rate of
1664 change of a) PET, b) the radiative component and c) the aerodynamic component. The first five
1665 (four; three) bars are the contribution to the rate of change of annual mean PET from the rate
1666 of change of each of the variables, calculated per pixel, than averaged over each region. Each
1667 bar has an error bar showing the 95% CI on each value. Since the pixels are highly spatially
1668 correlated, we use the more conservative CI calculated by applying this analysis to the regional
1669 means. The next bar is the sum of the other bars and shows the attributed rate of change of
1670 annual mean PET. The final bar shows the slope and its associated CI obtained from the linear
1671 regression of the mean annual PET for each region.
1672



1673



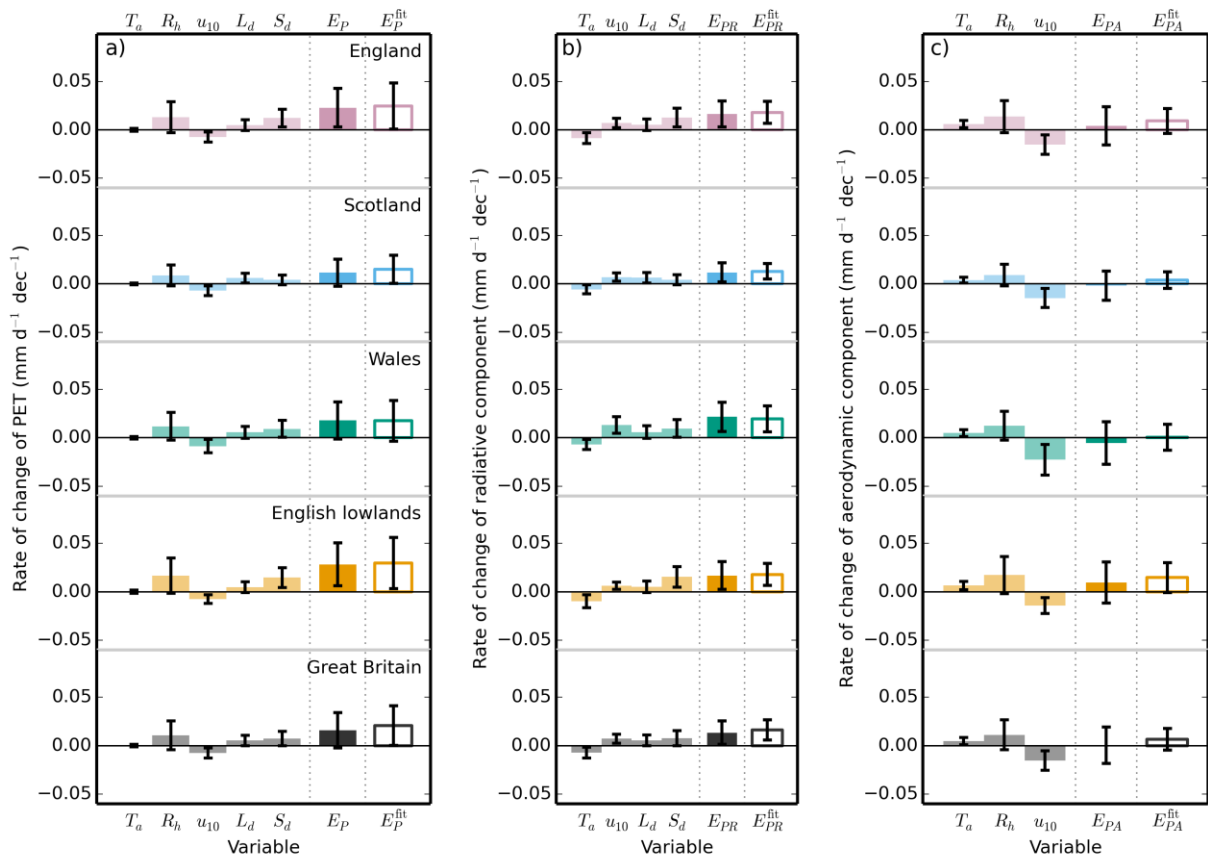
1674

1675

1676

1677

Figure 14. Regional annual means (a), regional mean-monthly climatology (b) and regional rates of change of relative humidity for the years 1961-2012.

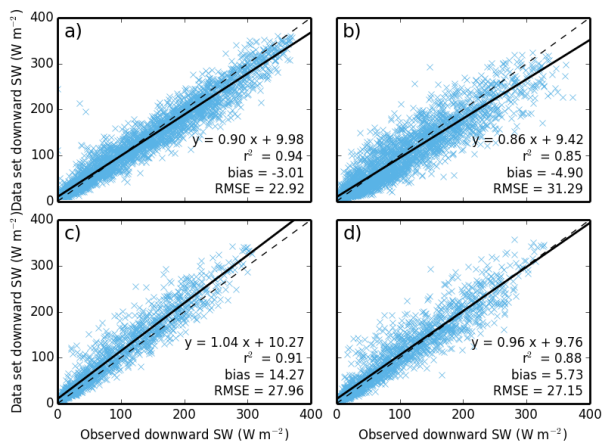


1678

1679 Figure 15. The contribution of the rate of change of each meteorological variable to the rate of
 1680 change of a) PET, b) the radiative component and c) the aerodynamic component, with relative
 1681 humidity instead of specific humidity. The first five (four; three) bars are the contribution to
 1682 the rate of change of annual mean PET from the rate of change of each of the variables,
 1683 calculated per pixel, than averaged over each region. Each bar has an error bar showing the
 1684 95% CI on each value. Since the pixels are highly spatially correlated, we use the more
 1685 conservative CI calculated by applying this analysis to the regional means. The next bar is the
 1686 sum of the other bars and shows the attributed rate of change of annual mean PET. The final
 1687 bar shows the slope and its associated CI obtained from the linear regression of the mean annual
 1688 PET for each region.

1689

1690



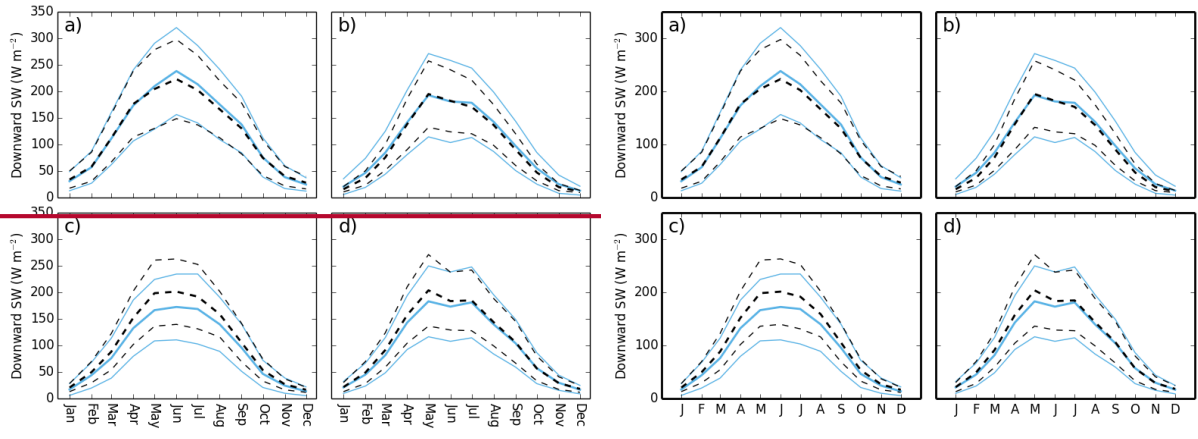
1691

1692

1693

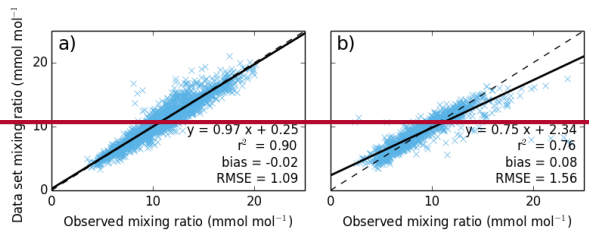
1694

Figure A1. Plot of data set downward SW radiation against daily mean observed downward SW radiation at four flux sites. Symbols and sites as in Fig. 4.

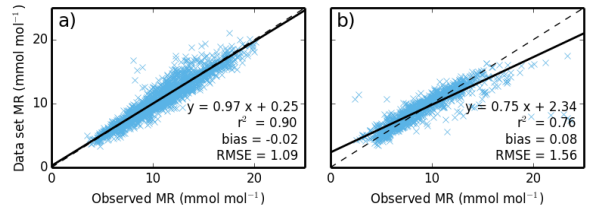


1697 Figure A2. Mean monthly climatology of the dataset (black, dashed lines) and observed (blue,
1698 solid lines) and observed air temperatures (black, dashed lines), downward SW radiation,
1699 calculated for the period of observations. Symbols as in Fig. 5, sites as in Fig. 4.

1701



1702



1703

Figure A3. Plot of mixing ~~ratio~~ratio calculated using dataset meteorology against daily mean

1704

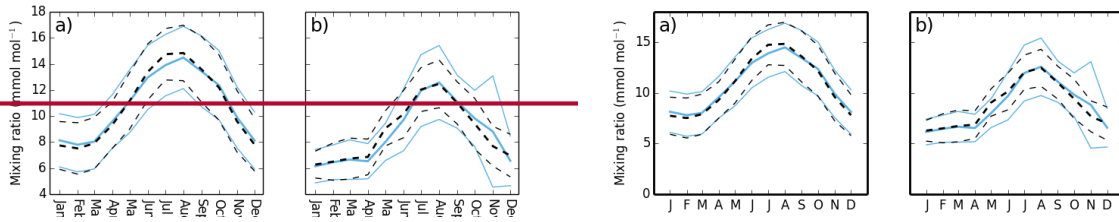
observed mixing ratio at four sites. Symbols as in Fig. 4. The sites are a) Alice Holt and b)

1705

Griffin Forest.

1706

1707

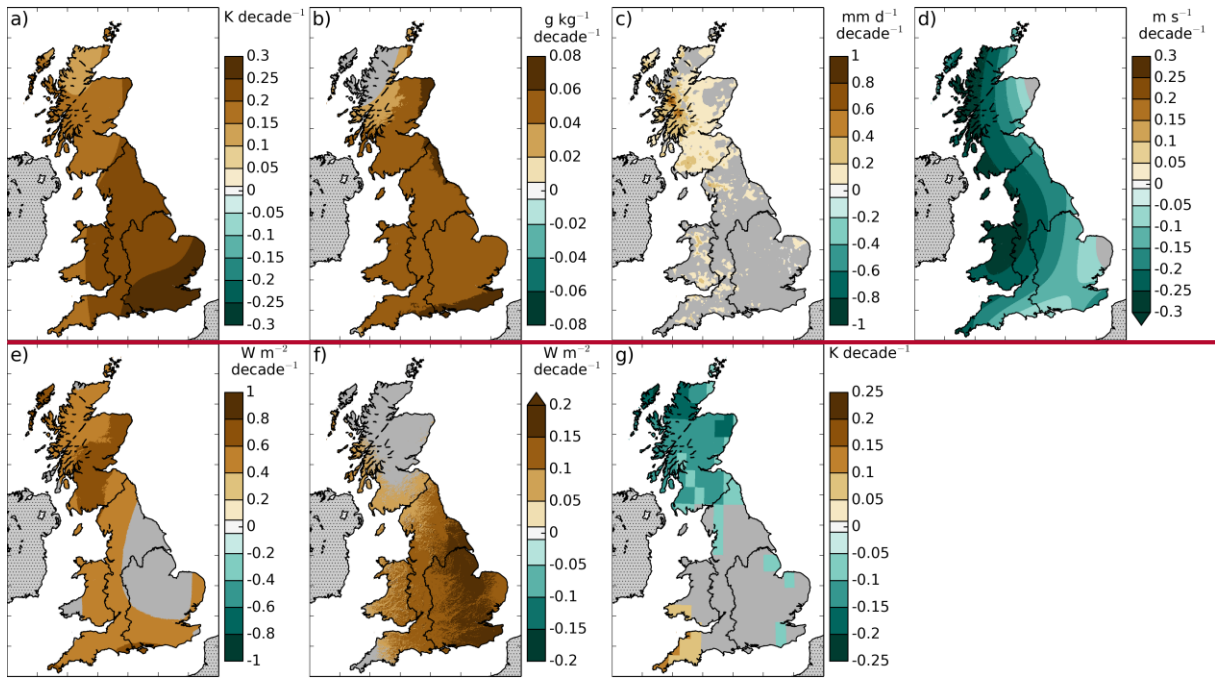


1708

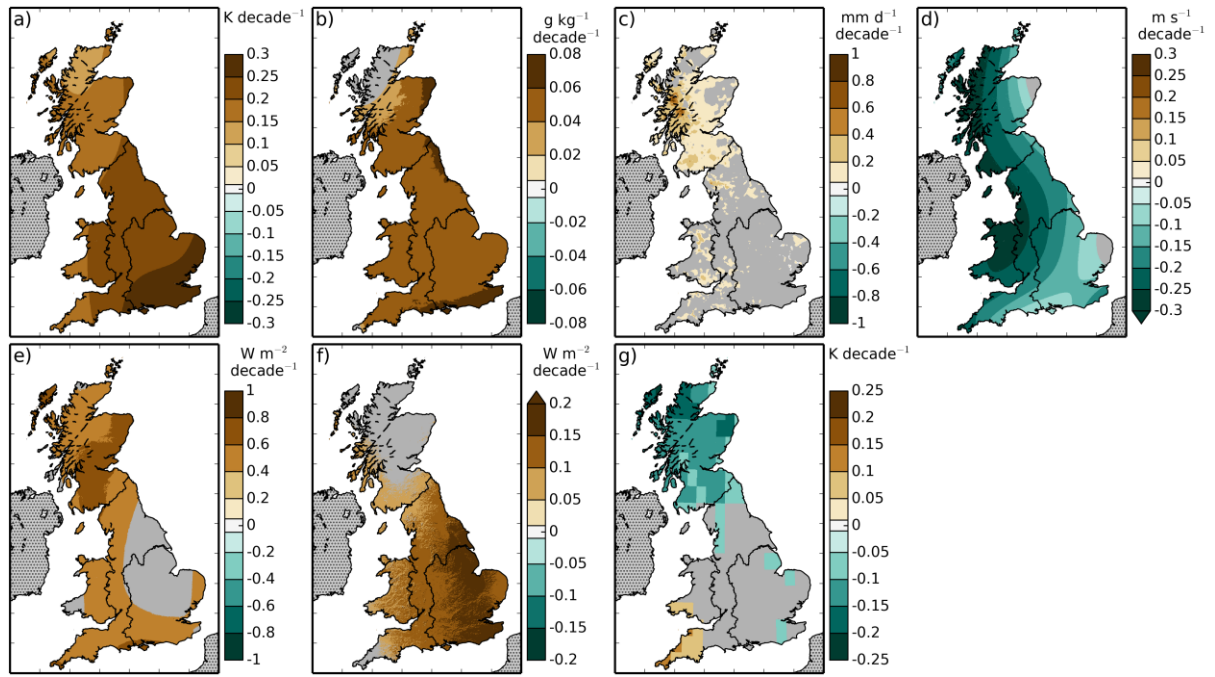
1709 Figure A4. Mean monthly climatology of the dataset (black, dashed lines) and observed (blue,
1710 solid lines) ~~and observed~~ mixing ratio (~~black, dashed lines~~),₂ calculated for the period of
1711 observations. Symbols as in Fig. 5. Sites as in Fig. A3.

1712

1713



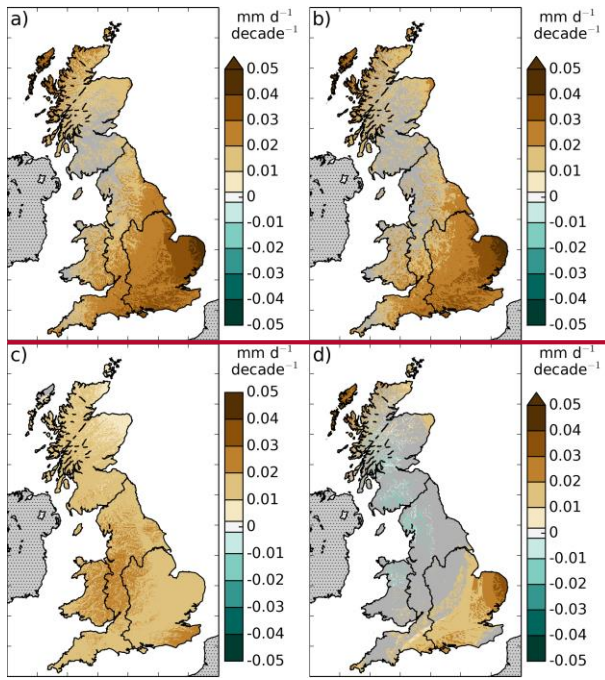
1714



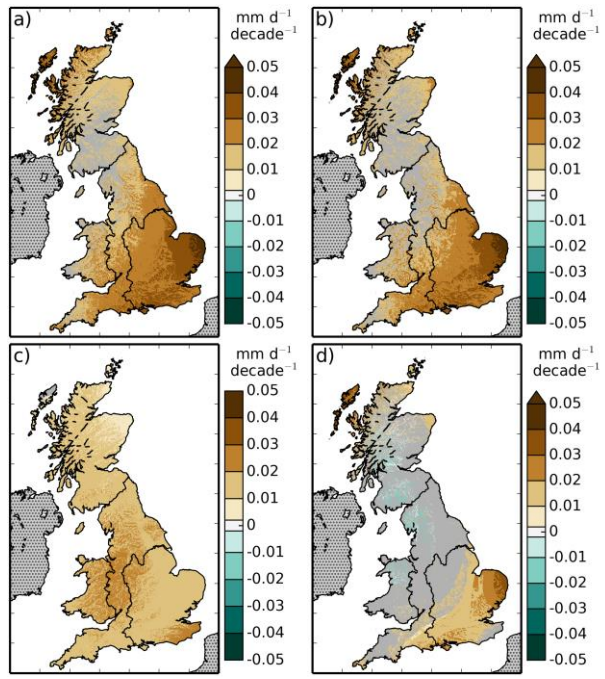
1715 Figure B1. Rate of change of the annual means of the meteorological variables, a) 1.2 m air
 1716 temperature, b) 1.2 m specific humidity, c) precipitation, d) 10 m wind speed, e) downward LW
 1717 radiation, f) downward SW radiation, g) surface air pressure, ~~h) daily air temperature range~~
 1718 over the period 1961-2012. Areas for which the trend was not significant are shown in grey.

1719

1720



1721



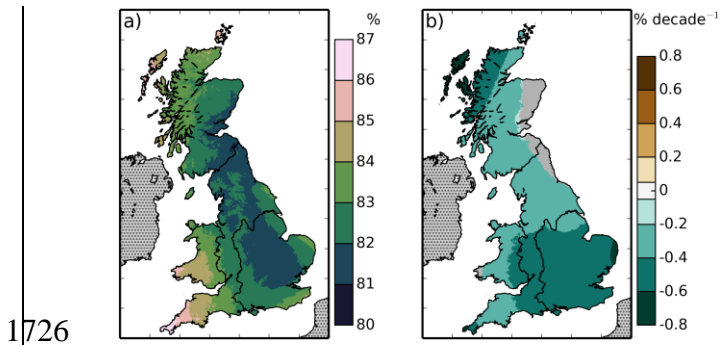
1722

Figure B2. Rate of change the annual means of a) PET, b) PETI, c) the radiative component of PET, d) the aerodynamic component of PET over the period 1961-2012. Areas for which the trend was not significant are shown in grey.

1723

1724

1725



1726

1727

1728

1729

1730

Figure B3. Mean of the relative humidity over the years 1961-2012 (a). Rate of change of the annual mean of relative humidity (b). Areas for which the trend was not significant are shown in grey.